Atrial Myocyte Physiology and Pharmacology in Health and Disease

Cynthia Laura Sandra SAM

Kingston University and St George's, University of London

2013

Atrial myocyte physiology and pharmacology in health and disease
Cynthia Laura Sandra Sam
Kingston University, 2013
Ethos persistent id: uk.bl.ethos.587410

Please do not digitise the following:

Figure 1.5 p.13
Figure 1.6 p.13
Figure 1.7 p.14
Figure 1.8 p.18

Anything after p.228

"Art is a passion pursued with discipline,

Science is a discipline pursued with passion"

Sir James Black

(*Founder of the β blockers*)

Abstract

Atrial fibrillation is the most common form of cardiac dysrhythmia in the world. According to the British Heart Foundation, about 1 million people in the UK are currently living with this condition and they are up to five times more likely to suffer a stroke than the rest of the population. Atrial fibrillation is the result of irregular spontaneous contractions of the atrial chambers of the heart separate to the contractions generated by the sino-atrial node activity. At a cellular level, pro-arrhythmogenic calcium handling has been observed upon the stimulation of atrial cells with the partial agonist CGP12177 at a novel low affinity β1-AR ($\beta1_L$-AR).

The aim of this thesis is to characterise the relationship between the morphology of the left and right atrial myocytes and the initial calcium release sites, and alterations in calcium handling protein phosphorylation state during cardiomyocyte contraction. We study how this relates to atrial arrhythmias via spontaneous calcium release activity in quiescent rat atrial myocytes by stimulating the propranolol-insensitive β1-ARs using CGP12177. We aim to contribute towards understanding specific alterations at the cellular level in atrial myocytes during arrhythmias and heart failure (HF).

Quiescent WKY rat left and right atrial cells were obtained from Langendorff perfusion of the whole heart and subsequent atrial cell isolation. Left atrial cells (13.6 ± 0.3 μm) were wider on average compared to right atrial cells (9.9 ± 0.25 μm). Di-8ANEPPS stained cells confirmed networks of t-tubules in left atrial myocytes that facilitate t-tubular transportation of calcium during excitation contraction coupling. However no t-tubules were reported for right atrial myocytes presumably due to their narrower widths which are sufficient for calcium diffusion. Cardiac dysfunction results in cardiac proteins (sarco(endo)plasmic calcium ATP-ase (SERCA2a) protein, phospholamban (PLB) and ryanodine receptors (RyR2) having abnormal expressions. Western blotting studies have demonstrated high abundance of PLB and a tendency for lower abundance of SERCA2a in hypertensive and volume overload HF tissues as a result of the increased the workload on the heart and prolonged calcium release from the calcium store. Phosphorylated proteins of PLB in hypertensive tissues have lower population of β-ARs and hence there is a reduction in the stimulation of these receptors in the heart. On the other hand, a deterioration of RyR2 of the sarcoplasmic reticulum leads to a reduced amount of calcium being stored in the calcium store and consequently contributes to a contractile deficit. This may eventually result in arrhythmias, commonly observed in people with HF.

A pharmacological study of spontaneous calcium release (calcium sparks, wavelets and waves) using a series of cardioactive agents suggests pathways of pro-arrhythmogenic calcium release via the low affinity β1-ARs. In particular, CGP12177 stimulating the $\beta1_L$-ARs of quiescent rat atrial myocytes has revealed that there may be a pro-arrhythmogenic pool of calcium in these atrial cells and a β-blocker such as bupranolol may be efficient in supressing such stimulation as a therapeutic solution.

Table of Contents

List of Abbreviations and Acronyms

2-APB - 2-aminoethoxydiphenyl borate

AC - Adenyl cyclase

AF - Atrial fibrillation

AM – Acetoxymethyl

AP – Action potential

ANF - Atrial natriuretic factor

AV - Atrioventricular

β-ARs - β-Adrenoceptors

$\beta 1_H$-AR - high affinity β-adrenoceptor

$\beta 1_L$-AR - low affinity β-adrenoceptor

BHF - British Heart Foundation

BRF - Biological Research Facilities

BRL37344 - (±)-4-(2-[2-hydroxy-2-(3chlorophenyl)ethylamino]propyl) phenoxyacetate sodium salt sesquihydrate

BSA - Bovine serum albumin

CaM Kinase II - calmodulin-dependent protein kinase 2

cAMP - cyclic adenosine monophosphate

cGMP - cyclic guanosine monophosphate

CGP12177 - (4-(3-tertiarybutylamino-2-hydroxypropoxy)-benzimidazole-2-on hydrochloride

CHF - Congestive heart failure

CICR - Calcium-induced calcium release

CSQ - Calsequestrin

EC - Excitation contraction

ECL - Enhanced chemiluminescence

ER - Endoplasmic reticulum

DHPR - Dihydropyridine

Di-8ANEPPS - di-8-aminoaphthylethenylpyridinium

DMSO - Dimethyl sulfoxide

DPBS - Dulbecco's phosphate buffered saline

ECL - enhanced chemiluminescence

EDTA - Ethylenediaminetetraacetic acid

EGTA - Ethylene glycol tetraacetic acid

eNOS - endothelial nitric oxide synthase

FBS - Fetal bovine serum

Fluo-4AM - fluo-4 acetoxymethyl ester

GAPDH - Glyceraldehyde 3-phosphate dehydrogenase

GC - Guanylate cyclase

GPCR - G-protein coupled receptors

HEPES - 2-[4-(2-hydroxyethyl)piperazin-1-yl]ethanesulfonic acid

HF - Heart failure

HRP - Horseradish peroxidise

I_{Ca} - inward calcium current

ICI - Imperial Chemical Industries

IgG - Immunoglobulin G

IHF - Induced heart failure

i.p - Intraperitoneal injection

IP3R - Inositol 1, 4, 5-triphosphate receptors

ISO - Isoprenaline

kDa – Kilodalton

LA - Left atria

LP - Long pass

LTCC - L-type calcium channel

LSM - Laser scanning microscope

LV - Left ventricular

M199 - Medium 199

MI - Myocardial infarction

MW - Molecular weight

NA - Numerical aperture

NCX - Sodium calcium exchange

PAGE - Polyacrylamide gel electrophoresis

PDE - Phosphodiesterase

PI3K - Phosphoinositide 3-kinase

PKA - Protein kinase A

PKG - Protein kinase G

PLB - Phospholamban

PLB-Ser16 - Phosphorylated Serine 16

PLB-Thr17 - Phosphorylated Threonine 17

PP1 - Protein phosphatase 1

PTP - Protein phosphotyrosyl phosphatase

PVDF - Polyvinylidene fluoride

RA - Right atria

Rpm - revolutions per minute

RT - Room temperature

RV - Right ventricular

RyRs - Ryanodine receptors

RyR2 - Cardiac ryanodine receptor

RyR-Ser 2808 - Ryanodine phospho Serine-2808

RyR- Ser 2814 - Ryanodine phospho Serine-2814

RyR-Ser 2030 - Ryanodine phospho Serine-2030

SA - Sino-atrial

SD - Sprague-Dawley

SDS - Sodium dodecyl sulfate

S.E.M - Standard error of the mean

SERCA2a - Sarco(endo)plasmic calcium ATP-ase pump

SHR - Spontaneously hypertensive

SR - Sarcoplasmic reticulum

TBST - Tris buffered saline with Tween-20

TEMED - Tetramethylethylenediamine

T-tubules - Transverse-tubules

TATS - Transverse axial tubular system

WGA - Wheat germ agglutin

WKY - Wistar-Kyoto

List of Abbreviations and Acronyms

(Relevant chemical formulae)

Ca^{2+} - Calcium

$CaCl_2$ - Calcium chloride

CO_2 - Carbon dioxide

H - Hydrogen

K - Potassium

KCl - Potassium chloride

KOH - Potassium hydroxide

$MgCl_26H_2O$ - Magnesium chloride hydrate

$MgSO_47H_2O$ - Magnesium sulphate heptahydrate

Na - Sodium

NaCl - Sodium chloride

NaF – Sodium fluorate

$NaH_2PO_4H_2O$ – monosodium dihydrogen phosphate monohydrate

NaOH – Sodium hydroxide

$Na_4P_2O_7$ – Sodium orthophosphate

NO - Nitric oxide

NTA - Nitrilotriacetic acid

O_2 - Oxygen

List of Figures

CHAPTER 4

CHAPTER 5

List of Tables

ACKNOWLEDGEMENTS

My PhD is one of the best things I have done so far in my life, it has not only furthered my knowledge, critical thinking and understanding in cardiac physiology and pharmacology, but also I have learnt to be self-motivated, stronger in both mind and body and to be grateful and appreciate everything in life. My thesis would not have been possible without the support of several people who in one way or another have provided me with guidance and unselfishly extended their help, support and encouragement.

First and foremost, I dedicate my heartfelt gratitude to my Director of Studies, **Dr Nicholas Freestone** who has been a first class supervisor, mentor and friend. His valuable guidance, unique sense of humour and unfailing support has kept me motivated and enthusiastic throughout the rollercoaster ride of my PhD studies. I am thankful to **Dr Ian Piper** who is my co-supervisor, for his unwavering encouragement and helpful ideas during my PhD. Thank you to **Professor Tom Bolton** for being my supervisor, I am grateful for his moral support and advice during my research in the laboratories at St George's, University of London and I am honoured to be his last PhD student.

To **Drs Oleksandr Povstyan** and **Maksym Harhun**, I thank them sincerely for helping me during the early stages of my training on the confocal microscope at St George's, University of London, despite having their own gruelling research to do. Their exemplary work ethic has certainly made a positive impact on me. Thank you to **Mr Nick Brill** for his helpful assistance in IT support. Thank you to my brother, **Laurent Sam** who has always kept me grounded and sane during my PhD!

Last but not least I want to say thank you with all my heart to my **Mum and Dad** back home in the Seychelles who have sacrificed a lot for me. Even though I am so far away, their unconditional love, encouragement and support have always made it here to me. My sincere gratitude also goes to everyone else who has helped me in one way or another, I have not forgotten them or ever will.

*†Financial support for my PhD studentship was from the **BPSRG** at Kingston University and **SWAN grant** from St George's, University of London.*

I dedicate my thesis to Papa et Maman

CHAPTER 1

Introduction

1.0 Introduction

1.1. Introduction to the anatomy and physiology of the mammalian heart

The mammalian heart is an important life-sustaining muscle in the body (Figure 1.1). It continuously and involuntarily propels blood around the body to deliver oxygenated blood to nourish the organs with vital nutrients and oxygen, as well as to deposit de-oxygenated blood in the lungs to expel carbon dioxide and collect oxygen (Levick, 2012). Unlike other muscle groups in the body, the heart is unique in that it beats continuously and will continue to do so rhythmically even when the body is at rest. The mammalian heart is situated slightly to the left of the centre of the body and is obliquely positioned, so that the apex of the heart leans slightly towards the left side of the body with the base of the heart lying towards the right of the body. The heart is surrounded by a pericardium which is a fibrous sac enveloping the epicardial muscle that constitutes the outside layer of the heart and provides some anchorage of the heart and protection behind the sternum and rib cage (Levick, 2012). The healthy heart is crucial in the normal function of the body since alteration in its activity would bring about consequences to the sustainability of one's life.

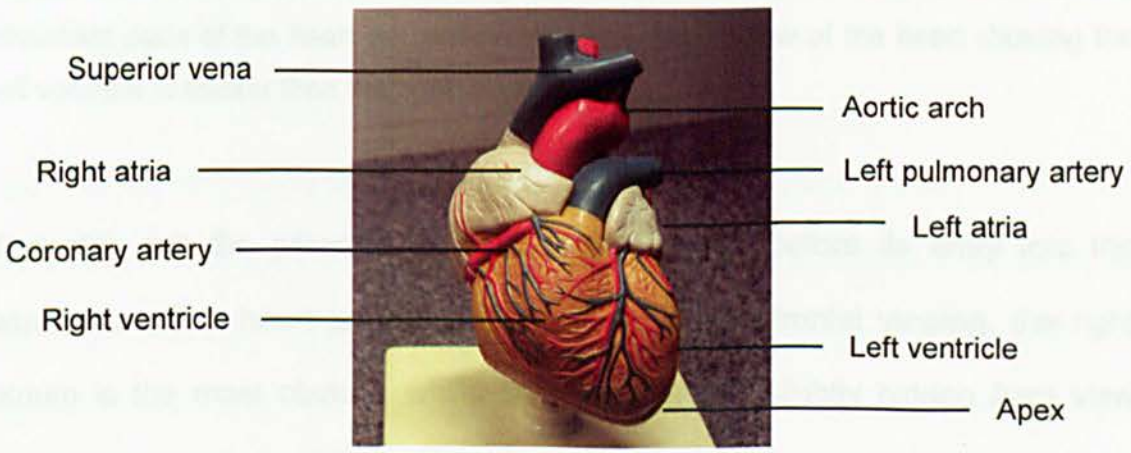

Figure 1.1 The mammalian heart. A posterior view of a typical mammalian heart.

1.2. Structure and function of the heart

1.2.1 Atria and ventricles

The mammalian heart is made up of four chambers (Figure 1.2). The left and right atria make up the upper cavities of the heart, whilst the left and right ventricles are larger muscular chambers that are at the apex of the heart.

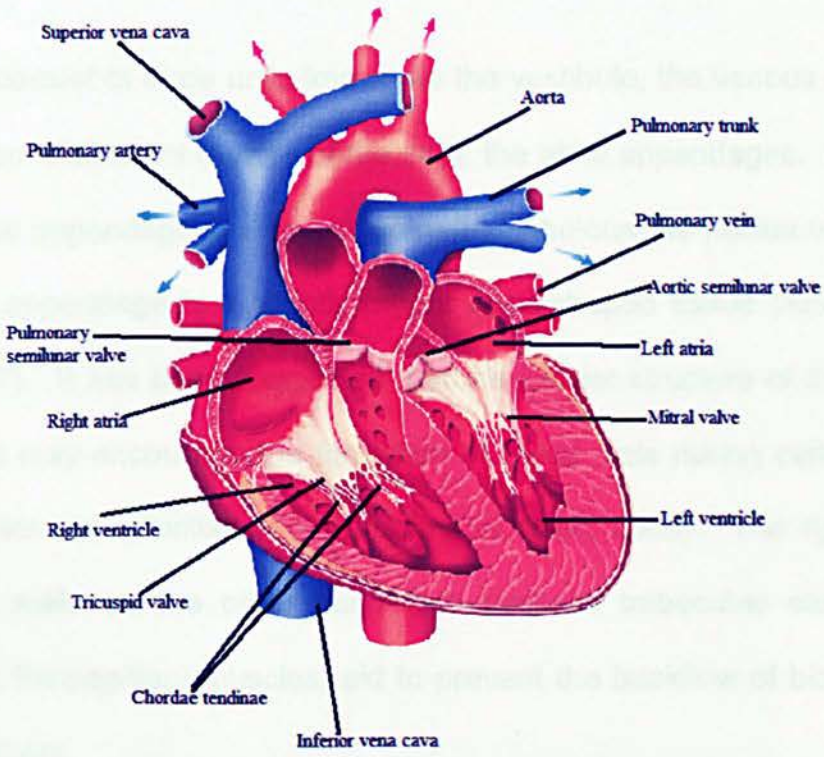

Figure 1.2 The anatomical interior of the mammalian heart. The fundamental and important parts of the heart are annotated. The frontal view of the heart showing the left ventricle is thicker than the right ventricle.

The atria are the primary recipients of blood just before its entry into the ventricles. The heart is orientated such that upon frontal viewing, the right atrium is the most obvious whilst the left atrium is slightly hidden from view (Anderson and Cook, 2007). The left atrium is made up of a smooth inner wall with relatively thick muscle fibres which accounts for the higher pressure

required to pump blood to the largest chamber of the heart, the left ventricle. On the other hand, the right atrium has a thinner muscular wall as it does not require much force to push blood into the right ventricle. The right atrium consists of extensive muscular protrusions known as trabeculae which serve to prevent the atrioventricular (AV) valves from inverting and these develop into ridges called the pectinate muscles (Ho *et al.*, 2002 ; Anderson and Cook, 2007).

Both atria consist of three units known as the vestibule, the venous component and the most prominent feature of the atria, the atrial appendages. In humans, the left atrial appendage is a small, protruding lobulous-like pocket whereas the right atrial appendage is a slightly bigger cone-shaped tissue (Anderson and Cook, 2007). It has been suggested that the lobular structure of the left atrial appendage may encourage the formation of blood clots during certain cardiac disorders like atrial fibrillation (AF) (Johnson *et al.*, 2000). The right and left ventricular walls on the other hand also possess trabeculae carnae which similarly to the papillary muscles, aid to prevent the backflow of blood into the atrial chambers.

1.2.2 Circulation of the blood in the heart

Upon arrival to the atria, the majority of the blood flows passively into the ventricular chambers whereas a smaller proportion of the blood is pumped by atrial contraction which contributes about 15 - 20% of the blood in the ventricles (Kaasik *et al.*, 2001). The replenishing of the ventricles with blood from the atria is called the "atrial kick" (Lo *et al.*, 1999). The contraction of the mammalian

atrial chambers occurs momentarily just before that of the ventricles. The contraction of the atria is less forceful and less prolonged than for the ventricles (Korecky and Michael, 1974) since the distance for blood to travel from atria to ventricles is relatively short. The right atrium receives deoxygenated blood from the body via the two caval veins, the superior vena cava (from the upper parts of the body) and the inferior vena cava (from the lower parts of the body). The left atrium receives oxygen-rich blood via the pulmonary vein.

Each side of the heart possesses an AV valve whereby, the right side of the heart has a 3-cusp valve known as the tricuspid valve while the AV valve on the left side of the heart is known as the bicuspid or mitral valve. Upon atrial contraction, blood flows from the right and left atria and through the respective AV valves which prevent backflow of the blood and into the corresponding relaxed ventricles. During systole, when the right and left ventricles contract, the cusps of the pulmonary and aortic semilunar valves are forced outwards to enable blood to flow out of the ventricles. Chordae tendinae are strong tendons made of connective tissue which prevents prolapse of AV valves under high systolic pressure and they are situated on the inner ventricular walls attached to papillary muscles of the heart.

Upon exit from the right ventricle, deoxygenated blood flows via the pulmonary artery towards the lungs. On the other hand, the left ventricle which is also the most muscular and thickest ventricle, pumps blood rich with oxygen towards the rest of the body via the aorta.

1.3 Cardiac Excitation Contraction Coupling

1.3.1 Ventricular Excitation Contraction coupling

Excitation Contraction (EC) coupling is the electrical excitation event in cardiomyocytes which activates the contractile machinery of the heart, first resulting in cardiac sarcoplasmic reticulum (SR) calcium release and eventually, contraction of the heart muscle (Fabiato, 1985 ; Cheng *et al.*, 1993 ; Bers, 2002 ; Eschenhagen, 2010). Calcium ions play the main role in orchestrating EC coupling (Figure 1.3). During the cardiac action potential, the cardiac cell undergoes depolarisation whereby the L-type calcium channels (LTCCs) open and calcium enters the cell as a calcium current (Bers, 2002). Invaginations of the surface membrane of the cardiac cell called t-tubules facilitate the transport of depolarisation deep into the ventricular cell for EC coupling (Kirk *et al.*, 2003 ; Smyrnias *et al.*, 2010).

The entry of calcium into the myocyte then triggers the release of more calcium from the SR via calcium release channels called ryanodine receptors (RyR2) (Tunwell *et al.*, 1996 ; Dulhunty *et al.*, 2012). This process of calcium movement is known as Calcium-Induced Calcium Release (CICR) (Fabiato, 1985). This increase in intracellular calcium concentration enables calcium to bind to a myofilament protein called troponin C, causing a conformational change of the latter which causes tropomyosin to be displaced from the troponin body. This in turn allows the myofilaments actin and myosin to interact by sliding past one another in a rowing motion as outlined in the sliding filament theory (Huxley and Hansen 1954 ; Huxley and Niedegerke, 1954) which facilitates contraction of the cardiomyocyte.

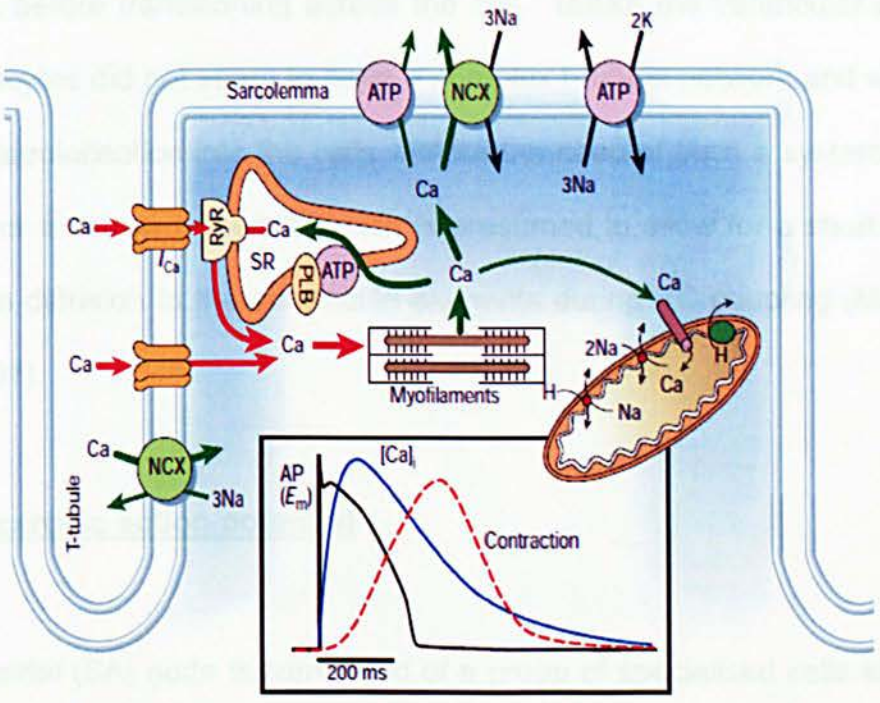

Figure 1.3 The action of calcium ions during excitation contraction (EC) coupling. Red arrows show the movement of calcium ions during systole. Green arrows represent events during diastole when the intracellular calcium is low and the cardiomyocyte is relaxed. The inset diagram illustrates the action potential time course, the calcium events and the resulting contractile activity in a ventricular myocyte. Adenosine triphosphate (ATP), sodium calcium exchanger (NCX), action potential (AP), ryanodine receptor (RyR2), phospholamban (PLB), sarcoplasmic reticulum (SR), sodium (Na) and calcium (Ca). Courtesy of Bers, 2002.

1.3.2 Atrial Excitation Contraction coupling

EC coupling in isolated ventricular cells has been frequently studied but recently there has been a sudden increase in interest for this event in atrial cells. EC coupling in atrial cells is similar to that in ventricular cells. However, differences occur regarding the handling of intracellular calcium events. Work carried out by Hüser and colleagues (1996) on isolated cat atrial myocytes showed that

calcium release was frequently being initiated from the periphery of the myocytes before transitioning across the cell. Unlike the ventricular cells, the atrial myocytes did not seem to have a complex t-tubule network and were able to carry depolarisation into the cells without the need of such a system. This is because of a narrow cell width which is presumed to allow for a short distance of calcium diffusion to the contractile elements during EC coupling (Mackenzie *et al.*, 2001).

1.4 The cardiac action potential

The sinoatrial (SA) node is composed of a group of specialised cells situated in the right atrial muscular wall (Figure 1.4), close to the superior vena cava, and its function is to trigger continuous and precisely timed electrical signals known as action potentials (Boyett *et al.*, 2000). The action potential spreads over the right and left atrial walls and causes the atria to contract. By this time, the action potential reaches the AV node causing the Purkinje fibres, which are specialised fibrous conductive tissues on the inside wall of the ventricles to send a signal of contraction to the ventricles (Eliška, 2006). This causes the right ventricle to propel the de-oxygenated blood via the pulmonic valve, into the pulmonary artery and towards the lungs. At the same time, the left ventricle contracts powerfully to enable the oxygenated blood to be distributed to the rest of the body via the aortic valve.

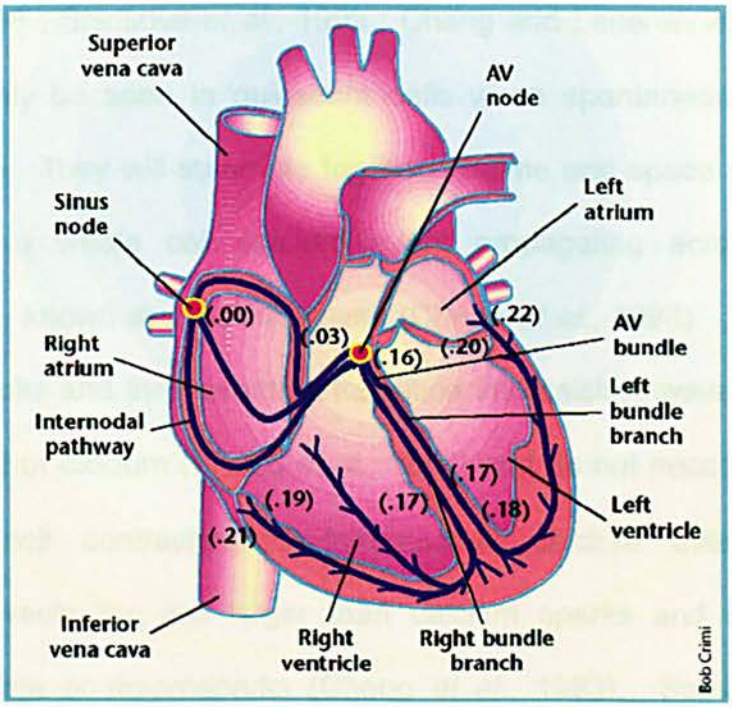

Figure 1.4 Cardiac action potential pathway. An electrical impulse originates from the sino-atrial (SA) node (or sinus node) and arrives at the atrioventricular (AV) node within 30 ms before travelling down the Purkinje fibres and causing the ventricles to contract. Courtesy of Robbins and Dorn II (2000).

1.5 Calcium Sparks

Calcium sparks are the fundamental units of quantal calcium release arising from the SR as a response to an action potential during EC coupling (Benham and Bolton, 1986 ; Cheng *et al.*, 1993 ; Venetucci *et al.*, 2008). Initially, calcium sparks were identified in isolated single rat cardiomyocytes under the laser scanning confocal microscope in 1993 by Lederer's group (Cheng *et al.*, 1993). In quiescent cells, the calcium sparks were described as being localised and discrete areas of increased fluorescence observed under the confocal

microscope when cardiomyocytes were loaded with a fluorescent calcium indicator such as fluo-4 acetoxylmethyl (AM) (Cheng *et al.*, 1993 ; Bolton and Gordienko 1998 ; Shirikova *et al.*, 1999 ; Cheng and Lederer, 2008). Calcium sparks can only be seen in quiescent cells when spontaneous SR calcium release occurs. They will summate together in time and space and eventually will result in a whole cell calcium event propagating across the entire cardiomyocyte, known as calcium waves (Cheng *et al.*, 1993). The frequency of calcium sparks and their eventual transition into calcium waves is increased by an overload of calcium (Cheng *et al.*, 1993) and do not necessarily result in co-ordinated cell contractions. Intermediate calcium events are non-propagating events but are larger than calcium sparks and are known as calcium wavelets or macrosparks (Cheng *et al.*, 1993). Sometimes excess catecholamines can activate the arrhythmogenic inward current which generates an extra cardiac contractions separate to the action potential generated contractions and they are known as arrhythmias.

Calcium sparks have been observed to be of a bigger size in spontaneously hypertensive rats (SHR) (Shorofsky *et al.*, 1999). This is due to the size and the increase in population of RyR2 that function as the calcium channels on through the LTCC to accommodate the increasing pressure of blood upon the heart. SHRs are outbred strains of the Wistar rat produced by the Kyoto School of Medicine and they naturally develop hypertension as they get older. Therefore, cardiomyocytes from SHR hearts are a common experimental animal model to study left ventricular hypertensive heart disease at the cellular level because of their ability to demonstrate the stages of hypertension evident in human disease (Shorofsky *et al.*, 1999).

1.5.1 Pathology of cardiac tissues

In humans, pathological hypertrophy in the left ventricular chamber increases the chances of myocardial infarction (MI), congestive heart failure (CHF) and stroke (Gradman and Alfayoumi, 2006 ; Bauml and Underwood, 2010). During cardiac hypertrophy, the muscular wall of the heart thickens progressively as a result of the increase in the sizes of cardiomyocytes (Frey *et al.*, 2004). The increase in the thickness of the cardiac muscle is due to compensatory mechanisms responding to the pathological cardiac wall stress when the heart has to work harder to keep up cardiac demand by pumping blood around the body. Furthermore, collagenous substances begin to accumulate on the cardiac cell surface which reduces the elastic compliance of the cardiac muscle (Katz and Zile, 2006). Heart failure (HF) is due to the weak pumping action of the heart causing insufficient blood reaching the organs of the body to deliver oxygenated blood or to remove deoxygenated blood. In order to compensate for a low cardiac output, the heart has to work harder and faster. During HF, the flow of blood being pushed by the atria into the ventricles during contraction can be significantly affected since the heart does not have enough power to pump the blood (Maisel and Stevenson, 2003).

The incidence of AF in patients with HF is between 10 - 15% (Maisel and Stevenson, 2003). The spontaneous electric impulses of the atria result in the irregularity in atrial calcium signalling events causing the atria to contract sporadically and randomly leading to AF which is the most commonly occurring cardiac arrhythmia (Benjamin *et al.*, 1998). Initially, AF is not a danger to health since the blood still reaches the ventricles although less forcefully. The irregular

atrial contraction however could then lead to the possibility of thrombus formation in the atria due to blood not being pumped consistently and rhythmically and this may eventually result in a stroke.

1.6. Atrial and ventricular cardiomyocytes

1.6.1. Morphology

Atrial and ventricular cells have well-adapted structures to suit their specific functions during EC coupling. The morphology of human atrial and ventricular cells is not significantly different from each other (Bustamante *et al.,* 1982), however it has been widely demonstrated that there are pronounced differences in terms of morphological structures between the atrial and ventricular myocytes of other mammals such as cats (Hüser *et al.*, 1996), sheep (Dibb *et al.*, 2009), guinea pigs (Hume and Uehara, 1985) and rats (Kirk *et al.*, 2003 ; Walden *et al.*, 2009 ; Smyrnias *et al.*, 2010).

Rat hearts are popular choices for use in many cardiac related studies due to their physiological relevance to the human heart function, their relatively small handling sizes and availability (De Young *et al.*, 1989). However, the rat atrial and ventricular cell morphologies are different to that of the human myocytes. Rat atrial cells in particular usually have a narrow worm-like shape with tapered ends (Figure 1.5) which is very different from that seen in humans which have a rod shape.

Figure 1.5 An isolated rat atrial myocyte. The atrial myocyte photomicrograph taken with an objective magnification of 20 x and a calibration bar indicating 20 μm, has the expected smooth tapered end morphology. Courtesy of Sam *et al.*, 2009.

Isolated human atrial cells are larger and have a rod-shaped morphology (Figure 1.6) (Bustamante *et al.*, 1982). Previously it has been shown that rat ventricular cells (Figure 1.7) are noticeably wider than the rat atrial cells and have a rod-shaped morphology (Kirk *et al.*, 2003 ; Smyrnias *et al.*, 2010). Hence, the rat ventricular cell is similar to the shape of the human atrial cell (Bustamante *et al.*, 1982). Despite the differences in morphology, both human and rat atrial myocytes can demonstrate arrhythmic events.

Figure 1.6 An isolated human atrial myocyte. The calibration bar indicates 20 μm. The human atrial cell has a long straight-edged body and has a rod-shape morphology. Courtesy of Bustamante *et al.*, 1982.

Figure 1.7 An isolated rat ventricular myocyte. The photomicrograph depicts a calibration bar of 50 μm. The characteristically rod-shaped rat ventricular cell is similar in morphology to the human atrial cell but completely different to the rat atrial cell. Courtesy of Freestone *et al.*, 2000.

1.6.2 Structure and function of t-tubules

T-tubules are intricate intracellular invaginations of the sarcolemmal membrane (Lipp *et al.*, 1995 ; Brette and Orchard, 2003 ; Kirk *et al.*, 2003 ; Smyrnias *et al.*, 2010) found in ventricular cells and some mammalian atrial cells (Dibb *et al.*, 2009 ; Richards *et al.*, 2011). T-tubules serve to propagate a depolarising action potential throughout the myocytes to enable the co-ordinated and simultaneous release of calcium to be discharged from the SR (Cheng *et al.*, 1994 ; Song *et al.*, 2000 ; Brette and Orchard, 2003 ; Brette and Orchard, 2007 ; Kirk *et al.*, 2003 ; Smyrnias *et al.*, 2010).

T-tubules are normally non-existent at birth but they soon start to develop rapidly in number and structure (Chen *et al.*, 1995). In situations where there are ailments of the heart or through ageing, t-tubules begin to deplete considerably (Smyrnias *et al.*, 2010). T-tubules can be studied once the

cardiomyocytes are isolated and stained with a suitable probe such as di-8ANEPPS, a fluorescent dye which detects differences in membrane potential. The dye only becomes activated and fluoresces upon binding to the lipophillic membranes of the cell and observed under a laser scanning confocal microscope.

The t-tubules of the rat ventricular cells are normally about 200 nm in length and are apparent regularly at every 1.8 μm along the myocyte (Soeller and Cannell, 1999). In atrial cells derived from small mammals however, there are significant variations concerning this ultrastructural detail. It has been reported that rat atrial cells do not have an organised t-tubule system unlike for the ventricular cells (Mackenzie *et al.*, 2001 ; Orchard and Brette, 2008 ; Walden *et al.*, 2009 ; Richards *et al.*, 2011 ; Orchard *et al.*, 2013). Other groups have reported that the atrial cells have a similar network of t-tubules which are however not fully developed and they lack the organisation observed in ventricular cells and may be orientated transversely (Leeson *et al.*, 1980 ; Tidball *et al.*, 1991). In other studies, the tubular network of the atrial cells has often been reported as being disorganised in both longitudinal and transverse manner (Soeller and Cannell, 1999 ; Kirk *et al.*, 2003). This rudimentary network of atrial tubules, similar to those in ventricular cells has been named the Transverse Axial Tubular System (TATS) (Kirk *et al.*, 2003). The functional characteristics of TATS are similar to ventricular t-tubules, yet their existence in atrial cells is thought to be dependent upon the morphology of these cardiomyocytes.

As discussed previously, atrial cells are narrower than the ventricular cells and so therefore there is a smaller distance for the released calcium load to travel to activate contraction (Dobrev *et al.*, 2009). In rats, wider atrial myocytes (>20 μm in width) were reported to have more TATS than narrower atrial myocytes (Kirk *et al.*, 2003 ; Smyrnias *et al.*, 2010) possibly facilitating the EC coupling process in these wider cells (Dobrev *et al.*, 2009). Upon contraction, left atrial myocytes provide higher pressures than the right atrial myocytes and thus may have adapted to be wider (Kirk *et al.*, 2003). There is also considerably more heterogeneity in the morphology of atrial cells than for ventricular cells. For example, horse atrial cell widths were considerably larger than those for cows and sheep, but there were no significant variations in ventricular cell widths between the different mammals investigated (Richards *et al.*, 2011).

In atrial cells with TATS (more often found in the left atrium), fundamental units of calcium release events observed by augmentation of fluorescence under the confocal microscope (calcium sparks) were shown to be initiated more frequently from groups of cardiac RyR on the cell periphery but also with some occasional initiations from the cell interior (Hüser *et al.*, 1996 ; Kirk *et al.*, 2003 ; Smyrnias *et al.*, 2010). The relationship between the existence of t-tubules and the occurrence (and location of initiation) of calcium sparks has been studied by co-labelling the single atrial cells with both di-8ANEPPS and fluo-4AM (Smyrnias *et al.*, 2010). In wider atrial cells, more calcium sparks occurred originating from the centre of the cell but in narrower atrial cells where there are no TATS, calcium sparks were mainly restricted to the cell periphery. When line-scanned under the confocal microscope the wider atrial cell is seen to produce calcium waves with a "W" shape (Kirk *et al.*, 2003) and progressively

the waves propagate through the cell in this manner (Hüser *et al.*, 1996 ; Mackenzie *et al.*, 2001 ; Kirk *et al.*, 2003 ; Smyrnias *et al.*, 2010). However, in narrower atrial cells, where TATS are less likely to occur, a "U" shaped calcium wave is produced (Kirk *et al.*, 2003 ; Freestone *et al.*, 2007). This is due to calcium sparks being triggered on the periphery of thinner cells and these sparks tend to be notably bigger and have a longer duration before progressing as a propagated wave across the cell in a "U" shape (Woo *et al.*, 2003).

Recently, it has been suggested that the size of atrial cells, and hence the probability of the presence of a t-tubule network may be dependent upon the animal size (Dibb *et al.*, 2009 ; Richards *et al.*, 2011). Hüser *et al.*, (1999) studied atrial cells from a small mammal (cat) stained with di-8ANEPPS and suggested that the t-tubule system does not exist in these cells. In larger mammals such as sheep, the isolated atrial cells show evidence of having many more t-tubules structures, though they are still less in numbers than those in the corresponding ventricles (Dibb *et al.*, 2009). The t-tubular structures existing in these larger mammalian atrial cells such as in horse atrial cells were observed by incubating the cells in wheat germ agglutinin (WGA) (Figure 1.8) (Richards *et al.*, 2011). WGA is commonly used in conjunction with a fluorescent conjugate and it selectively binds to N-acetyl-D-glucosamine and sialic acid residues which are found on intracellular cell surfaces such as t-tubules (Savio-Galimberti *et al.*, 2008).

Figure 1.8 Horse right atrial myocyte t-tubule network. The calibration bar depicts 10 μm. A network of t-tubules is clearly shown in isolated horse right atrial cells incubated with wheat germ agglutinin (WGA), which have a rod-shaped morphology, a shape similar to the ventricular cell of a rat. Courtesy of Richards *et al.*, 2011

1.6.3 Pathophysiology of t-tubules

T-tubules carry depolarisation deep within the cell which results in cardiomyocyte contraction but in the pathological state t-tubules may become damaged. The symptomatic stage of hypertension in humans is rather challenging to work on experimentally hence the SHRs are commonly used for such studies as they provide an experimental model of hypertensive heart disease leading to HF. The SHRs still retain t-tubules even though the cardiomyocytes may not be in a healthy condition. Despite this, EC coupling still occurs in these SHR cardiomyocytes (Fowler *et al.*, 2007). It has been suggested that SHR rats of 6 months have already developed signs of hypertrophy such as increased heart mass and increased systolic blood pressure (Bell *et al.*, 2004). Temporal features such as the dimensions of the SHR ventricular myocytes by this stage differs to the normotensive Wistar-Kyoto (WKY) counterparts, whereby both the ventricular cell width and cell lengths are larger than for WKY rats (Bell *et al.*, 2004).

Ageing and any underlying cardiac diseases are factors which will cause a depletion of t-tubules in cardiomyocytes and interrupt the EC coupling process (Smyrnias *et al.*, 2010). To study this effect, rat ventricular myocytes were detubulated chemically by formamide to re-enact the situation of the deletion of t-tubules (Smyrnias *et al.*, (2010). The same group went on to show that di8-ANEPPS stained rat atrial cells showed similar fluorescence intensity as for ventricular cells which have been artificially detubulated (Smyrnias *et al.*, 2010). The detubulated rat ventricular cells showed similar patterns in whole cell calcium waves as for atrial cells, both forming "U" shape calcium waves propagating through the cell which is normally characteristic of the narrower atrial cells.

1.7 Expression of calcium handling proteins

Cardiac phosphoproteins in the heart, such as phospholamban (PLB), phosphorylated versions of PLB (phospho Ser-16 and phospho Thr-17), sarco(endo)plasmic reticulum calcium ATP-ase (SERCA2a), cardiac RyR2 and its phosphorylated proteins (RyR2 phospho-Ser2808, RyR2 phospho-Ser2814 and RyR2 phospho-Ser2030), calsequestrin (CSQ) and calreticulin (Figure 1.9) regulate and maintain the normal function of the heart.

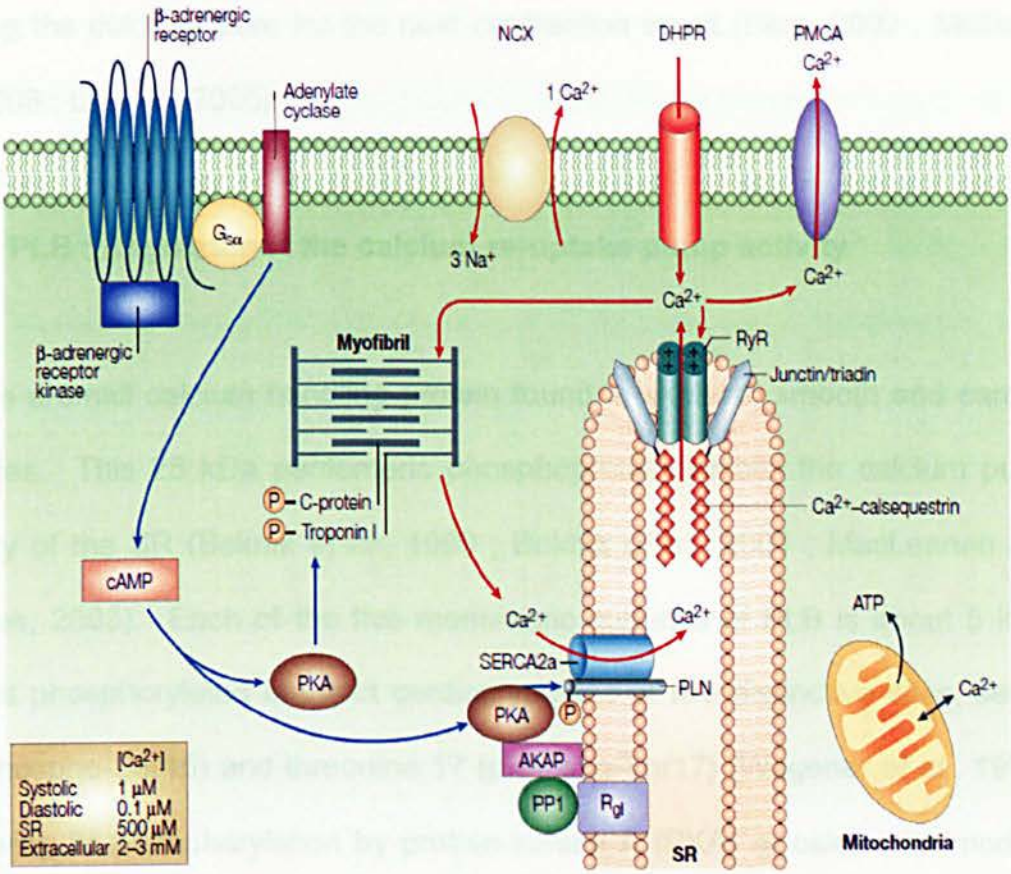

Figure 1.9 Calcium handling protein signalling pathways. The pathways show how the levels of the intracellular second messengers-cyclic adenosine monophosphate (cAMP) in blue arrows and calcium in red arrows play a role in triggering the actions of phospholamban (PLN also known as PLB) and sarco(endo)plasmic reticulum 2-ATPase (SERCA2a) respectively on the sarcoplasmic reticulum (SERCA2a). Other acronyms include ryanodine receptor (RyR2), protein kinase (PKA), protein phosphatase 1 (PP1) and adenosine triphosphate (ATP). Courtesy of MacLennan and Kranias, 2003.

1.7.1 SERCA2a : Cardiac calcium pump of the SR

Depolarisation of cardiac cells causes calcium release from the intracellular calcium store, the SR. The resulting transient elevation in intracellular calcium concentration enables cardiac contraction to occur. SERCA2a is a 100 kDa cardiac isoform forming the SR calcium pump (Hasenfuss *et al.*, 1997). It

allows cardiac relaxation to occur when it pumps calcium back into the SR thus refilling the calcium store for the next contraction event (Bers, 2002 ; Müller *et al.*, 2003 ; Li *et al.*, 2005).

1.7.2 PLB : Regulator of the calcium re-uptake pump activity

PLB is a small calcium handling protein found in skeletal, smooth and cardiac muscles. This 25 kDa pentameric phosphoprotein inhibits the calcium pump activity of the SR (Bokník *et al.*, 1999 ; Bokník *et al.*, 2001 ; MacLennan and Kranias, 2003). Each of the five monomeric subunits of PLB is about 5 kDa. PLB is phosphorylated in intact cardiomyocytes at two distinctive sites, serine 16 (phospho-Ser16) and threonine 17 (phospho-Thr17) (Wegener *et al.*, 1989). Following its phosphorylation by protein kinase A (PKA) or calcium/calmodulin dependent protein kinase 2 (CaM Kinase II) via the β-adrenergic receptor pathway (MacLennan and Kranias, 2003), the inhibition of SERCA2a activity is then reversed. When the calcium pump is active, the calcium content of the SR is increased and cardiac relaxation is hastened (Goldman *et al.*, 1984 ; Solaro *et al.*, 1998 ; Bokník *et al.*, 2001 ; Kaasik *et al.*, 2001 ; Bers, 2002). When PLB becomes dephosphorylated by protein phosphatase 1 (PP1), the activity of SERCA2a pump is again inhibited (Hasenfuss *et al.*, 1997 ; MacLennan and Kranias, 2003). If calcium re-uptake into the SR increases, this results in more calcium being released at the next contraction cycle and this in turn leads to positive inotropy of the whole heart and an increase in cardiac output (Simmerman *et al.*, 1998).

1.7.3 RyR2 : Calcium release channel of the SR

The intracellular calcium release channel on the SR membrane is known as the RyR and it was initially mentioned in cardiac muscles by Nakai and colleagues in 1990. RyRs are usually found close to the surfaces of sarcolemma especially at the t-tubules (Franzini-Armstrong *et al.*, 1999). The cardiac isoform of RyR known as RyR2 exists as a homotetramer unit of about 565 kDa, consisting of four RyR2 monomers (Kushnir and Marks, 2010). RyR2 is activated by the inward flow of calcium into the cell during EC coupling (Hasenfuss *et al.*, 1997 ; Lanner *et al.*, 2010). β-stimulation then increases the L-type calcium current which increases SR calcium release via the RyR2 (Eschenhagen, 2010).

1.7.4 Other calcium handling proteins

Other less major cardiac calcium handling proteins exist and may be relevant to this work. CSQ is a 44 kDa calcium binding protein attached hydrophobically on the inside of the SR and aids the regulation of EC coupling of the cardiomyocytes (MacLennan and Wong, 1971) by managing the release of calcium through the RyR2 (Chopra and Knollmann, 2009). Calreticulin is a 46 kDa protein, first reported by Ostwald and MacLennan, 1974. It is located on the interior surface of the SR which contributes to the healthy early development of the human heart (Gelebart *et al*, 2005). It is normally highly expressed in the human embryonic heart, however after birth, the level decreases naturally (Nakamura *et al.*, 2001 ; Gelebart *et al.*, 2005). Calreticulin at this repressed level helps the folding of new developing proteins and glycoproteins and regulating the binding and storage of calcium for intracellular

calcium events (Michalak *et al.,* 1999 ; Gelebart *et al.*, 2005). Abnormal increases in calreticulin levels in the adult human heart are associated with development of congenital arrhythmias and heart block (Nakamura *et al.*, 2001).

The expressed abundances of the major cardiac proteins and their phosphorylation states involved in calcium handling ; for example PLB and SERCA2a in mammalian atrial cells may differ significantly to calcium handling in mammalian ventricular cells and be related to the different functions carried out by the various cardiac chambers.

1.7.5 Pathophysiology of calcium handling proteins

Calcium handling proteins which are altered or abnormally distributed were often found to be those involved in the elimination of calcium from the cytosol (Hasenfuss *et al.*, 1997). The resulting mishandling of calcium in the cardiomyocytes may underlie the pathophysiology of several cardiac disease states, such as cardiac hypertrophy, arrhythmias and HF (Hasenfuss *et al.*, 1997 ; Kubo *et al.*, 2001).

In experimental studies of systemic hypertension, the SHR and its normotensive control, the WKY strains are used. On the other hand, a volume-induced overload model of HF (Scheuermann-Freestone *et al.*, 2001) in rats can be used as a means to study the effects of heart failure on calcium handling proteins and CICR.

During HF, there is impairment to the intracellular calcium uptake into the SR which therefore leads to an upset in normal calcium handling. It has been found in the human heart in terms of calcium handling proteins that there are no changes in the abundances of PLB protein upon the onset of HF however there is a decrease in SERCA2a activity levels (Schwinger *et al.*, 1995 ; Kubo *et al.*, 2001). On the other hand, MacDonnell and colleagues (2005) have shown in left ventricular tissue of female rats that the levels of PLB and SERCA2a remained the same, both in normotensive and hypertensive animals.

The release of calcium from the SR is enhanced when stimulants of the β-adrenoceptor (β-AR), adrenaline and noradrenaline, bind to trigger the phosphorylation of the Ser-2808 site on the RyR2 (Eschenhagen, 2010). However, during HF, RyR2 becomes continuously phosphorylated or hyperphosphorylated by PKA at the Ser-2808 site of RyR2 (Marks *et al.*, 2002 ; Wehrens *et al.*, 2005 ; Wehrens *et al.*, 2006 ; Shan *et al.*, 2010 ; Eschenhagen, 2010 ; Bers, 2012 ; Zhang *et al.*, 2012). These calcium channels are therefore not able to regulate the calcium efflux from the calcium store normally resulting in a depletion of calcium in the SR. Less calcium in the SR means a decrease in inotropy, and hence less blood being pumped out of the heart.

1.8 β-signalling pathways

1.8.1 β1/β2-ARs

Initially, β-ARs were classified into two subtypes called β1-ARs and β2-ARs (Lands *et al.*, 1967). It has been suggested since that there are four β-ARs subtypes in the human heart (Kaumann and Molenaar, 1997). These subtypes

are namely, a low affinity β1 ($\beta1_L$-AR), a high affinity β1 ($\beta1_H$-AR), the β2 and β3-ARs, and each regulates the heart in different ways depending on the subtypes' specific signalling pathway (Kaumann and Molenaar, 1997). β-ARs are responsible for connecting the sympathetic nervous system and the cardiovascular system mediated by the endogenous catecholamines, adrenaline and noradrenaline (Zheng *et al.*, 2005).

The stimulation of the β1-AR active site by specific agonists triggers the Gs-protein signalling pathway, whereby adenylate cyclase (AC) is activated leading to an increase in the levels of cAMP and stimulation of PKA activity (Zhu *et al.*, 2005). This results in positive inotropic, chronotropic and lusitropic responses.

In humans, β2-ARs are found in smooth, cardiac and skeletal muscles, as well as the bronchial, genitourinary and vascular areas of the body. The β-AR signalling pathway is linked to both Gs and Gi proteins (Xiao *et al.*, 2004). Upon stimulation of the β2-AR, the Gs pathway results in positive inotropy and chronotropy. However, the persistent stimulation of the β2-AR will trigger a switch from Gs protein coupling to a Gi pathway whereby phosphoinositide 3-kinase (PI3K) will be activated and this leads to negative inotropy (Chen-Izu *et al.*, 2000 ; Xiao *et al.*, 2004). Upon stimulation of the Gi sub-unit, nitric oxide (NO) is produced by endothelial nitric oxide synthase (eNOS). The production of NO activates guanylate cyclase (GC) which catalyses the production of cyclic guanosine monophosphate (cGMP). An increase in cGMP levels activates protein kinase G (PKG) and calcium entry via the LTCC is inhibited hence causing cardioinhibitory effects. Triggering the Gi signalling pathway has also shown evidence of being a cardioprotective mechanism, whereby apoptosis of

cardiomyocytes is avoided in HF (Bernstein *et al.*, 2005). It has been shown that β2-ARs are up-regulated during HF to protect the heart from excess catecholamines (Moniotte *et al.*, 2001).

1.8.2 β3-ARs

A third cardiac β-AR was reported in ventricular cells from a number of species including humans (Gauthier *et al.*, 1998). β3-ARs produce a negative chronotropic and inotropic effect promoted by β3 specific agonists and are usually coupled to Gi proteins in the human heart (Gauthier *et al.*, 1996).

1.8.3 Designation of the novel propranolol-insensitive and pro-arrhythmic $\beta1_L$-ARS

One of the most important treatments for HF and arrhythmias is a class of drugs known as the β-blockers. β-blockers were initially introduced in the 1960s by Sir James Black at the Imperial Chemical Industries (ICI) (Black *et al.*, 1995) and this success triggered a surge of interest in this set of drugs. β-blockers inhibit the ability of catecholamines to bind to their receptors hence inhibiting cardiac stimulation. However, a specific sub-class of these β-blocking drugs was discovered not to block cardiostimulation but instead to cause stimulation. These drugs were designated as non-conventional partial agonists and they have been discovered to work upon a specific β receptor variant, known as the $\beta1_L$-AR previously known as the putative β4-AR (Kaumann *et al.*, 1998 ; Kaumann and Molenaar, 2008). An example of a non-conventional partial agonist is pindolol which was studied in an investigation by Podrid and Lown

(1982). Pindolol has since been contra-indicated as a result of the sympathomimetic activity observed in the treatment of ischaemic HF (Podrid and Lown, 1982). Freestone and colleagues (1999) have shown that the non-conventional partial agonist, CGP12177, which is structurally similar to pindolol, is 40 times more potent than isoprenaline (ISO) (a potent synthetic analogue of adrenaline and noradrenaline) in causing arrhythmias in electrically paced mouse ventricular myocytes. A study carried out by Kaumann and Lynham (1997) in WKY rats, showed that CGP12177 mobilised less cAMP and PKA via the β-AR signalling pathway than ISO. Furthermore, in a study carried out by Lowe (1998), in ferret ventricle, CGP12177 caused an increase in the plateau phase of the action potential however the duration of the action potential was shortened more abruptly compared to noradrenaline stimulating the conventional β1-ARs. CGP12177 also caused cardiostimulatory and arrhythmic effects in rat ventricular and atrial myocytes (Sarsero *et al.*, 1999).

Propranolol, a β-blocker was unsuccessful in hindering the stimulatory effects of CGP12177 though another β-blocker known as bupranolol has been shown to be moderately effective in blocking the pro-arrhythmic activity (Lowe *et al.*, 1998). This has led to the designation of a new receptor variant – β_{1L}-AR. However, the mechanism for the arrhythmogenic effects mediated by this receptor is currently unknown.

1.9 Objectives of the thesis

The objectives of this thesis will focus upon studying the physiology and pathophysiology of the rat atrial myocyte and pharmacological studies of the propranolol-insensitive low affinity β-AR in relation to atrial arrhythmias.

Chapter 3 : Pharmacological studies of β-AR cardio-active drugs in embryonic chick ventricular myocytes will seek to confirm the presence of the four β-AR subtypes and the combinations of drugs required to individually characterise these receptors.

Chapter 4 : The morphology and dimensions of isolated left and right rat atrial myocytes and how these features relate to the occurrence of the t-tubular network and its relation to EC coupling in these cells will be studied.

Chapter 5 : Calcium handling proteins that contribute to the functioning of the EC coupling processes will be studied. Particular focus will be upon the differences and quantification of calcium handling protein abundances and degree of phosphorylation in left and right chambers of the rat atrial and ventricular myocytes in healthy and pathological conditions.

Chapter 6 : Spontaneous calcium release events resulting from calcium handling in quiescent rat atrial myocytes under various perfusate conditions will be studied for pro-arrhythmogenicity or inhibition of SR calcium release activity. This would hopefully contribute to a better understanding of the specific alterations at the cellular level in atrial myocytes during arrhythmias and HF.

CHAPTER 2

General Methods

2.0 General Methods

2.1 Materials

2.1.1 General reagents

All chemicals including Foetal Bovine Serum (FBS) (Gibco), Bovine Serum Albumin (BSA), penicillin, streptomycin and amphotericin B solution and trypan blue were purchased from Sigma Aldrich Company Ltd with the following exceptions : sodium chloride, M199 cell culture media and Dulbecco's phosphate buffered saline (DPBS) (without calcium and magnesium) which were from Fisher Scientific UK Ltd. Trypsin extracted from bovine pancreas and Type II collagenase enzyme (both Worthington) were obtained from Lorne Laboratories. Pluronic F-127 solution, di-8ANEPPS and fluo-4AM (all Invitrogen) were obtained from Fisher Scientific Ltd whilst sodium orthovanadate was purchased from Sigma Aldrich Company Ltd. Protease inhibitor cocktail tablets for the lysis buffer were obtained from Roche Products, Ltd. All blue standard marker was purchased from BioRad Laboratories Inc.

2.1.2 General instruments and equipments

Instruments and equipment for western immunoblotting were purchased from BioRad Laboratories Inc. Quantification of the protein of interest was carried out using a densitometer (BioRad G-800) and QuantityOne software which was also obtained from BioRad Laboratories, Inc. Glassware for the Langendorff perfusion system set-up was purchased from Fisher Scientific Ltd, with bespoke additions obtained from the glass blowing workshop at Kingston University. The perfusion pump and the platinum cured silicone tubings were obtained from Watson-Marlow Pump Group. Pure oxygen medical gas (100% O_2) was obtained from St George's Hospital. The Axiovert 100M or Axiovert 200M inverted microscopes attached to LSM 510M laser scanning units, as well as the LSM 510M software were from Carl Zeiss, Oberkochen, Germany. The 488 nm argon laser was from Laser-Fertigung Hamburg, Germany.

2.1.3 Drugs

All drugs for the chick embryonic cardiac cell culture study and calcium imaging study in rat atrial cells were purchased from Tocris Bioscience. Bupranolol was a kind gift from Professor Kiec-Kononowicz (Poland) and ruthenium red was purchased from Abcam plc.

2.2 Embryonic chick cardiac cell culture

Under aseptic conditions, chick embryonic ventricular cells were isolated and cultured according to the methods of DeHaan (1967) and Rabkin and Sunga (1987) with slight modifications. In brief, white chick eggs (53 g - 63 g) were incubated in an automatic egg incubator (Maino MPS 24 and Brinsea Octagon 10) for 7 - 8 days at 37.8°C and 87% humidity. Chick hearts were isolated under sterile conditions from the embryos. Using a standard laboratory dissecting microscope, ventricular tissues were separated from the atria and minced using single edged razor blades in DPBS solution. The tissue was digested by a series of 5 min digestion periods at 37°C, in 0.05% w/v trypsin. The tissue digests were then bathed in a growth media solution made up of 90% v/v M199 solution, 10% w/v FBS and 0.1% v/v antibiotic/antimycotic solution of penicillin, streptomycin and amphotericin B.

Cells obtained by this enzymatic digestion were then spun at 216 rpm for 5 mins in a standard laboratory centrifuge. Cell pellets were collected and diluted in the growth media solution. Cell number and therefore the volume of cell-containing media to be plated was determined by mixing the cell suspension and trypan blue in a 1:1 ratio and using a haemocytometer (Neubauer chamber) under the light microscope. Cells were plated ($3x10^5$ - $9x10^5$ cells/ml) to be maintained in a sterile incubator (37.5°C and 95% O_2 and 5% CO_2) for 48 hrs to allow for cell proliferation and initiation of spontaneous contractile activity prior to drug exposure.

2.2.1 Basal beating rate studies

Cultured chick embryonic ventricular cells were aseptically replenished with fresh pre-warmed growth media after 48 hrs incubation. Culture plates containing the cultured ventricular cells were placed on a heated microscope stage 37°C for 5 mins. The spontaneous basal beating rates of the chick cardiomyocytes were studied using the Leica Application Suite V3.2.0 application. The contraction rate was recorded for 20 s.

2.2.2 Pharmacological classification of β-ARs in chick embryonic ventricular cells

Upon the consistent beating of the cultured cells, the following cardioactive agents (Table 2.1) were aseptically introduced to the single wells ; ISO (100 nM), propranolol (200 nM), CGP12177 (1 μM) and propranolol (200 nM) and BRL37344 (300 nM and 600 nM).

Table 2.1 List of drug experiments for study of β-ARs on chick embryonic ventricular myocytes in culture. Basal counts were carried out prior to drug additions. The drug agents were cardiostimulatory, eg. ISO, or cardioinhibitory eg. BRL37344 and were added to cell media of proliferated chick cardiomyocytes and allowed to equilibrate for 10 mins before beating rates were taken under the microscope.

β-AR agents	Concentration (M)
ISO	100 nM
Propranolol	200 nM
CGP12177 + propranolol	1 μM and 200 nM respectively
BRL37344	300 nM, 600 nM

2.3 Rat atrial and ventricular cell isolation

2.3.1 Animals

Adult (8 - 10 weeks old) WKY, Sprague-Dawley (SD) and SHR rats (250 - 350 g) from Charles River, UK were used. Animals were maintained at the Biological Research Facilities (BRF), St Georges Hospital, UK, in a specialised environment, fed daily on rat chow and water *ad libitum*. Male rats were initially sacrificed by stunning followed by cervical dislocation in accordance to the guidelines of Schedule 1 of the Animal (Scientific Procedures) Act 1986. For the majority of the studies, rats were deeply anaesthetised i.p by a single dose (40 mg/ml per 250 g body weight) sodium pentobarbital before being dissected to remove the heart also in accordance to the guidelines of Schedule 1 of the Animal (Scientific Procedures) Act 1986.

2.3.2 Enzymatic dissociation of cardiac myocytes: Langendorff method

Male WKY rats were sacrificed as previously described and the diaphragm was cut open via an abdominal thorax intersection. The whole heart including a generous section of the aorta was dissected out and bathed immediately in cold (4°C) Tyrode's solution composed of (mM); 130 NaCl, 5.4 KCl, 1.4 $MgCl_26H_2O$, 0.4 $NaH_2PO_4H_2O$, 10 glucose 4.2 HEPES, 20 taurine, 10 creatine, 0.5 $CaCl_2$, pH 7.3 (NaOH). Glucose was added and the pH of the Tyrode's solution was adjusted accordingly on the day of experiment. Fat and extra tissue was dissected off and a mixture of heparin (12.5% v/v) and Tyrode's solution was flushed into the heart using a small needle syringe via the aorta in an attempt to prevent blood clots. The heart was then suspended immediately onto the cannula of the Langendorff apparatus (Figure 2.1). Initially, the isolated heart was perfused with Tyrode's solution (0.5 mM calcium) at a flow rate of 10 ml/min and the heart was observed to be beating vigorously and ejecting blood. Once the medium collecting in the reservoir ran clear, the second perfusate (calcium free) with EGTA (100 µM) was switched to run for 6 mins. Once the heart ceased to beat, the third perfusate consisting of calcium-free Tyrode's solution with collagenase (1 mg/ml) was allowed to run for 10mins. All buffers in the Langendorff apparatus were gassed continuously with 100% O_2 medical gas and maintained at 37°C and only the collagenase perfusate was re-circulated.

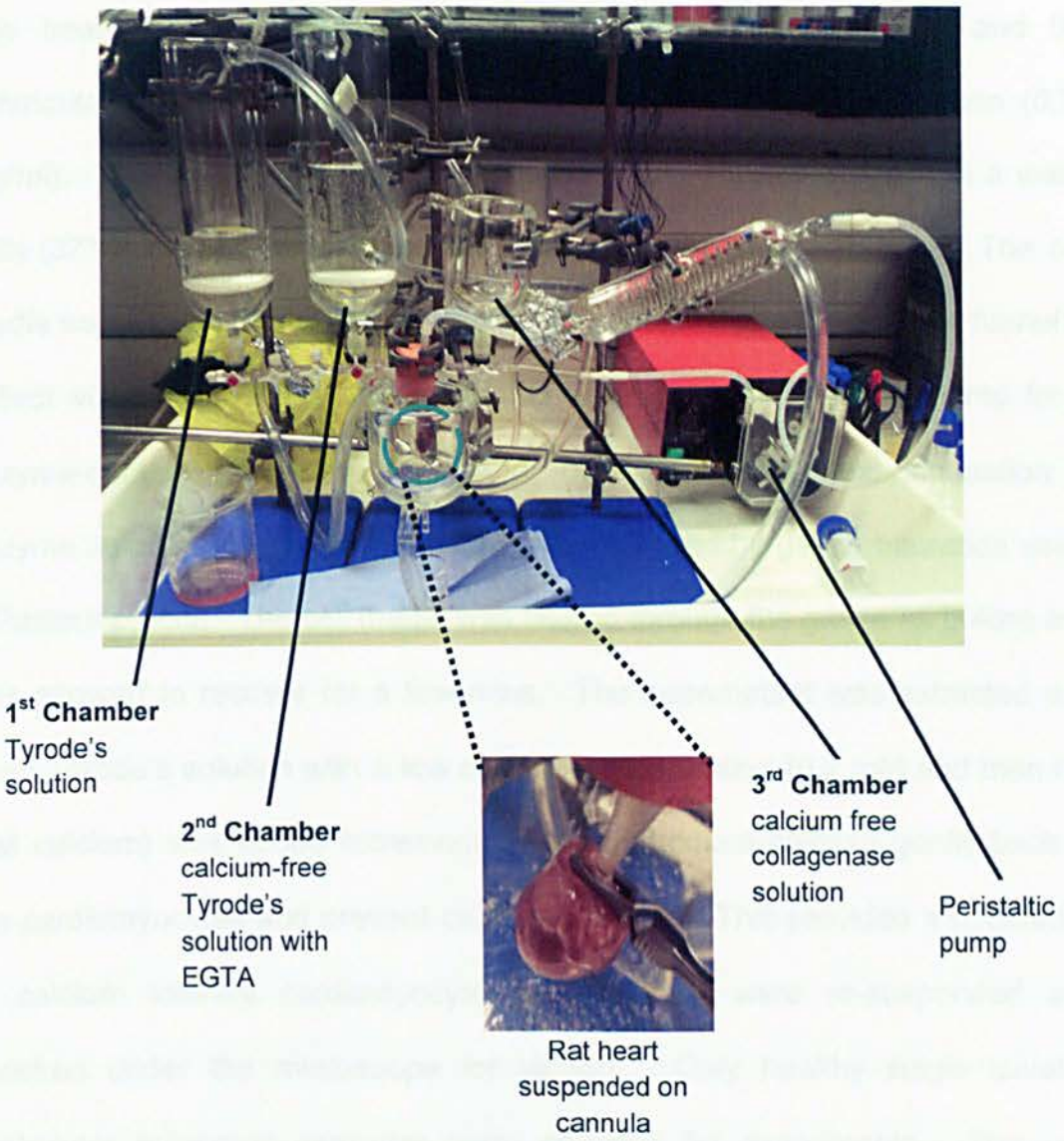

Figure 2.1 Langendorff apparatus. Perfusion of warm Tyrode's solution (0.5 mM calcium) maintains a rhythmic contraction of the rat heart before becoming static due to the subsequent perfusion of EGTA. Final perfusate includes the enzyme collagenase for tissue digestion.

2.3.2.1 Ventricular cell isolation

The heart was then removed from the Langendorff apparatus and the ventricular tissue was minced up in fresh warm collagenase solution (0.75 mg/ml). The tissue was manually agitated in the enzyme solution in a water bath (37°C) whilst being gassed with 95% O_2 : 5% CO_2 for 5 mins. The cell media was filtered through nylon gauze (250 μm pore size) in a plastic funnel to collect viable cells whilst the remaining tissue was scraped back into fresh enzyme-containing solution for further digestion. The next incubation in enzyme solution (1 mg/ml) was for 25 mins followed by gentle trituration using a Pasteur pipette. The cell media was filtered through the gauze as before and was allowed to recover for a few mins. The supernatant was extracted and fresh Tyrode's solution with a low calcium concentration (0.2 mM and then 0.5 mM calcium) was added incrementally to re-introduce calcium gently back to the cardiomyocytes and prevent calcium overload. This provided a population of calcium tolerant cardiomyocyte pellets which were re-suspended and checked under the microscope for viability. Only healthy single isolated ventricular quiescent myocytes were selected for experiments. The cell-containing media was then transferred to eppendorf tubes for use in subsequent experiments.

2.3.2.2 Atrial cell isolation

The steps for atrial cell isolation differed slightly from that of the ventricular cell isolation. Following the Langendorff perfusion of the heart, the left and right atria were microdissected immediately and bathed in some enzyme perfusate (0.75 mg/ml). The left and right atria were minced up using sharp single edge razor blades and placed into separate boiling tubes for incubation and manual agitation in the water bath (37°C). Agitation in enzyme solution was carried out three times, each session lasting 15 mins. Each time, the supernatant was collected and fresh enzyme-containing solution added to the remaining tissue in the boiling tubes and cell pellet was re-suspended. In the final session, the tissue was gently triturated. The cells were allowed to rest in Tyrode's solution (0.2 mM calcium then 0.5 mM calcium added incrementally) to prevent calcium overload and recover from the mechanical agitation. The cell media was then checked under the microscope for any viable cells. Viable cells are isolated single cells with a worm-shaped morphology and visible striations observed under the microscope. Cells with blebs or contracting erratically were excluded from the subsequent analyses. The media was then transferred to eppendorf tubes in preparation for experiments.

2.4 Confocal Microscopy

The confocal microscope is now an essential tool for studying and characterising the subcellular calcium signalling events on single isolated quiescent cells (Minsky, 1988 ; Bolton and Gordienko, 1998). Confocal, or "stationary spot" (Parker *et al.*, 1996) microscopy is a specific optical imaging technique in combination with fluorescence whereby the microscope utilises a narrow laser beam projected precisely onto a specific point of interest through an objective of high numerical aperture (NA) (Amos and White, 2003). The laser excites the fluorescence loaded in the cell of interest to a high energy state and when the energy is lost, light is emitted at lower energy to produce an image. A pinhole aperture on the microscope enables irrelevant light rays to be ignored and only illuminates onto a single point on the specimen of interest without sacrificing the light intensity (Minsky, 1988).

A laser scanning microscope (LSM) 510M version 2.01 (Carl Zeiss) of the confocal microscope was employed for all the experimental work involving cardiomyocyte morphological studies, t-tubule studies and calcium imaging. The SCsi interface of the confocal microscopes was hosted by a Pentium PC (32-bit Windows NT. 4.0 operating system) running the LSM 510M software. An argon laser light source of 488 nm (3%) was used as exciting light and 4.8 A tube current was selected. Low intensity laser excitation was used to prevent the risk of photobleaching. Plan-Neofluar x 20 / 0.5 Ph2 objectives, numerical aperture (NA) oil-immersion objective, long pass (LP) wavelength 505 nm and a pinhole size of 95 µm (to optimise signal quality of the images being captured) were selected for all studies.

The line-scan method which provides information only from a one-dimensional perspective (Lipp and Niggli, 1993) was run with the selected line on the cell specimen being scanned at every 2.09 ms for 20000 ms. In order to minimise any photobleaching or potential damage to the cell caused by the laser beam during line scanning, only a maximum of 3 line scan image videos were obtained from one particular section and none lasted for more than 20 s at any time.

The high spatial fast X-Y whole cell time series imaging was also used whereby the whole cell images produced are from repetitively scanning the specimen of interest multiple times in two dimensions. However the acquisition rate of the X-Y time series mode is theoretically not as fast as for the line-scan mode with a scan speed of 10, bi-directionally at 40 whole frame image scans s^{-1} and it also depends on the population of pixels in one image frame. The lowest possible X-Y frame pixel size (128) which maximises frame rate, minimises noise-signal disruptions and reduces photobleaching was used for time series and calcium spark images.

2.4.1 Incubation of fluo-4AM loaded cardiac cells

The high affinity calcium-sensitive fluorescein indicators such as fluo-3 or fluo-4, are favoured for use with the laser scanning confocal microscope to study calcium events in cardiomyocytes. Calcium fluorescent indicators are not lipophilic and hence are unable to enter the cell membrane. Therefore, calcium indicators are usually pre-combined with AM esters which act as protective groups rendering the fluorescent dye neutral to enable it to cross the lipid

membranes (Figure 2.2). Upon entering the cytoplasm, de-esterification occurs whereby the AM groups are digested by the intracellular esterases. This enables the trapped fluophore molecules to be excited by a blue excitation light (laser beam) and triggers emission of a green light which can be detected by the confocal microscope (Semwogerere and Weeks, 2005).

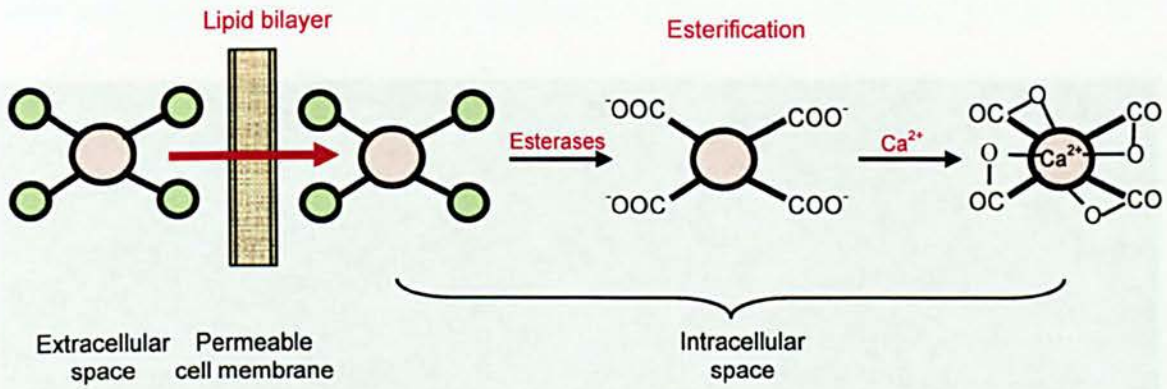

Figure 2.2 Fluo-4AM calcium indicator crosses lipid bilayer. The dye is excited by the laser and leads to the detection of calcium cytosolic events. The fluorescent dye molecule is shown in pink and the acetoxymethyl (AM) units which are eventually cleaved off upon entry into the intracellular space are shown in green.

The fluo-4AM dye is an AM ester dye used as an intracellular calcium indicator (Gee *et al.*, 2000). For this study, pluronic F-127 solution (2 µl) and fluo-4AM in dimethyl sulfoxide (DMSO) (1 mM, 5 µl) was added to a calcium-containing Tyrode's solution (0.5 mM calcium, 1 ml) in the dark, to make up fluo-4AM (4 µM) stock solution. The cell preparation was re-suspended and incubated in some fluo-4AM stock solution for 30 mins at room temperature (RT), away from any light source. The supernatant was extracted leaving the cardiac cell suspension behind in an eppendorf tube and was replaced with Tyrode's solution (1 mM calcium) to incubate at RT for 5 mins to allow for intracellular

de-esterification of the dye. The cells were then examined under the laser scanning confocal microscope using an Axiovert 100M or Axiovert 200M inverted microscope attached to LSM 510M laser scanning units. An increase in calcium intensity detected by fluorescence is able to be captured by the confocal microscope (Figure 2.3) and experiments were carried out accordingly.

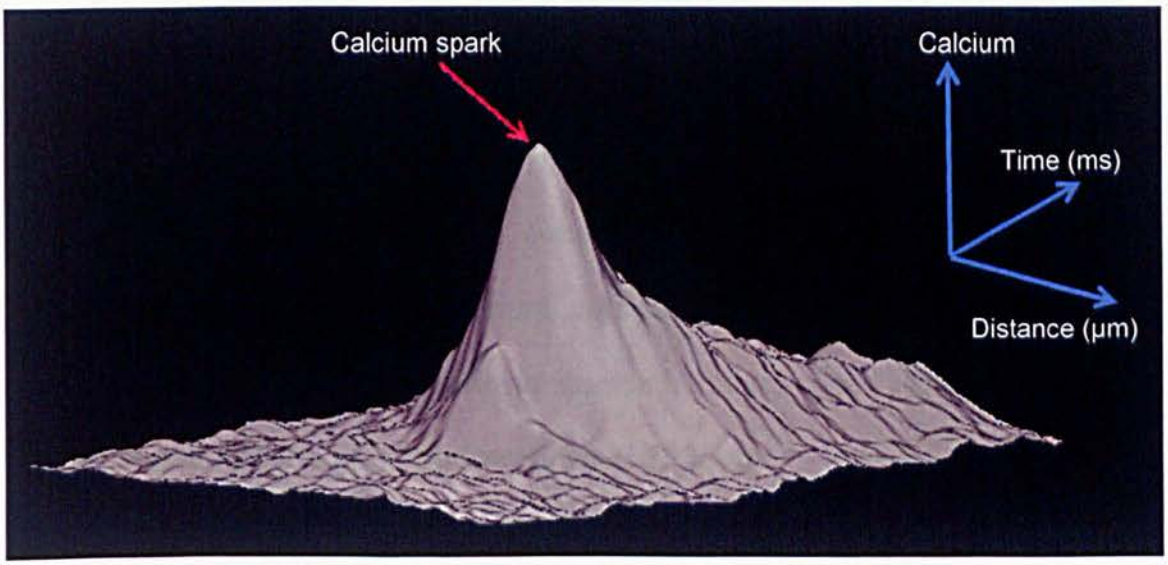

Figure 2.3 Histogram showing an example of calcium spark arising in time and space. The increase in calcium intensity in a cardiomyocyte is detected by calcium fluorescence under the confocal microscope.

2.4.2 Incubation of di-8ANEPPS loaded cardiac cells

Di-8ANEPPS is a membrane potential dye which is highly fluorescent upon excitation by a laser from the confocal microscope. It binds to membranes as it is very lipophilic. Di-8ANEPPS (5 mg) in pluronic F-127 solution (1 µl) was added to DMSO (4.2 ml) to make up the 2 mM di-8ANEPPS stock solution. This was aliquoted (10 µl) into eppendorf tubes for storage at -20°C. For immediate use, the stock solution of di-8ANEPPS (5 µl) was added to Tyrode's solution (0.5 mM calcium, 5 ml) to make up a final di-8ANEPPS solution (2 µM). This was then added to an aliquot of cells in an eppendorf tube and incubated at RT for 7 mins. The supernatant was then removed and fresh Tyrode's solution (0.5 mM calcium) was added and the cells were then inspected under the laser scanning confocal microscope. Di-8ANEPPS is excited at 498 nm and emits fluorescence at 713 nm.

2.5 Western Blotting

Western blotting was used to identify and quantify proteins from samples of tissue homogenates. Briefly, it involves gel electrophoresis whereby proteins of interest are separated according to their molecular weight (MW) and then transferred onto a suitable membrane and blocking non-specific protein binding before being detected by interactions between antibodies and the specific proteins in question. In this thesis, western blotting was carried out to determine the presence and to provide quantification of the following calcium

handling proteins ; total PLB, the phosphorylated versions of PLB - phospho-Thr17 and phospho-Ser16, SERCA2a, total RyR2 and the phosphorylated versions of RyR2, Ser-2808, Ser-2814 and Ser-2030. Anti-PLB was purchased from Merck Millipore. Phosphorylation specific antibodies of PLB, anti-phospho-Thr17 and anti-phospho-Ser16 and phosphorylation specific antibodies of RyR2 such as anti-phospho Ser-2808, anti-phospho Ser-2814, anti-phospho Ser-2030 were purchased from Badrilla Ltd. Anti-RyR2 was purchased from Abcam plc. Actin, α-actinin and glyceraldehyde 3-phosphate dehydrogenase (GAPDH) antibodies used as housekeeping proteins were obtained from Insight Biotechnology Ltd. Polyclonal IgG sheep anti-mouse horse radish peroxidase (HRP), polyclonal IgG donkey anti-goat HRP and IgG anti-rabbit HRP were obtained from GE Healthcare as was the enhanced chemilumiscence (ECL) analytical system for protein blot detection.

2.5.1 Preparation of cardiac homogenates

Upon cervical dislocation of WKY, SHR and HF-induced by volume-overload (shunt) and sham-operated (sham) rats, the hearts were quickly excised and the left and right atria and ventricles were micro-dissected. WKY and SHR adult male rats were from Charles River, UK and cardiac samples from shunt and sham-operated rats were kindly donated by Dr Aarne Feldheiser (Germany). Tissues were immediately immersed in ice cold (4°C) physiological solution composed of (mM); 120 NaCl, 5.4 KCl, 5 $MgSO_4 7H_2O$, 5 pyruvate Na, 20 glucose, 10 HEPES, 20 taurine, 5.5 NTA, 0.5 $CaCl_2$, pH 6.96 (HCl, NaOH). Left and right atrial and ventricular samples were immediately snap frozen in liquid nitrogen and stored at -80 °C.

Atrial and ventricular homogenates were prepared on dry ice. Frozen tissues were weighed before being manually homogenised using a hand held glass tissue grinder. Homogenisation was performed on ice in a lysing buffer composed of (mM); 0.5 NaCl, 0.5 NaF, 0.5 $Na_4P_2O_7$, 0.5 EDTA, 0.5 EGTA, Triton x 100 (1%), including one protease inhibitor cocktail tablet and sodium orthovanadate (50 µl), an inhibitor for protein phosphotyrosyl phosphatases (PTPs). Lysed tissue samples were centrifuged at 4°C, 15000 x g for 10 mins before adding the supernatant to β-mercaptoethanol and sodium dodecyl sulphate (SDS) containing sample buffer. SDS in the sample buffer encourages protein denaturation by taking the role of a surfactant, whilst β-mercaptoethanol acts as a mild reducing agent for cleaving disulfide bonds of proteins, hence disrupting their conformation.

2.5.2 Western blot of calcium handling proteins

Protein homogenates were boiled at 95°C for initial use and dry-heated to 37°C for subsequent uses. Polyacrylamide gel percentage depends on the protein of interest (Table 2.2) and once loaded, the proteins were separated according to their individual MW during gel electrophoresis at 200 V.

Table 2.2 Polyacrylamide gel percentage for various protein of interest : Cardiac RyR2 and phosphorylated RyR2s (4% gel), SERCA2a (6% gel) and PLB and the phosphorylated PLB (15% gel). The recipe makes up a total of 10 ml volume.

Reagent	Stacking Gel	4% Running Gel	9% Running Gel	15% Running Gel
4X Buffer	2.5 ml	2.5 ml	2.5 ml	2.5 ml
Acrylamide	1.16 ml	1.5 ml	3.0 ml	5.0 ml
10% APS	100 µl	100 µl	100 µl	100 µl
dd H2O	6.23 ml	5.89 ml	4.39 ml	2.39 ml
TEMED	10 µl	10 µl	10 µl	10 µl

The protein on the gel was then transferred to a membrane such as a nitrocellulose membrane (8.5 x 6.0 cm^2) following the method of Towbin *et al.*, (1979) or polyvinylidene fluoride (PVDF) membrane (8.5 x 6.0 cm^2). After protein transfer using semi-dry protein transfer unit (Figure 2.4) one of two blocking incubation processes were carried out either with 3% w/v BSA or with 5% w/v milk in 0.1% v/v Tween 20 buffer solution. The primary antibody, depending on the specific protein of interest, was incubated with the protein membrane overnight at 4°C. The membrane was incubated in the appropriate secondary antibody labelled by the highly specific HRP enzyme. The process was followed by ECL protein detection. Upon exposure to the substrate luminol from the ECL reagent, the HRP label on the secondary antibody is oxidised in the presence of hydrogen peroxide and light is produced. Briefly, when the western blot is exposed to an X-ray film, the light produced is captured and shows up on the film where the protein of interest has been attached by the HRP labelled antibody. This is represented on the X-ray film as a protein band which can be quantified using a densitometer (Biorad G-800) and analysed using QuantityOne software.

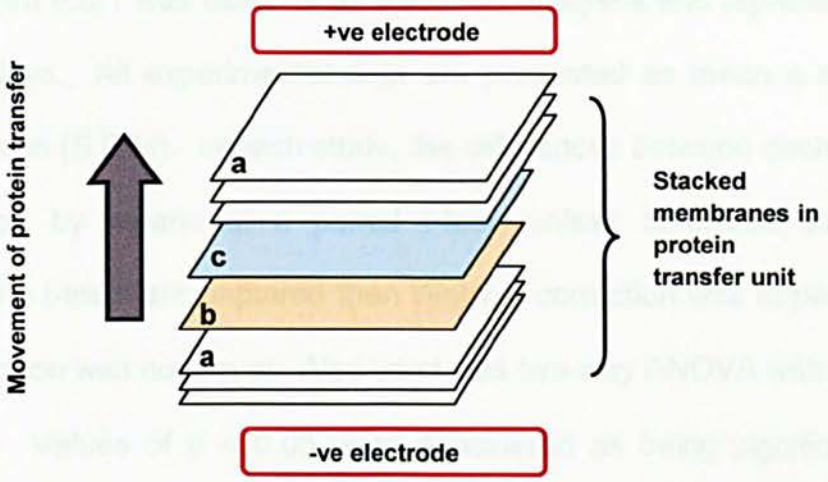

Figure 2.4 Western blotting semi-dry transfer unit. The layout of the transfer unit is such that the negatively charged proteins travel from the gel and onto the chosen blotting membrane (nitrocellulose or PVDF) towards the positive end of the unit. **(a)** stacking membrane in triplicate **(b)** gel **(c)** protein membrane.

2.5.3 PLB standards for the assessment of linearity

Pure PLB standard (50 µg/1000 µl) was loaded (10 µl) in increasing amounts in a polyacrylamide gel (15%) including 6 M urea. The protein samples were loaded and electrophoresed on an SDS-polyacrylamide gel electrophoresis (PAGE) gel at 200 V before being transferred to a PVDF membrane (8.5 x 6.0 cm^2). Following the semi-dry transfer of the proteins onto the PVDF membrane, the latter was immersed and incubated with a blocking solution of 5% w/v milk in 0.1% v/v Tween 20 buffer solution on a reciprocating shaker. The membrane was then incubated at 4°C overnight with a specifically labelled antibody for PLB (1 : 5000). The membrane was incubated in the appropriate secondary antibody labelled by the highly specific HRP enzyme. The process was followed by ECL protein detection.

2.6 Data analysis and statistics

GraphPad Prism 6.0.1 was used for all statistical analyses and representations of graph displays. All experimental data are presented as mean ± standard error of the mean (S.E.M). In each study, the differences between each subject were assessed by means of a paired t-test, unless otherwise stated as unpaired. If the t-tests are unpaired then Welch's correction was applied if the standard deviation was not equal. Also used was two-way ANOVA with Tukey's post-hoc test. Values of $p < 0.05$ were considered as being significant and were assigned * in graph representations.

QuantityOne analysis software was used for the quantitative analysis of densitometric data resulting from western blotting of calcium handling proteins in different cardiac chambers.

The LSM 510 Image Examiner was used for spontaneous calcium activity analyses in studies using quiescent isolated cardiac myocytes in time series and line scan mode as well as the di-8ANEPPS study of the t-tubules.

CHAPTER 3

Pharmacological characterisation of β-AR subtypes in cultured chick embryonic ventricular cells

3.0 Pharmacological characterisation of β-AR subtypes in cultured chick embryonic ventricular cells

3.1 Introduction

3.1.1 Chick embryo physiology

Cardiac myocytes derived from the chick embryo (*Gallus domesticus*) constitute a useful tool to study cardiovascular development and neurohormonal influences on cardiac function (McCain *et al.*, 1999). They are also of use in studying pharmacological effects on the cardiovascular system of a variety of cardioactive agents (Sperelakis, 1978). Chick embryos are favoured for experimental studies because of their availability, rapid embryological development and easy experimental handling (Fechner *et al.*, 2008). In this study the chick embryonic cardiomyocyte model facilitates the testing of various concentrations and combinations of β-blockers and β-agonists and hence to characterise the β-ARs present in chick embryonic heart.

The chick embryo undergoes developmental changes outside the maternal body and as such, the influences of the maternal hormones, metabolic or other haemodynamic changes will not have an influence on the development of the chick embryo (Ruijtenbeek *et al.*, 2002). Furthermore, the chick embryo in one chick egg is independent of other eggs growing from the same maternal body and hence there are no interactions or disturbances amongst the other embryos (Fechner *et al.*, 2008). Similar to the mammalian heart, the chicken heart also possesses four chambers. The right atrium of the chicken heart is the recipient of the deoxygenated blood from the body via the vena cava, whilst the left atrium obtains oxygenated blood from the lungs via the pulmonary vein. The

right ventricle pumps blood into the pulmonary circulation via the pulmonary artery whilst the left ventricle, via the aorta, supplies the blood to the rest of the body. Hamburger and Hamilton, (1951) have suggested that within 40 hrs after the formation of a chick embryo, the contracting heart is formed.

3.1.2 Cardiac cell and tissue culture

Cardiac cells are aseptically isolated from a suitable experimental animal model and cultured in a sterile artificial media that has similar environmental conditions to that which the cells are normally exposed to *in vivo* (Pedro de Magalhaes, 2004). The resulting network of a monolayer of spontaneously beating interconnected individual cardiac myocytes enables a range of experimental studies to be performed *in vitro* (Sperelakis, 1978).

Burrows and colleagues (1912) were the first to successfully culture cardiac cells that were observed to spontaneously beat. Cardiac cells in culture possess a unique characteristic in that they are able to beat spontaneously, independent of innervations from the nervous system (Weaver, 2007). Cultured cardiac cells are suitable for studying various pharmacological properties, for example they are robust enough to be exposed to drugs at a range of concentrations so that dose-response curves of drugs can be obtained (Sperelakis, 1978). Another advantage of cultured cardiac myocytes is that despite the artificial environment the cells are exposed to, they still possess their normal pharmacological receptors which make them excellent models for pilot studies for determining drug actions (Sperelakis, 1978). However, in spite of all the favourable features of cultured cardiomyocytes, it is important to keep

in mind that some negative aspects do exist for this model. It has been suggested for instance, that significant variability in the spontaneous beating of cardiac cells in culture is possible (Sperelakis, 1978), even in various locations of the same cell culture. Nevertheless, the chick embryonic tissue culture remains useful for carrying out pilot studies for determining suitable working concentrations of pharmacological agents targeted at specific receptors on cardiac cells.

3.1.3 Classification of β-ARs subtypes in cardiomyocytes

β-ARs are G-protein coupled receptors (GPCRs) present on cardiac cells made up of 7-transmembrane domains with an extracellular N-terminus and an intracellular C-terminus (Dzimiri, 1999). When the catecholamines bind to β-ARs, stimulation of the receptors occurs which results in the enhancement of a series of physiological processes such as cardiac contractility, cardiac pacemaker activity, as well as metabolism of glucose and lipids (Zheng *et al.*, 2005). β-ARs are responsible for a number of intracellular signalling components being triggered such as AC, GC, phospholipase C and a variety of ion channels (Dzimiri, 1999).

It was initially suggested that the cardiac activity stimulated by β-ARs was exclusively via the stimulation of a subclass of the β-ARs called the β1-ARs. However, several other subtypes of the β-ARs were discovered through radioligand binding studies and various pharmacological assays using β-agonists and antagonists in human hearts (Baker, 2005 ; Zheng *et al.*, 2005). Lands and colleagues (1967) famously classified the β-ARs into two subtypes

called β1-ARs and β2-ARs. However, recently it has been proposed that there are four β-ARs subtypes in the human heart (Kaumann and Molenaar, 1997). These subtypes are namely, $\beta1_L$-, $\beta1_H$-, β2- and β3-ARs, and each sub class possesses various characteristics to regulate the heart in different ways depending on the subtypes' specific signalling pathway (Kaumann and Molenaar, 1997). β-ARs exert a characteristic property that is known as constitutive activity (Seifert and Wenzel-Seifert, 2002). This means that an agonist is not required to be present at the specific active site of the cardiac cell in order for a receptor to be spontaneously active. GPC Rs consist of an active and an inactive form (Kenakin, 2004). Upon the vacancy of an active site or its occupation by an agonist, the active conformation is favoured and hence, the receptor becomes coupled to the G-protein (Chidiac *et al.*, 1995). However, the inactive form is favoured when an inverse agonist settles at the specific active site and the receptor is uncoupled from the G-protein (Chidiac *et al.*, 1994). As a result, the conformational forms of the receptor rely upon the particular structure of the ligand as well as its efficacy for binding to the active site (Bhattachaya *et al.*, 2008).

3.1.3.1 $\beta1_H$-ARs

The β1-AR is a subclass of the β-ARs of the cardiac cells. It is made up 477 amino acids and it is located on chromosome 10 (Frielle *et al.*, 1988). The stimulation of the β1-AR active site by a specific agonist triggers the Gs-protein signalling pathway, whereby AC is activated leading to an increase in the levels of cAMP and stimulation of PKA activity (Zhu *et al.*, 2005). The resulting response involves the increase in the phosphorylation of LTCCs, causing

increase in calcium influx into the cell which leads to more calcium release from the SR, causing increased inotropy and chronotropy (Bers, 2002 ; Creazzo *et al.*, 2004). It has been suggested that 75% of the total β-ARs found in the human heart are of the β1 subtype (Naga Prasad *et al.*, 2001 ; Taira *et al.*, 2008). There are two particular subtypes of the β1-AR that have been suggested recently; $\beta1_H$ and $\beta1_L$-ARs (Figure 3.1) both of which stimulate the Gs signalling cascade and when the high affinity and low affinity sites of β1 respectively, are triggered, positive inotropism, chronotropism and lusitropism have been reported (Kaumann *et al.*, 1989 ; Taira *et al.*, 2008). However, for these two affinity sites of β1-AR, different pharmacological characteristics have been reported (Molenaar *et al.*, 2007).

Adrenaline has double the potency of noradrenaline on the atria of the human heart (Kaumann *et al.*,1989) even though both stimulate and occupy the binding sites of the $\beta1_H$-AR. However, ISO which is a potent synthetic analogue of adrenaline and noradrenaline has been found to have the highest potency of them all at the $\beta1_H$-AR (Brodde and Michel, 1999). Examples of a selective agonist and antagonist at the $\beta1_H$-AR are fenoterol (Xiao *et al.*, 2003) and bisoprolol (Taira *et al.*, 2008) respectively. It has been suggested that upon acute stimulation of the $\beta1_H$-ARs, the PKA-dependent coupling pathway becomes predominant, however, chronic stimulation will eventually cause desensitisation of the receptor which occurs in HF and cardiac cell death (Koch *et al.*, 2000).

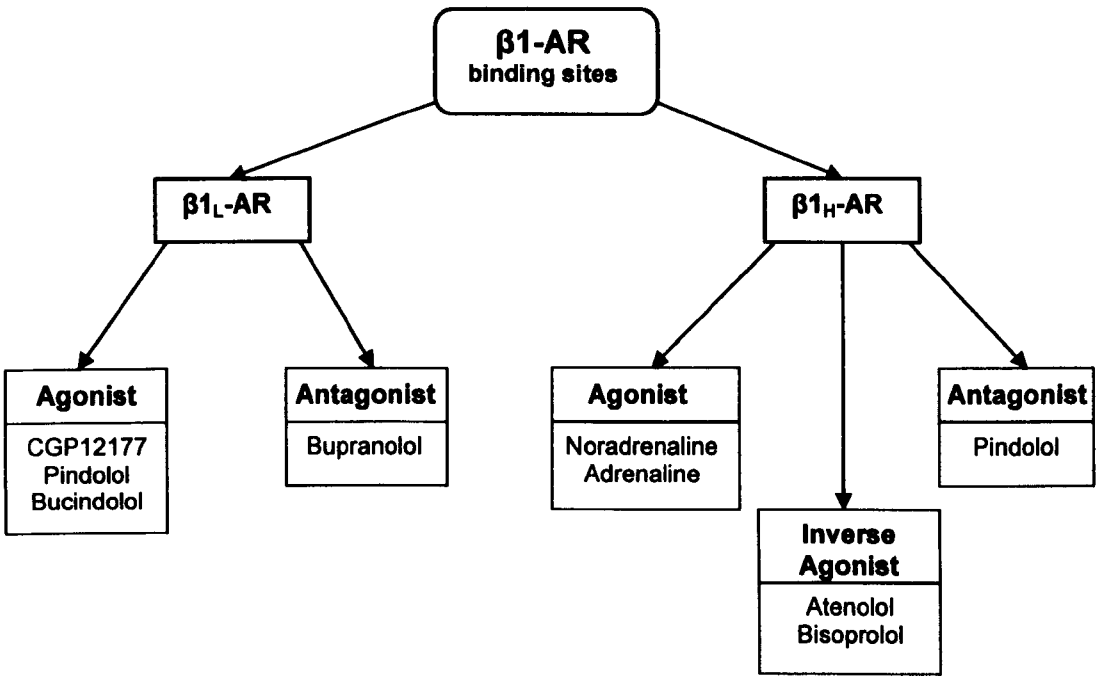

Figure 3.1 Agonists and antagonists of the β1-Adrenoceptor (β1-AR) binding sites on cardiomyocytes. A selection of examples of agonists and antagonists that have affinity for β1-ARs namely $\beta1_H$-ARs (high affinity) and $\beta1_L$-ARs (low affinity).

3.1.3.2 β2-ARs

The β2-AR protein is coded by a gene on chromosome 5, made up of 413 amino acids (Bristow *et al.*, 1986). In the human heart, β2-ARs accounts for 30 - 40% of the total β-ARs found mainly in the ventricles and atria (Bristow *et al.*, 1986). β2-ARs are also found in smooth muscles and skeletal muscles, as well as the bronchial, genitourinary and vascular areas of the body. It has also been suggested that β2-ARs play a role in assisting the regulation of cardiac contraction and rhythm by being located in the pacemaker and conducting sites

of the heart (Bartel *et al.*, 2007 ; Dzimiri, 1999). ISO has been found to have an affinity at the β2-AR, as well as the endogenous catecholamines (Brodde, 1991). Selective agonists and antagonists of the β2-AR, include terbutaline and ICI118551 respectively (Brodde and Michel, 1999).

The β2-AR signalling pathway in human and rat ventricular myocytes is able to couple to both Gs and Gi proteins (compared to β1-AR which couples to only the Gs protein) (Chen-Izu *et al.*, 2000 ; Xiao *et al.*, 2004 ; Johnson, 2006). This results in more opportunity to accommodate various agonists that activate different signalling pathways, and this behaviour is known as agonist trafficking (Zheng *et al.*, 2005). This characteristic may be of potential use in the development of specific β2 Gi agonists since Gi protein coupling has a cardioprotective effect which might be beneficial in the treatment of HF (Zheng *et al.*, 2005).

It has been speculated that the ability of β2-ARs to couple to both Gi and Gs proteins may be due to the polymorphism of the active site. McGraw and colleagues (2005) have shown the existence of 9 different polymorphisms of the β2-AR whereby binding to each polymorphism produces different behaviour following the coupling of an agonist to the active site of the receptor. The Gs protein pathway in β2-ARs is identical to that of the β1-ARs, therefore upon stimulation, positive chronotropy and inotropy will occur (Lohse *et al.*, 2003). It has been proposed that β2-ARs coupling can also promote relaxation (Taira *et al.*, 2008) which is thought to be as a result of cAMP-dependent phosphorylation of PLB and the depletion of calcium stores (Bartel *et al.*, 2003).

As previously mentioned, persistent stimulation of $\beta1_H$-ARs will result in death of cardiomyocytes via the CaM kinase II pathway (Xiao *et al.*, 2004). On the other hand, it has been suggested that the Gi pathway when coupled with β2-ARs will prevent the apoptosis of cardiomyocytes in HF (Bernstein *et al.*, 2005 ; Zheng *et al.*, 2005). This cardioprotective property of β2-ARs results from its persistent stimulation which forces the receptor G protein coupling to change from the Gs to the Gi signalling cascade via the activation of PI3K (Chen-Izu *et al.*, 2000 ; Xiao *et al.*, 2004). This has been demonstrated in experiments involving cultured rat myocytes and inhibition of β2-ARs showing an increase in β1-AR-induced apoptosis (Communal *et al.*, 1999) compared to when β2-ARs were not inhibited.

3.1.3.3 β3-ARs

The β3-AR gene was successfully cloned in 1989 by Emorine and colleagues and is located on chromosome 8 and produces a protein with 402 amino acids. In terms of the amino acid sequence, β3-ARs are 51% and 46% similar to β1-ARs and β2-ARs respectively (Emorine *et al.*, 1989). β3-AR is the other β-receptor that produces a cardio-inhibitory effect apart from β2-AR (upon its persistent stimulation only) and its functional role in the human heart remains controversial. In the human heart, β3-ARs are usually coupled to Gi proteins and are responsible for the negative chronotropism and inotropism promoted by specific agonists (Gauthier *et al.*, 1996). β3 mRNA gene expression has been reported to be upregulated and hence advance the progression of HF in canine models (Cheng *et al.*, 2001)

The stimulation of the β3-ARs (Figure 3.2) by a suitable agonist such as BRL37344 activates the enzyme eNOS and as a result produces NO (Rozec *et al.*, 2006). NO causes the activation of GC which in turn increases the intracellular cGMP concentration. A rise in the levels of cGMP leads to the activation of PKG which controls several proteins including one which decreases the opening frequency of the LTCCs and hence reducing calcium entry into the cardiomyocytes (Williams *et al.*, 2006 ; Napp *et al.*, 2009). Gi protein activation is also thought to be linked with the inhibition of AC which decreases the levels of intracellular cAMP although the mechanism for this pathway is still currently unknown (Ursino *et al.*, 2009). BRL37344 remains the agonist of choice for selectively stimulating the active site of β3-ARs (Gauthier *et al.*, 1996 ; Baker, 2005).

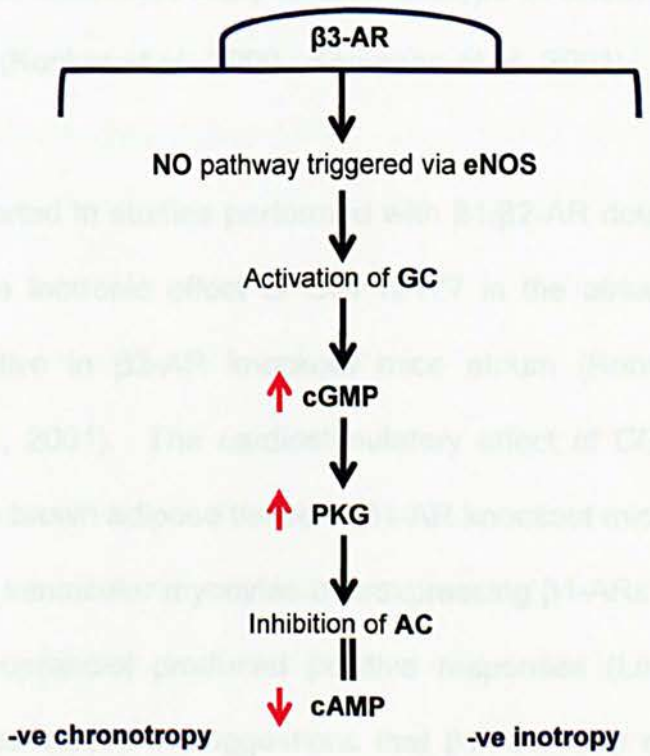

Figure 3.2 β3-Adrenoceptor (AR) cardiac signalling pathway. Upon stimulation by a β3-AR agonist upon the receptor, nitric oxide (NO) is produced and causes cardioinhibitory effect.

3.1.3.4 The novel low affinity β1-ARs

Initially, it was suggested that a third cardiostimulatory β-AR existed and that this receptor was activated by non-conventional partial agonists which caused raised heart rate and increased force of contraction (Kaumann, 1989). It was towards the late nineties when a putative β4-AR, thought to be similar to the β3-AR subtype, was reported to exist in the atria and brown adipose tissue of mice (Kaumann and Molenaar, 1998). Kaumann and Molenaar (1998) carried out studies on β3-AR knock-out mice to find that CGP12177 still triggered stimulatory activity in the atria and brown adipose tissue implying that the β3-AR and the putative β4-AR were separate receptors mediating opposite effects. However, no genes were confirmed for the putative β4-AR which suggests that this new receptor was more likely to be a subtype of another binding site that already existed (Konkar *et al.*, 2000 ; Kaumann *et al.*, 2001).

It was also reported in studies performed with β1/β2-AR double-knockout mice that the positive inotropic effect of CGP12177 in the atrium was absent but remained effective in β2-AR knockout mice atrium (Rohrer *et al.*, 1999 ; Kaumann *et al.*, 2001). The cardiostimulatory effect of CGP12177 was also abolished in the brown adipose tissue of β1-AR knockout mice (Kaumann *et al.*, 2002) but in rat ventricular myocytes overexpressing β1-ARs, CGP12177 in the presence of propranolol produced positive responses (Lewis *et al.*, 2004). Recently, this concluded in suggestions that β1-ARs may exist in two affinity states, the high affinity state, $\beta1_H$-AR and the novel low affinity state, $\beta1_L$-AR (Konkar *et al.*, 2000 ; Kaumann *et al.*, 2001 ; Lewis *et al.*, 2004 ; Molenaar and Parsonage, 2005 ; Molenaar *et al.*, 2007; Taira *et al.*, 2008).

3.2 Aim of study

There is conflicting evidence regarding the existence of various β-AR subtypes in cardiac tissue. This work therefore forms a pilot study of the cardioactive drugs being used in aseptically cultured chick embryonic ventricular myocytes to confirm the working conditions required to pharmacologically isolate the contributions of the four cardiac β-ARs described and relate them to the physiology of the cardiac cells.

3.3 Materials

All materials obtained are from the UK unless stated otherwise. Fertile white chick eggs were purchased from Henry Stewart and Co. Ltd and incubated in conditions previously described. All cardioactive drugs for the study were purchased from Tocris Bioscience (UK).

3.4 Methods

3.4.1 Embryonic chick cardiac cell culture

Chick embryonic ventricular cells were aseptically isolated and cultured (Figure 3.3 and Figure 3.4) according to the methods of DeHaan (1967), Rabkin and Sunga (1987) and Rabkin *et al.*, (1994) with slight modifications, as previously described in Chapter 2.

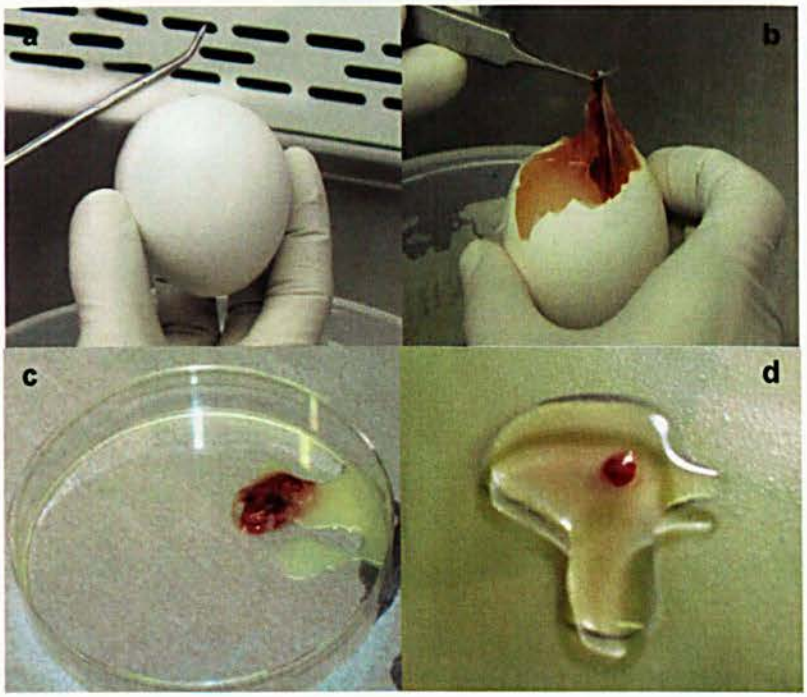

Figure 3.3 Extracting chick embryos from fertile chick eggs. **(a)** Eggs were cracked open **(b)** the embryo was gently removed from the egg **(c)** the embryo was gently placed onto a sterile petri dish **(d)** the ventricular tissue was separated from the atria and placed in Dulbecco's phosphate buffered saline (DPBS) solution to be minced into smaller chunks .

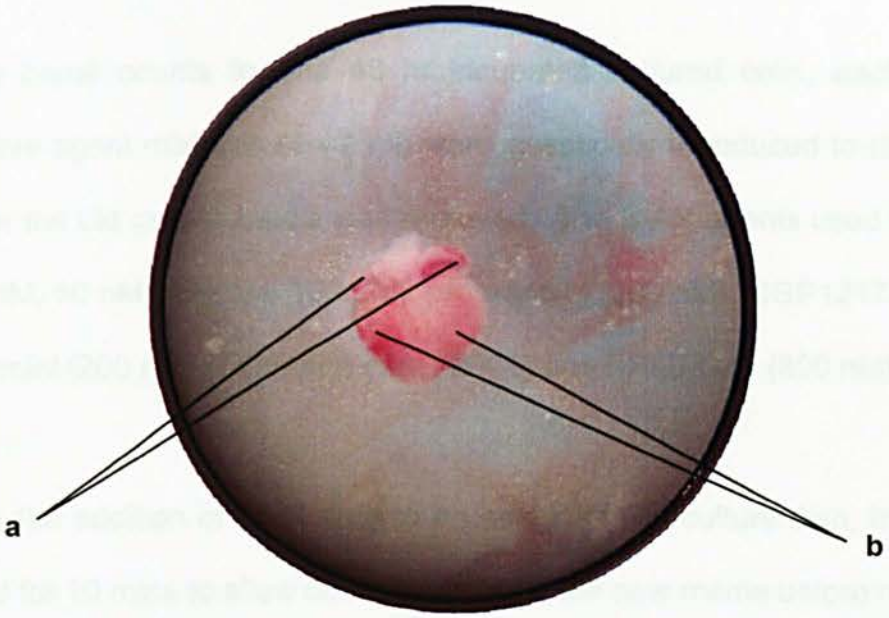

Figure 3.4 Chick embryo heart under the dissecting microscope. (a) atria and **(b)** ventricles.

3.4.2 Basal beating rate studies

The spontaneous basal beating rates of the chick cardiomyocytes were recorded as previously described with slight modifications. The contraction rate was recorded for 20 s from assigned quadrants of the culture dish in a 10 min period.

3.4.3 Cardioactive drugs used for pharmacological characterisation of β-subtypes in chick ventricular myocytes

Following basal counts for the 48 hr incubated cultured cells, each of the cardioactive agent mixtures (1 - 2 ml) were aseptically introduced to the single wells after the old growth media was removed. The β-AR agents used included ISO (25 nM, 50 nM, 100 nM, 100 μM), propranolol (200 nM), CGP12177 (1 μM) + propranolol (200 nM) (Kaumann *et al.*, 2001) and BRL37344 (600 nM).

Following the addition of each drug to an assigned cell culture dish, they were incubated for 10 mins to allow cell adaptation to the new media before recording the contraction rate of the cardiomyocytes.

3.5 Statistical analysis

Experimental data are presented as mean ± S.E.M. The differences between the average beating rates of the cultured ventricular cardiac cells at basal conditions and after administration of drugs were assessed by means of the paired t-test unless otherwise stated as unpaired. Values of $p < 0.05$ were considered as being significant.

3.6 Results

3.6.1 Culturing chick embryonic ventricular cardiomyocytes

Following the 48 hr incubation, the chick ventricular cardiomyocytes culture formed elaborate long lobular shaped colonies that have spontaneous rhythmic contractions.

3.6.2 Drugs acting on β-ARs

3.6.2.1 ISO

In an attempt to investigate the cardioactive activities mediated by β1/β2 ARs, ISO was introduced aseptically to proliferated chick embryonic ventricular cells at the following concentrations ; 25 nM, 50 nM and 100 nM to culture dishes containing ~700,000 cells/ml. ISO (25 nM) significantly increased the mean spontaneous contraction rate from basal at 74.6 ± 7.23 bpm to 129.6 ± 10.32 bpm. However, with the introduction of ISO (50 nM), the mean spontaneous contraction rate decreased slightly and when more ISO (100 nM) was added, there was another decrease in contraction rate from 121.2 ± 8.24 bpm to 89.5 ± 7.57 bpm (Figure 3.6). However, all three sample groups of ISO produced higher contraction rates than at basal.

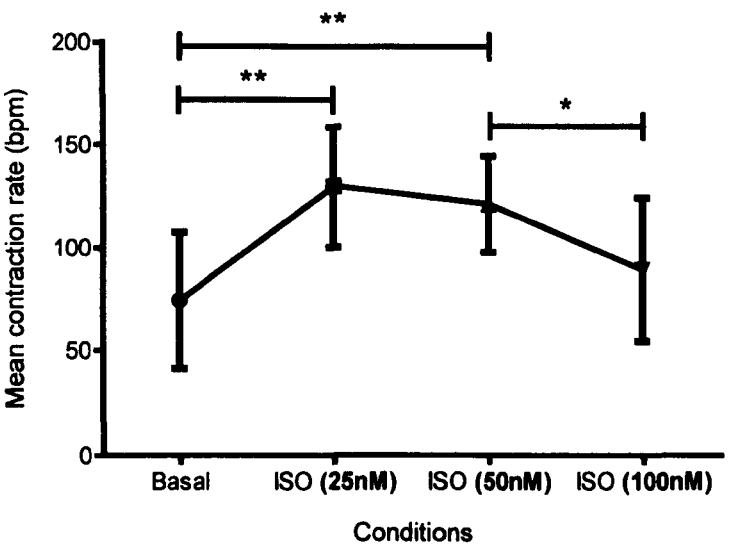

Figure 3.5 The cardiostimulatory effect of a range of ISO concentrations. Isoprenaline (ISO) at 25 nM caused a positive cardiostimulatory effect but the mean beating rate decreased slightly upon the addition of 50 nM ISO. The addition of ISO (100 nM) caused a significant decrease (*$p < 0.03$) in the mean spontaneous beating rate but tends to be cardiostimulatory in the unpaired ANOVA test compared to the beating rate at basal conditions ($n = 21$ where n = number of cells) and error bars signify S.E.M.

3.6.3.2 Propranolol

Propranolol (200 nM) which is a β1/β2 antagonist decreased the mean basal spontaneous contraction rate (~750,000 cells/ml). It is demonstrated (Figure 3.7) that compared to the basal condition the mean spontaneous contraction decreased from 89.6 ± 5.28 bpm to 71.0 ± 5.03 bpm upon the addition of propranolol. This paired sample study shows inverse agonism mediated by the occupancy of propranolol at β1/β2-ARs that results in significantly lower mean contraction rate compared to that for basal conditions where these sites are unoccupied.

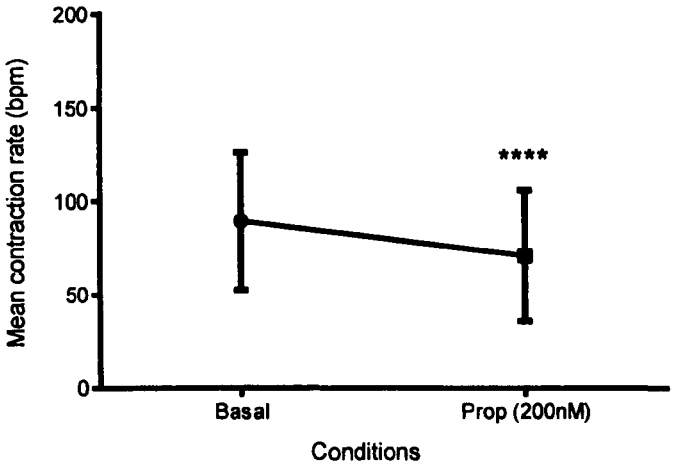

Figure 3.6 Propranolol demonstrates inverse agonism. Addition of propranolol (200 nM) to proliferated chick ventricular myocytes, decreased the contraction rate by 20.8% in relation to its basal count (n = 48 where n = number of cells ; ****p < 0.0001) and error bars signify S.E.M.

3.6.3.3 CGP12177 + propranolol

CGP12177 (1 μM) in the presence of propranolol (200 nM) caused an increase in the spontaneous beating rate in cells pre-treated with propranolol in a paired study (Figure 3.8). Propranolol decreased the contraction rate of chick ventricular cells from 47.5 ± 1.05 bpm to 34.4 ± 4.19 bpm (n = 16 ; p = 0.0015). However, the addition of CGP12177 caused the beating rate to increase sharply to 115.1 ± 5.08 bpm (n = 16 ; p < 0.0001).

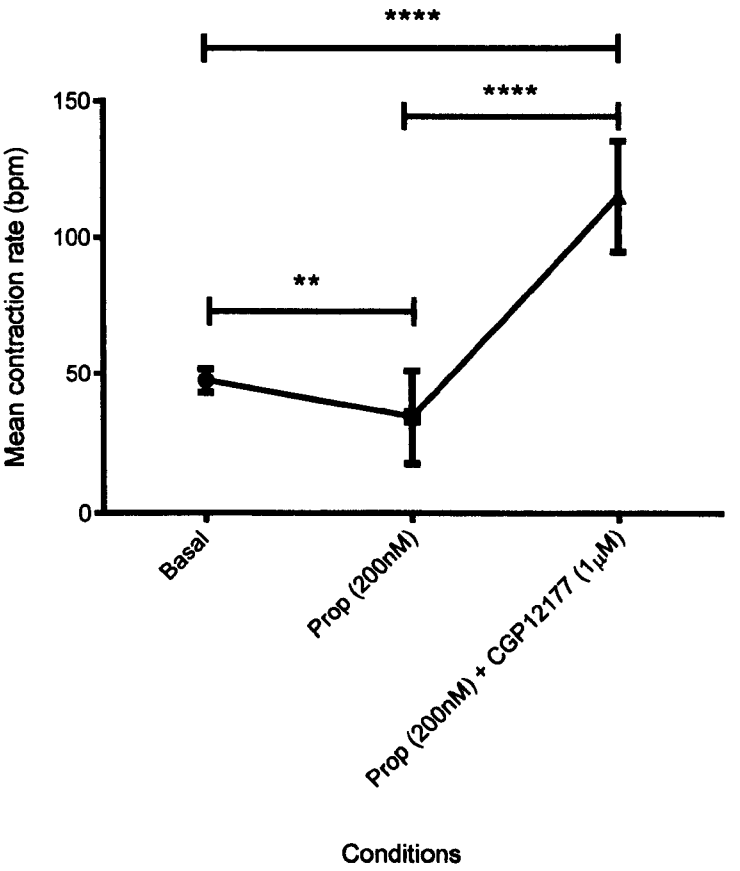

Figure 3.7 The cardiostimulatory effect of the addition of CGP12177 in the presence of β-blocker propranolol. Propranolol (200 nM) significantly decreased the mean contraction rate (n = 16 where n = number of cells ; **p < 0.005) from basal conditions. When CGP12177 (1 μM) was added in the presence of propranolol (200 nM) in a paired study, the contraction rate of the ventricular cells increased by 70% which was statistically significant compared to basal rates (n = 16 where n = number of cells ; ****p < 0.0001) and error bars signify S.E.M.

3.6.3.4 BRL37344

Upon the addition of BRL37344 (600 nM), the mean spontaneous contraction rate of ventricular cultured cells (~650,000 cells/ml) decreased from a basal rate of 37.6 ± 2.43 bpm to 27.5 ± 4.25 bpm (n = 13 ; p < 0.001) (Figure 3.9). BRL37344 was observed to promote negative inotropic effects via β3-ARs due to activation of a PKG-dependent pathway via cGMP (Gauthier *et al.*, 1998).

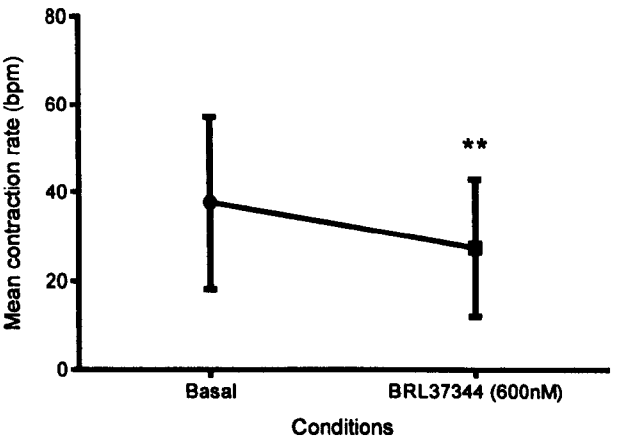

Figure 3.8 BRL37344 causes negative inotropy in chick ventricular myocytes. After the addition of BRL37344 (600 nM) to cultured ventricular myocytes, the contraction rate was observed to decrease significantly compared to the basal rate (n = 13 where n = number of cells ; **p < 0.001) and error bars signify S.E.M. The mean difference in beating rate of ventricular myocytes between the paired basal condition and BRL37344 at 600 nM is 10.1 bpm.

3.6.3.5 Cumulative addition of cardiostimulatory and cardioinhibitory drugs

Data was gathered from un-paired experiments to summarise the cardiostimulatory and cardioinhibitory activity exerted by cardioactive drugs on their specific β-ARs in chick ventricular cardiomyocytes in a cumulative manner. The mean beating rate of the chick ventricular myocytes at basal condition was 90.3 ± 4.50 bpm (n = 119). The addition of propranolol (200 nM) showed an inverse agonist behaviour whereby the mean beating rate showed a statistically significant decline to 34.4 ± 4.19 bpm (n = 16 ; $p < 0.0001$). However, the mean contraction rate increased when CGP12177 (1 μM) was introduced in the presence of propranolol (n = 16 ; p = 0.006) demonstrating the stimulatory effect of this partial agonist acting upon the $\beta1_L$-AR. BRL37344 (600 nM) resulted in a sharp decrease in mean contraction rate to 42.0 ± 2.88 bpm (n = 13 ; p = 0.0001). However, ISO (100 nM) showed cardiostimulatory behaviour whereby the mean beating rate was shown to be 89.5 ± 7.57 bpm (n = 21) (Figure 3.10).

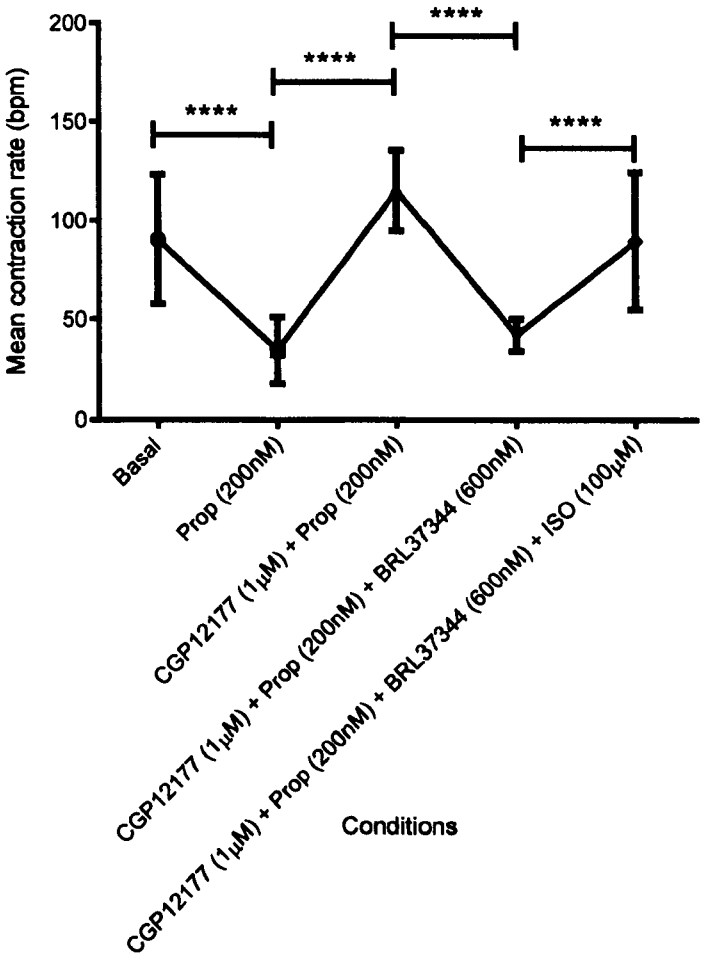

Figure 3.9 The effect of consecutive addition of cardioactive drugs to cultured chick ventricular myocytes. Propranolol shows inverse agonism in cultured chick myocytes (****$p < 0.0001$). Addition of CGP12177 (1 μM) and propranolol (200 nM) caused a significant increase in the mean contraction rate (n = 16 where n = number of cells ; ****$p < 0.0001$). BRL37344 (600 nM) exerts cardioinhibitory behaviour whereas ISO (100 nM) shows a significant cardiostimulatory effect (n = 21 where n = number of cells ; ****$p < 0.0001$). The horizontal bars represent the individual comparisons between the groups and error bars signify S.E.M.

3.7 Discussion

The classic $\beta 1_H$-AR agonist, ISO has been shown to result in positive inotropism and positive lusitropism of rat atrial and ventricular myocytes (Sarsero *et al.*, 1999) mouse ventricular myocytes (Freestone *et al.*, 1999 ; Shen *et al.*, 2006), mediated by the PKA-dependent pathway in cardiac cells. ISO has been shown to stimulate both $\beta 1_H$ and β2-AR sites causing an increase in the rate of contraction and relaxation in humans (Brodde, 1991).

In the present study, ISO has been proven to be a cardiostimulant on immature chick cardiac cells whereby a concentration of 25 nM for 10 mins resulted in an increase from basal conditions in the mean spontaneous contraction rate. It was also observed that a large number of cardiac cells responded with positive inotropism and chronotropism upon the addition of ISO though a means of measuring the force of the contraction was not possible and is therefore a limitation of the technique used. However, when the ISO incubation time exceeded 20 mins, the cardiomyocytes was observed to be either highly arrhythmic or static. This confirms that ISO, a potent $\beta 1_H$ and β2 agonist, becomes cardiotoxic through a period of persistent stimulation as suggested by Brodde (1991). The cardiotoxicity arising from prolonged exposure of ISO in chick cardiac cells arises from the activation of the CAM kinase II pathway which has been suggested to be linked to cardiomyocyte apoptosis and desensitisation of the receptor site of the cardiac cell (Wang *et al.*, 2004).

On the other hand, propranolol is a competitive antagonist at the $\beta 1_H$ and β2-AR active sites. Through the addition of propranolol to a culture of non-stimulated chick ventricular cardiomyocytes, the mean spontaneous contraction rate showed a significant decrease of 20.8% demonstrating inverse agonism. This behaviour has also been observed in propranolol by Baker's group (2003).

The addition of CGP12177 in the presence of propranolol to spontaneously beating cardiac cultured cells increased the contraction rate more than that resulting from ISO at 25 nM, 50 nM and 100 nM, despite the fact that ISO is a full agonist and CGP12177 is only a partial agonist in cardiac cells from several other species. This is a similar behaviour to a study in 1999 in mouse ventricular myocytes carried out by Freestone and colleagues whereby it was shown that CGP12177 was much more likely to cause a more potent arrhythmic response compared to ISO even though CGP12177 only triggered 30% of the intracellular calcium levels of ISO. For example, there was an increase of 70% in spontaneous beating rate of chick ventricular myocytes upon the addition of CGP12177 (in the presence of propranolol) compared to the sole addition of propranolol. However, for ISO at 25 nM (which was also the most potent dose) the increase was by just 42.4% compared to its basal conditions. The effect of CGP12177 in the presence of a propranolol therefore confirms the presence of $\beta 1_L$-AR in chick ventricular cardiomyocytes and that this receptor is resistant to blockade by propranolol.

BRL37344 is a selective agonist that has a significant affinity for the β3 receptor which has been shown to be present in the mammalian myocardium (Gauthier *et al.*, 1998). Usually, BRL37344 is used at a concentration of 300 nM (Gauthier *et al.*, 1996), however in this study, no cardioactivity was observed when this concentration was used. BRL37344 at 600 nM was then added to the chick ventricular cardiomyocytes in culture and was seen to decrease the mean spontaneous contraction rate. BRL37344 has been described as a β-agonist for β1, β2 and β3-ARs though it is much more selective for the latter receptor site (Gauthier *et al.*, 1998). When the β1 and β2-ARs are not occupied by for example propranolol, BRL37344 favours the β3-ARs resulting in negative chronotropism. It has been suggested in cardiomyocytes of dogs that BRL37344 produces positive chronotropy, however this could possibly be due to baroflex mechanisms rather than cardiac β-ARs (Tavernier *et al.*, 1992). The presence of β3-ARs in chick ventricular myocytes is therefore supported by the negative chronotropism that results when β3-AR is stimulated by BRL37344 alone in these cardiac cells.

3.8 Conclusion

- The agonists for $\beta 1_H$, $\beta 2$ and $\beta 1_L$-ARs are all cardiostimulatory whereas the $\beta 3$ agonist causes a cardioinhibitory effect.

- Pharmacological evidence for four distinct β-AR sites in 7-days incubated chick embryo ventricular myocytes.

- This will be of use in Chapter 6 for the pharmacological investigation of the propranolol-insensitive β1-ARs in rat atrial cells and how they can promote atrial arrhythmias.

CHAPTER 4

Atrial cell morphology and calcium spark localisation

4.0 Atrial cell morphology and calcium spark localisation

4.1 Introduction

4.1.1 Physiological characteristics of rat atrial and ventricular myocytes

The function of individual atrial and ventricular myocytes has been widely studied in rats. Recently there has been a surge of interest in studying the specific morphology and size of the atrial myocytes with regard to considering the different functions exhibited by the atrial chambers with a specific focus on AF, a pathophysiological cardiac condition.

The presence of certain ultrastructural features of the cardiomyocytes may depend upon the size of the cells as they seem to be important for the conduction of calcium sparks. In other words, it is possible that a relationship exists between the morphology of the cardiomyocytes and calcium release sites. This then contributes to initiation of cell contraction either in response to a depolarizing action potential arising from the SA node or without such an impulse in the instance of an arrhythmic event.

The ventricle has been widely studied compared to the atria due to the ease and convenience of obtaining a significant number of isolated individual ventricular myocytes for experimental studies (De Young *et al.*, 1989). However, atrial cells are currently becoming subjects of interest for the study of AF. Single isolated rat ventricular cells are larger in both length and width compared to the atrial cells. This is because the ventricles are larger muscles and have to work harder to pump blood to the lungs and other more distant

organs. Freshly isolated calcium-tolerant (< 1 mM calcium) rat ventricular myocytes are wide and possess rod-like shapes (De Young *et al.*, 1989 ; Freestone *et al.*, 2000). On the other hand, rat atrial cells were found to have a fairly narrow and elongated shape with tapered ends (Freestone *et al.*, 2000). According to Kirk and colleagues (2003), atrial myocytes (mixed population of single left and right atrial cells) isolated from SD rats have relatively uniform widths across the length of the cells.

Rat atrial cells have been classified as being "wide" or "narrow" cells depending on whether they possess t-tubules or not (Kirk *et al.*, 2003 ; Smyrnias *et al.*, 2010). In cells with t-tubules present, the rat atrial cell is considered "wide" and according to Kirk's group (2003) has an average width of 13.2 ± 2.8 μm and according to Smyrnias' group (2010) the average width is 16.6 ± 0.4 μm. On the other hand, a typical "narrow" rat atrial cell has no t-tubules and according to Kirk's group (2003) has an average width of 11.7 ± 2.0 μm and according to Smyrnias' group (2010), has an average width of 13.7 ± 4.0 μm. Freestone and colleagues (2004) have reported WKY rat atrial cells having an average width of 13.0 ± 0.3 μm which is similar to the dimensions obtained by Kirk's and Smyrnias' group (Kirk *et al.*, 2003 ; Smyrnias *et al.*, 2010). According to Smyrnias et al., (2010) rat atrial cells which were wide, measuring more than 20 μm in width all possessed an ultrastructural feature similar to t-tubules. Such wide cells presumably were largely found in the left atria whilst narrower cells were predominantly found in the right atria.

4.1.2 T-tubules and EC Coupling

EC coupling is a critical mechanism needed to ensure synchronised cardiac contractility of the myocardium made up of millions of individual cardiomyocytes. A specific feature of the ventricular muscle cell ultrastructure called the transverse or t-tubules was initially discovered and reported in 1956 by Lindner. T-tubules are extensive and protruding invaginations of the sarcolemma which function to carry action potentials deep within the cell and therefore contribute to the regulation of contraction of these cardiomyocytes.

T-tubules are common features of rat ventricular cells and are about 200 nm in length and are regularly located every 1.8 μm along the length of ventricular myocytes (Smyrnias *et al.*, 2010). In cardiomyocytes, the majority of the LTCCs are located on the t-tubule membrane compared to a smaller proportion situated on the external sarcolemmal membrane (Brette and Orchard, 2003) and hence are in close proximity to the SR. As such, the most significant source of the calcium that triggers further calcium release from the SR is from the LTCC entry via the t-tubules (Brette *et al.*, 2006). This suggests that the position and function of the t-tubules within the ventricular cell contributes to a rapid and co-ordinated calcium release from the SR to all parts within the cell eventually causing a co-ordinated cellular contraction (Kirk *et al.*, 2003).

To a certain extent, the process of EC coupling in atrial cells is similar to that of the ventricular cells. Both atrial and ventricular cell contractions are triggered by the action potential reaching the membrane which causes the opening of the

voltage-gated LTCCs. However the propagation of the intracellular calcium mobilised by this event is quite different.

4.1.2.1 T-tubules in atrial myocytes

Recently studies have shown that the extensive and well organised t-tubule network system which is commonly observed in mammalian ventricular myocytes, does not exist in mammalian atrial cells (Orchard *et al.*, 2008 ; Walden *et al.*, 2009 ; Richards *et al.*, 2011). There have also been reports of atrial cells possessing a similar system which is not as well distributed and is rather disorganised compared to the ventricular t-tubular system (Leeson, 1980 ; Tidball *et al.*, 1991 ; Kirk *et al.*, 2003 ; Smyrnias *et al.*, 2010). This rudimentary network of tubules reported by Kirk and colleagues (2003) in wider rat atrial cells are known as TATS and these may facilitate EC coupling in such cells.

However, as previously suggested, narrower atrial cells lack the tubule system altogether (Kirk *et al.*, 2003; Smyrnias *et al.*, 2010). TATS in atrial cells have been described as having both randomly disorganised transverse and some occasional longitudinal tubules (Soeller *et al.*, 1999 ; Smyrnias *et al.*, 2010). Others have reported the tubules in atrial cells having primarily a lengthwise structural system rather than the usual invaginations of sarcolemma running across the cell as seen with ventricular myocytes (Leeson, 1980 ; Tidball *et al.*, 1991 ; Woo *et al.*, 2005 ; Dibb *et al.*, 2009 ; Smyrnias *et al.*, 2010). Furthermore, the electrical stimulation of narrower atrial cells tends to cause "U" shaped whole cell calcium transients with the calcium event originating from the cell periphery where calcium sparks are initiated (Kirk *et al.*, 2003).

On the other hand, wider atrial cells have been reported to produce "W" shaped calcium waves with calcium sparks originating from both the cell periphery and cell interior (Kirk *et al.*, 2003). This poses the question of whether there may be a relationship between the morphology of the atrial myocytes, the presence or absence of TATS and the site of initiation of calcium sparks.

4.1.2.2 T-tubules in SHR myocytes

SHR rats develop hypertension and eventually cardiac hypertrophy as they age. Hypertension is a chronic condition whereby the arterial blood pressure is elevated. Cardiac hypertrophy occurs when the myocardium thickens in response to working against this increased load and thus leads to a decrease in the volume capacity of heart chambers (Shorofsky *et al.*, 1999). This is an adaptive response to the increased after-load the heart is working against. In particular, the left atrium and left ventricular wall are thicker as more effort is required to pump the blood out of the heart. Therefore as a result, the hypertrophied rat heart is heavier than that for normotensive rats (Freestone *et al.*, 1996 ; Shorofsky *et al.*, 1999). SHR rats only develop cardiac hypertrophy from 6 months old onwards, but as shown in echocardiograph studies of these rat hearts, there are no signs of heart failure until after 12 months (Shorofsky *et al.*, 1999). As a result of the cardiac hypertrophy, individual cardiac cells show a prolonged relaxation period, increased calcium release from the SR and increased contractility of the individual heart cells (Shorofsky *et al.*, 1999 ; Bell *et al.*, 2004). There is a higher amount of free intracellular calcium ions in SHR cardiomyocytes which results in larger sparks compared to those from normal cardiomyocytes (Shorofsky *et al.*, 1999). The accumulation of calcium ions

seems to cause an increase in calcium storage capacity in the SR of SHR cardiomyocytes hence causing an increase in calcium release events (Shorofsky *et al.*, 1999).

4.1.2.3 T-tubules in large and small mammals

It has been reported in several studies that AF is a phenomenon that does not occur in small mammals (Hüser *et al.*, 1996 ; Mackenzie *et al.*, 2001 ; Dibb *et al.*, 2009 ; Richards *et al.*, 2011). Nevertheless, it is possible to initiate arrhythmic events in isolated rat atrial cells.

Dibb and colleagues (2009) showed that in terms of morphology and internal structure, small mammalian atrial myocytes (such as from rats) are very different to larger mammalian atrial myocytes (such as from sheep). The average width of the sheep atrial myocytes (14.5 ± 0.75 µm and 16.0 ± 1.16 µm) (Dibb *et al.*, 2009 and Richards *et al.*, 2011 respectively) is larger compared to rat atrial myocytes which has been reported to have an average width of 13.2 ± 2.80 µm, 13.0 ± 0.30 µm, 9.1 ± 0.98 µm and 10 µm (Kirk *et al.*, 2003 ; Freestone *et al.*, 2004 ; Dibb *et al.*, 2009 ; Walden *et al.*, 2009 respectively). Various studies have shown that human atrial cells have an average width of 17 µm, 17.9 µm and 17.3 ± 1.2 µm (Porciatti *et al.*, 1997 ; Polontchouk *et al.*, 2001 ; Richards *et al.*, 2011 respectively). This means they are narrower than the horse atrial width (22.7 ± 1.5 µm) but slightly wider than the atrial widths of cows (16.8 ± 0.93 µm) and sheep (16.0 ± 1.16 µm) (Richards *et al.*, 2011). In the larger atrial myocytes obtained from sheep, horses and humans, it was discovered that a t-tubule network exists (Dibb *et al.*, 2009 ;

Richards *et al.*, 2011) which supports the suggestion that these membranal invaginations function to facilitate the calcium release in the centre as well as the periphery of these wider atrial myocytes. Furthermore, the t-tubule network is noticeably absent in atrial myocytes from sheep with HF which is a similar occurrence in ventricular myocytes of horses with HF and human cardiomyocytes derived from patients with chronic HF (Dibb *et al.*, 2009).

4.2 Aim of study

There is no information in the literature about right and left atrial cell dimension comparisons but we hypothesise that left atrial myocytes are wider compared to right atrial myocytes. Wider atrial cells may provide a more heterogenous distribution of calcium sparks compared to the narrower atrial cells. We seek here to confirm the differences in width between the left and right atrial cardiomyocytes as well as to investigate the relationship between calcium spark initiation sites and cell morphology in rat atrial myocytes. In addition, important ultrastructural features of the ventricular myocytes, the t-tubules will be studied.

4.3 Materials

Materials used in this study are as previously described in Chapter 2, with the addition of sodium pentobarbital for anaesthesia which was purchased from Sigma Aldrich Company Ltd. Heparin was obtained from BD Healthcare Ltd.

4.4 Methods

4.4.1 Animals

Rats used in this study are as described in Chapter 2.

4.4.2 Langendorff method - Perfusing the whole rat heart

Male WKY rats were sacrificed and the procedure for whole heart perfusion using the Langendorff method was as previously discussed in Chapter 2.

4.4.3 Atrial cell isolation

Atrial cell isolation procedure is as described in Chapter 2 with a slight modification to the method. Gentle manual agitation of the minced tissues in collagenase enzyme solution and then Tyrode's solution (0.2 mM calcium) was carried out in sessions lasting 5 mins each in the water bath (37°C). After each session, supernatant was collected and fresh warm enzyme was added to the remaining atrial tissue in the boiling tubes for the last session of manual agitation at 37°C for 15 mins. Any remaining tissue was gently triturated using a Pasteur pipette to aid tissue digestion.

4.4.4 Incubation of fluo-4AM loaded cardiac cells

Fluo-4AM solution (4 μM) was made up as described in Chapter 2.

4.4.5 Incubation of di-8ANEPPS loaded cardiac cells

Di-8ANEPPS (2 μM) in DMSO was prepared as explained in Chapter 2. T-tubule studies consist of using di-8ANEPPS-stained cells to construct 3-D images which were obtained from a series of Z-slices of the specimen obtained in a specific time span.

4.5 Statistical analysis

Experimental data are presented as mean ± S.E.M. All t-tests were unpaired and values of $p < 0.05$ were considered as being statistically significant.

4.6 Results

4.6.1 Average weights of whole rat hearts

Upon dissection of the heart from WKY and SHR rats, a sample of hearts was weighed (Figure 4.1). The average wet weights of the hearts from SHR rats (2.0 ± 0.04 g) were found to be heavier than those obtained from WKY (1.5 ± 0.06 g) ($n = 5$ and 10 respectively, $p < 0.0001$). This is considered as being due to hypertrophy and thickening of the cardiac tissue (due to accumulation of collagen) characteristic of hypertension in these animals.

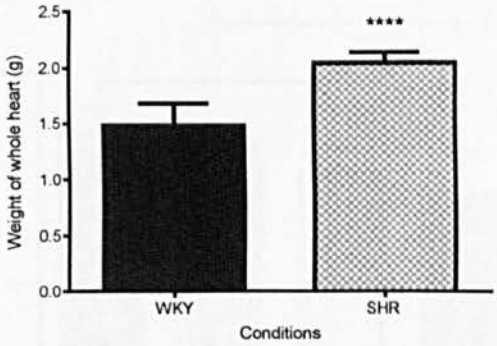

Figure 4.1 Comparison of the average wet weights of whole SHR and WKY rat hearts. SHR hearts are significantly heavier than WKY hearts (****$p < 0.0001$).

4.6.2 Average weights of WKY and SHR atrial tissue

Following microdissection of the left and right atria, the tissues were rapidly weighed out. The mean average weight of WKY left atria was 484.3 ± 23.2 mg and the WKY right atria was 464.8 ± 11.6 mg (although not significantly different). SHR left atria was 410.4 ± 19.7 mg and SHR right atria was 371.2 ± 32.7 mg (not significantly different). The mean average wet weights of WKY left and right atrial tissue were higher than the SHR counterparts (Figure 4.2) even though the whole SHR hearts had a significantly higher average weight than WKY hearts.

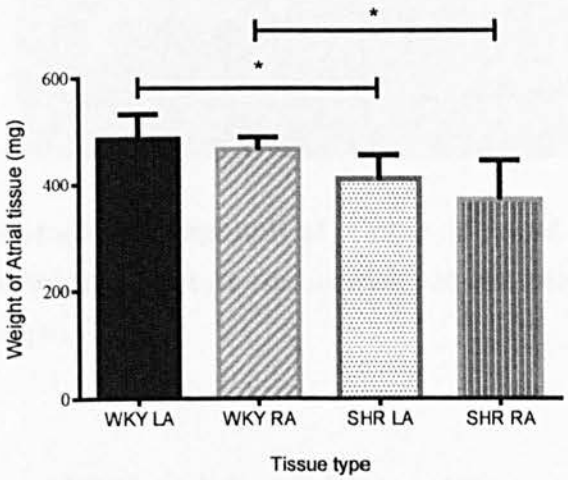

Figure 4.2 WKY left and right atria are on average heavier than SHR left and right atria. The mean weight of WKY left atria is significantly higher than the mean weight of SHR left atria, ($n = 4$ and $n = 5$ respectively, $^*p < 0.05$). The mean weight of WKY right atria is also significantly greater than the mean weight of SHR right atria ($n = 4$ and $n = 5$ respectively, $^*p < 0.05$). LA and RA depict left atria and right atria respectively. A similar observation was reported by Sonnenberg *et al.*, 1983.

4.6.3 Morphology of WKY rat ventricular myocytes

Different chambers of the heart possess cardiomyocytes with a specific morphology adapted to perform their specific functions. Ventricular cells isolated from WKY rats have a relatively wide and straight rod-shaped morphology (Figure 4.3). The mean ventricular width is 26.8 ± 1.71 µm and the mean ventricular length is 149.5 ± 5.07 µm (n = 14).

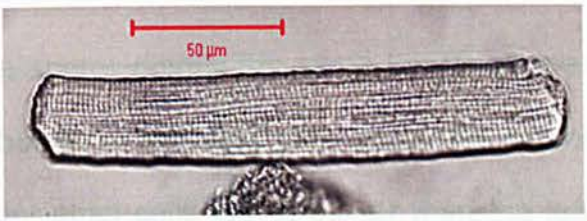

Figure 4.3 Morphological snapshot of single isolated WKY rat ventricular myocyte. The rat ventricular myocyte has a broad rod-like shape. The red scale bars indicate a scale of 50 µm.

4.6.4 Morphology of WKY rat left atrial myocytes

On the other hand, rat atrial cells have a long and thin worm-like morphology with tapered ends. Even though the left and right atria share the same general morphology, they differ in the widths of the cells. A selection of left atrial cells is shown (Figure 4.4). The mean left atrial myocyte width is 13.6 ± 0.30 µm (n = 91).

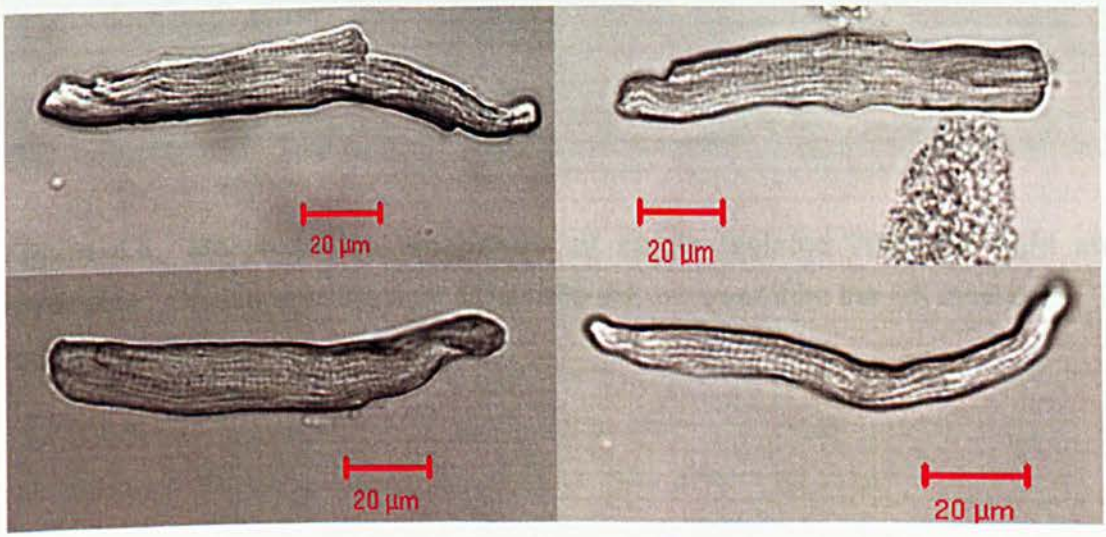

Figure 4.4 Morphological snapshots of single isolated WKY rat left atrial myocytes. Clear striations are seen under the microscope which are the sarcomere structures and are indications of healthy robust myocytes. The red bar indicates a scale of 20 µm.

4.6.5 Morphology of WKY rat right atrial myocytes

Right atrial cells are approximately the same length as the left atrial cells and resemble the morphology of left atrial cells under the microscope (Figure 4.5). On average, the right atrial cells are narrower than the left atrial cells, where the widths are 9.9 ± 0.25 μm compared to 13.6 ± 0.30 μm respectively (n = 125 and n = 91 respectively, $p < 0.0001$,). In terms of length, on average the right atrial cells are 96.5 ± 2.13 μm and the left atrial cells are 93.1 ± 2.01 μm respectively (n = 125 and 91 respectively) though not statistically significantly different.

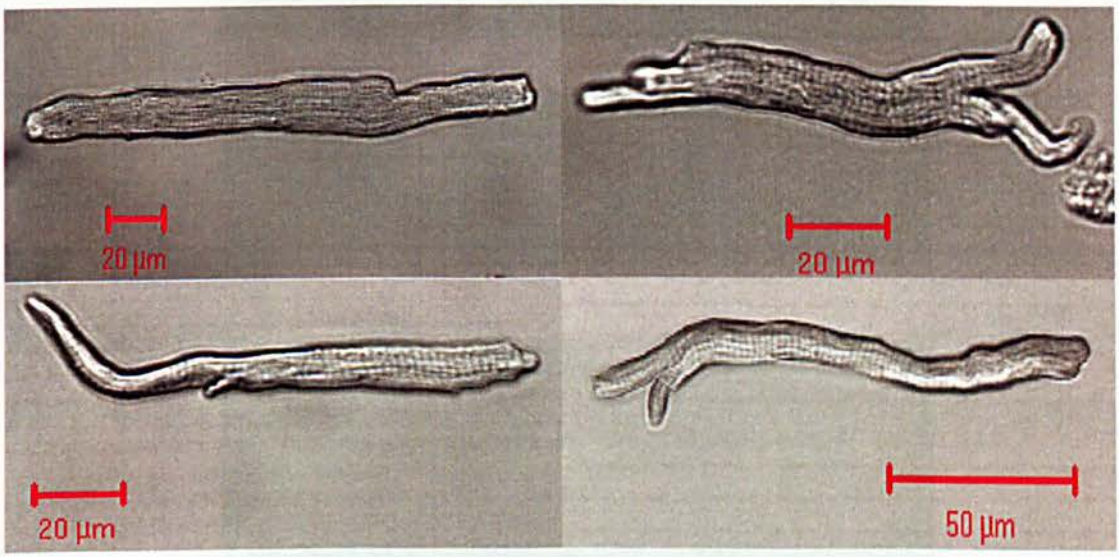

Figure 4.5 Morphological snapshots of single isolated WKY rat right atrial myocytes. On average, the right atrial cells are narrower than the left atrial cells. The red bar indicates a scale of 20 μm.

4.6.6 Morphology of SHR rat atrial and ventricular myocytes

Left SHR atrial cardiomyocytes are observed to be longer and wider than their WKY counterparts even though there is a proportion of atrial tissue death during hypertension. Similar observations have been reported by McCrossan's group (2004). SHR ventricular cells (Figure 4.6) had an average length of 144.5 ± 2.6 µm and WKY ventricular cell length was 149.5 ± 5.07 µm.

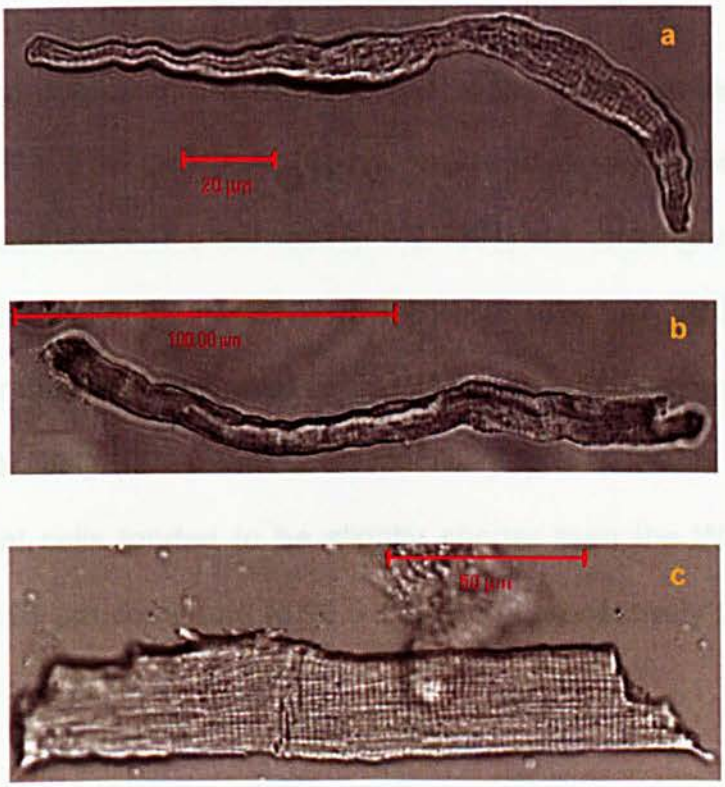

Figure 4.6 Morphological snapshot of single isolated SHR myocyte. (a) SHR left atrial cell **(b)** SHR right atrial cell and **(c)** SHR ventricular cell. All SHR cardiomyocytes are wider and longer compared to their WKY counterparts (*p = 0.05). Even though the above SHR ventricular myocyte is a diseased cell, it still maintains the striated sarcomere structures which are also seen in WKY ventricular cells.

4.6.7 Comparison between the average lengths of WKY and SHR atrial myocytes

The average length of WKY left atrial cells was 93.1 ± 2.01 μm which however was not significantly different from the average length of WKY right atrial cells which was 96.5 ± 2.13 μm (n = 91 and 125 respectively) (Figure 4.7). Furthermore, the average lengths of SHR left and right atrial cells also did not differ significantly from each other.

For comparison purposes, the mean length of the WKY ventricular cell was included (149.5 ± 5.07 μm) (n = 18) and was statistically significantly longer than the right and left WKY atrial cells ($p < 0.0001$) but not longer than the SHR atrial cells. On the other hand, SHR left atrial cells were shown to be on average longer than WKY left atrial cells, 123.9 ± 10.94 μm compared to 93.1 ± 2.01 μm respectively (n = 9 and 91 respectively, $p < 0.0002$). However, the SHR right atrial cells tended to be slightly shorter than the WKY right atrial cells, 94.6 ± 9.91 μm compared to 96.5 ± 2.13 μm respectively (n = 7 and 125 respectively, $p = 0.9$).

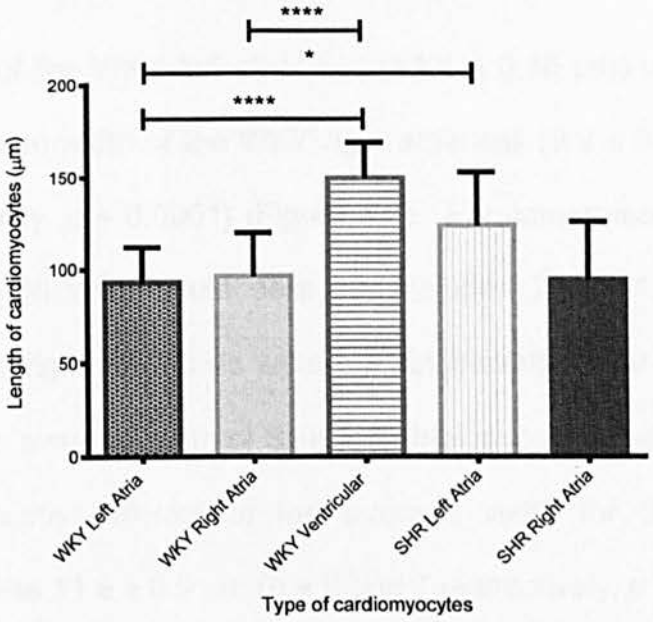

Figure 4.7 Comparison between the lengths of WKY and SHR left and right atrial myocytes. WKY ventricular myocytes are significantly longer than left and right atrial myocytes (****$p < 0.0001$) whereas SHR left atria is also significantly longer than WKY left atria (*$p < 0.01$). SHR left and right atrial myocytes did not show statistically different lengths and this was also observed in WKY left and right atrial myocytes.

4.6.8 Comparison between the average widths of WKY and SHR atrial myocytes

The mean width of the WKY left atrial cell (13.6 ± 0.30 µm) was significantly larger than the mean width of the WKY right atrial cell (9.9 ± 0.25 µm) (n = 91 and 125 respectively, $p < 0.0001$) (Figure 4.8). For comparison purposes, the mean width of the WKY ventricular cells was included, 26.8 ± 1.71 µm (n = 18). Both SHR left and right atrial cells were not significantly wider than their WKY counterparts. The average width of SHR left atrial myocytes was 15.1 ± 1.1 µm and was significantly different to the average width for SHR right atrial myocytes which was 11.9 ± 0.9 µm (n = 9 and 7 respectively, $p < 0.05$).

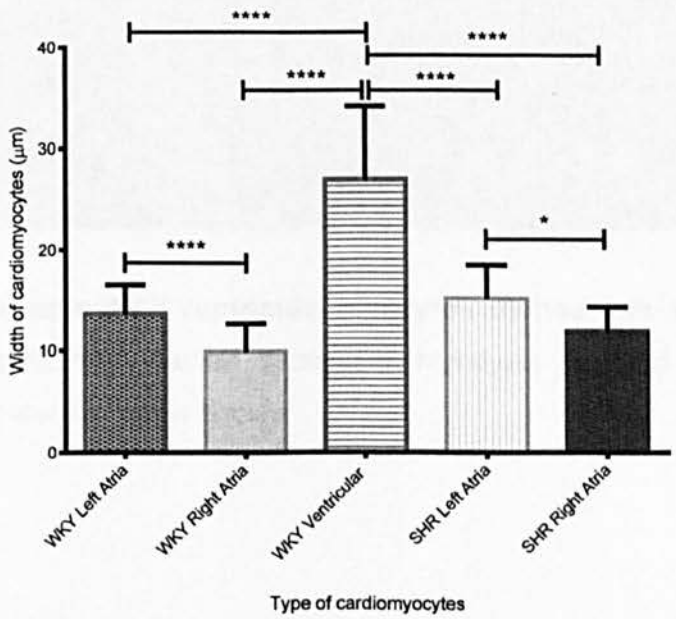

Figure 4.8 Comparison between the widths of WKY and SHR left and right atrial myocytes. SHR left atria is 3.23 µm wider than SHR right atria whereas WKY left atria is 3.70 µm wider than WKY right atria. Both SHR left and right atria tend to be wider than their WKY counterparts however SHR left atria is significantly wider than SHR right atria (*$p < 0.1$). WKY ventricular myocytes are significantly wider than both WKY and SHR left and right atrial myocytes (****$p < 0.0001$).

4.6.9 T-tubules in WKY rat ventricular myocytes

Di-8ANEPPS was used for the detection of the presence of t-tubule membranes within cardiomyocytes. As shown (Figure 4.9), t-tubules were present in WKY ventricular cells.

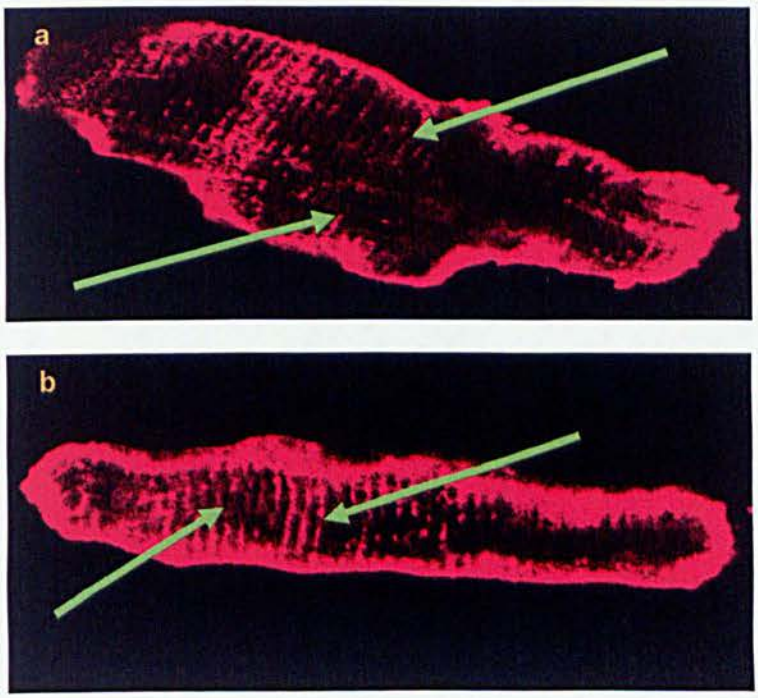

Figure 4.9 T-tubules in WKY ventricular myocytes stained with di-8ANEPPS. The striations in di-8ANEPPS stained ventricular myocytes **(a)** and **(b)** are t-tubule membranes annotated by green arrows.

4.6.10 T-tubules in WKY rat atrial myocytes

A sparse network of TATS can be observed in WKY left atrial cells (annotated by a white arrow) stained with di-8ANEPPS, however in the narrower right atrial cells, no t-tubule network was detected (Figure 4.10).

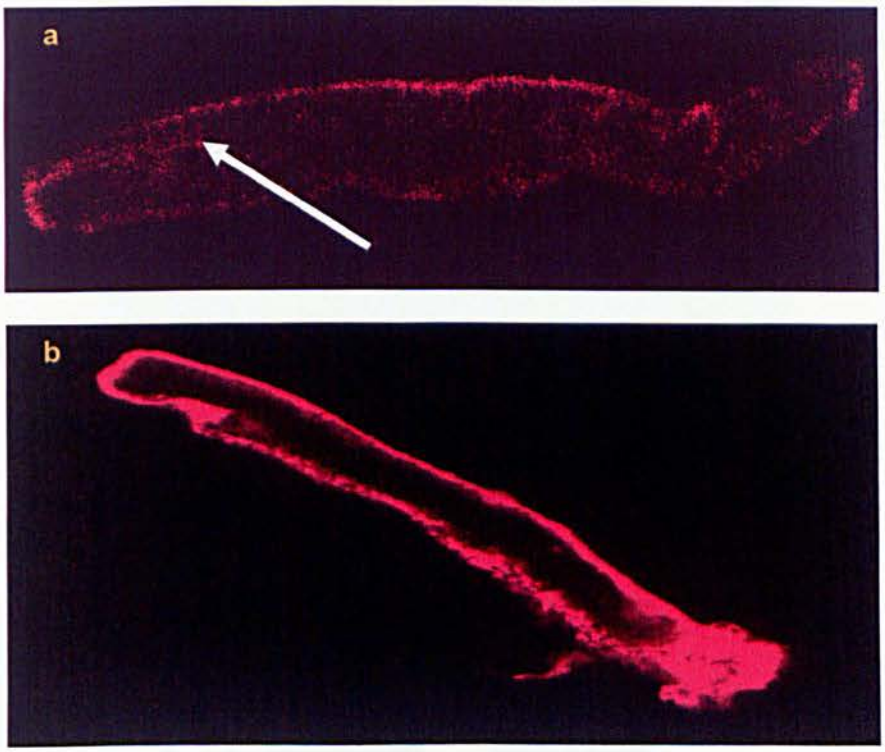

Figure 4.10 Single isolated WKY rat atrial myocytes labelled with di-8ANEPPS. **(a)** The left atrial myocyte shows some evidence of TATS annotated by the white arrow and **(b)** right atrial myocyte shows no evidence of TATS.

4.6.11 Calcium sparks originating from centre of atrial cells

Calcium sparks in atrial cells are initiated both on the cell periphery and from the central region of the myocyte and the frequency of the calcium sparks at each location depends on the size of the atrial cells. Left atrial cells are wider on average than right atrial cells (13.6 ± 0.3 μm compared to 9.9 ± 0.25 μm) and this means that a greater distance needs to be travelled to carry depolarisation across the width of the cardiomyocyte. As shown for the left atrial cell (Figure 4.11), some calcium sparks (51%) originate in the centre of the cell and this may be due to the presence of TATS (which are more likely to exist in left atrial cell than right).

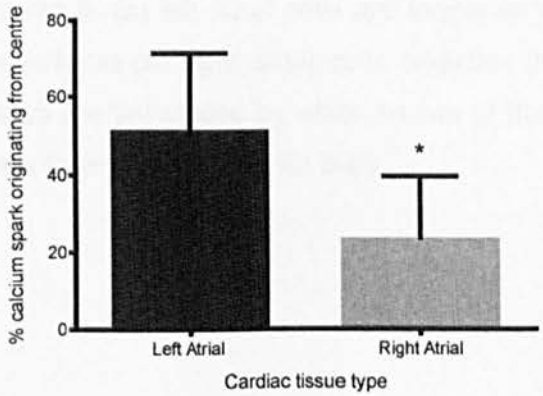

Figure 4.11 Percentage frequency of calcium sparks originating from centre of atrial cells. It was observed that 51% of calcium sparks occurring in the left atrial cells originated from the centre whereas 23% of calcium sparks in right atrial cells occurred in the centre of the cells (n = 6 and 5 respectively where n = number of cells ; *p = 0.03) and error bars signify S.E.M.

The following calcium fluorescent images (Figure 4.12) of atrial myocytes show examples of calcium sparks originating from the centre of the left atrial cell and calcium sparks being triggered from the periphery of the right atrial cell.

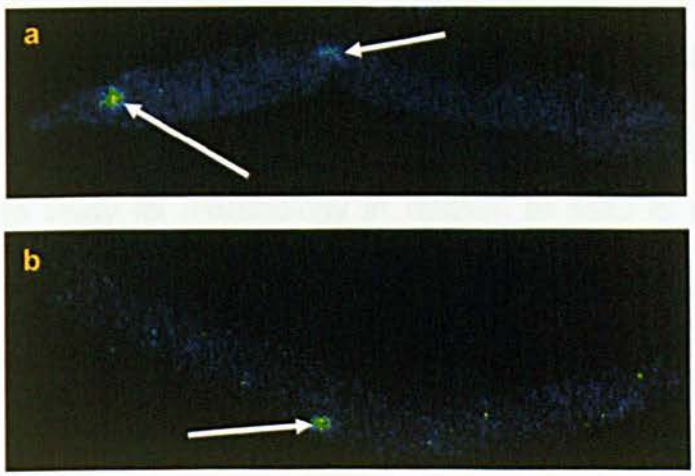

Figure 4.12 Initiation sites of spontaneous calcium sparks in atrial cells. The majority of calcium sparks in **(a)** left atrial cells are triggered from the centre however most of the calcium sparks in **(b)** right atrial cells originate from the periphery of the cell. The calcium sparks are annotated by white arrows in these confocal images and are observed as intense fluorescent-coloured blips.

4.7 Discussion

AF is the most commonly occurring type of cardiac dysrhythmia in the human population, currently affecting nearly 2% of the UK population according to the British Heart Foundation (BHF). However not much is known regarding whole cell calcium transient formation and EC coupling in the atria, unlike for the well-studied ventricles. The focus here has therefore been on the atrial cardiomyocyte to study its morphology in relation to sites of calcium release which contributes to cardiac contraction and which may be relevant to the spontaneous calcium release characteristic of arrhythmias.

Bell and colleagues (2004) have previously shown that SHR rats have heavier hearts compared to WKY which is consistent with the findings of this study. The mean weight of WKY hearts was found to be significantly lighter than for SHR hearts. This is possibly due to the thicker muscle of the left ventricular walls of the SHR rat hearts that produces more effort to pump blood out to the rest of the body (Freestone *et al.*, 1996 ; Shorofsky *et al.*, 1999 ; Bell *et al.*, 2004).

To our knowledge, this study is the first to have specifically separated out the right and left atrial tissue for comparison purposes. Both left and right SHR atrial tissue weighed less than the left and right WKY atrial tissue which suggests that there might have been significant cell death in this pathological state. A similar observation was reported by Sonnenberg and colleagues (1983) who did not specify the specific atrial tissue they used but reported the wet weight of the SHR atria was 295 mg and observed to be smaller and shrunken compared to the wet weight of the WKY atria at 386 mg. The loss of tissue mass of the SHR atria may be due to the constant and long term release

of the atrial natriuretic hormone factor (ANF) in SHR rats which results in death of atrial tissue (Sonnenberg *et al.*, 1983).

To add to the novel aspect of this study, the isolated left and right atrial myocytes have been specifically separated out unlike the other groups (Kirk *et al.*, 2003 ; Dibb *et al.*, 2009 ; Smyrnias *et al.*, 2010 ; Richards *et al.*, 2011). The average length of the single isolated SHR left atrial cells was significantly longer than that of the WKY left atria though there were no significant differences between the widths of these respective cells. This may account for the progressively longer process of cell shortening that occurs in SHR left atrial cells than in WKY (McCrossan *et al.*, 2004). SHR left atrial cells also need to work against a higher arterial pressure whereas the SHR right atrial cells might not experience this pressure increase greatly. Additionally there was no significant difference between the length of the SHR and WKY right atrial cells although the average width of SHR left atria was significantly wider than that of the SHR right atrial myocyte. This is possibly due to the higher pressure and hence higher workload subjected to the SHR left atria compared to the SHR right atria.

Ventricular cells were observed to be large rod-shaped like myocytes as previously described by Freestone and colleagues (2000). Upon staining with di-8ANEPPS, t-tubules were observed clearly in WKY and SHR ventricular cells. Bell and colleagues (2004) showed an average rat ventricular cell width of 26.1 ± 0.95 μm and an average rat ventricular cell length of 137.5 ± 5.53 μm. In this study, the ventricular myocytes were found to have an average width of

26.1 ± 1.71 μm and an average length of 149.5 ± 5.07 μm whereby the width measurement is similar to that reported by Bells' group (2004).

Many studies have shown that rat atrial cells do not possess a well organised t-tubular system as observed in mammalian ventricular cardiomyocytes (Tidball *et al.*, 1991 ; Woo *et al.*, 2002 ; Kirk *et al.*, 2003). Instead they posess TATS which perform the same task as the t-tubular system of the ventricular cells (Kirk *et al.*, 2003 ; Dibb *et al.*, 2009 ; Louch *et al.*, 2010; Smyrnias *et al.*, 2010). This shows that the action potential is still being propagated by the t-tubules deep into the cell to facilitate EC coupling. It has been shown that there is a correlation between the atrial cell widths and the quantity of t-tubules present in large mammals such as sheep, cow and horses (Richards *et al.*, 2011). Usually the wider the cells, then the more the t-tubules are present. These studies (unlike this present study) however did not analyse the extent of the t-tubular system separately in left and right atrial myocytes.

In this study, it has been discovered that the left rat atrial cells accounted for the majority of the wider atrial cells and in comparison the right rat atrial cells were significantly narrower. This observation has not been shown in previous literature. The atrial widths obtained by Kirk and colleagues (2003) are the most similar to the mean left atrial width obtained from this study. This indicates that in the rat, left atrial cells are wider than right atrial cells and show signs of possessing a tubular network which is required to facilitate EC coupling. The wider rat atrial myocytes consistently possess a tubular network to cause depolarisation-triggered calcium release over the larger distances compared to

the narrower cell where presumably calcium diffusion alone is significant to activate the myofilaments.

Furthermore, t-tubular systems have also been reported to alter in health and disease. Human atrial cells have mostly been studied in a pathological setting. However in the occasional studies where cardiomyocytes have been obtained from patients with normal heart rhythm, it has been shown that t-tubule networks are present in 69% of the atrial myocyte populations studied (Richards *et al.*, 2011). Healthy human atrial cells have been studied by Aptel and colleagues (2002) who showed evidence of two populations of calcium sparks occurring spontaneously, one being larger than the other. During AF, calcium handling is disrupted which suggests that the t-tubule membranes may be damaged in this pathophysiological state.

It was also noted in this study on WKY rats that the calcium sparks are statistically significantly more likely to originate from the centre of the left atrial myocytes compared to right atrial myocytes. It is also statistically significantly more likely that calcium sparks occur in the periphery of right atrial myocytes compared to the left. In the left atrial myocyte of the rat, 51% of calcium sparks occurred in the centre of the cell compared to 23% of calcium sparks that occurred in the centre of right atrial myocytes. It is likely then that left atrial myocytes have more calcium sparks deep within the cells because of a more developed t-tubule system compared to the right atrial myocytes (Kirk *et al.*, 2003 ; Smyrnias *et al.*, 2010).

4.8 Conclusion

- The majority of wider atrial cells are left atrial cells that possess TATS and the narrower atrial cells are right atrial cells that have no TATS.

- Left atrial cells had more calcium sparks originating from the centre of the cell body whereas right atrial cells had calcium sparks occurring mostly on the cell periphery. This may be relevant to the spontaneous calcium release characteristic of arrhythmias.

It may therefore be worthwhile to also quantitatively investigate the effect of health and disease on calcium handling proteins that regulate myocardial contractility in EC coupling.

CHAPTER 5

Cardiac calcium handling proteins:Abundance in normal and diseased states and regional specificity

5.0 Cardiac calcium handling proteins : Abundance in normal and diseased states and regional specificity

5.1 Introduction

Cardiac contractility is modulated by changes to intracellular calcium handling which can occur, for example by the binding of stimulatory agonists to the β-ARs. In healthy hearts, the Gs protein coupled β-ARs on the cell membrane are activated by stimulants such as catecholamines. This in turn activates AC and increases the intracellular level of cAMP (Levitzki, 1988). The rise in cAMP activates the cAMP-dependent PKA which phosphorylates a series of vital cardiac calcium handling proteins.

These proteins include PLB, a protein of the SR, which regulates the activity of SERCA2a, the calcium pump on the SR membrane (Kiss *et al.*, 1997 ; Bokník *et al*,. 1999 ; MacLennan and Kranias, 2003), RyR2, the cardiac isoform of the calcium release channel of the SR (Marx *et al.*, 2000 ; Eschenhagen, 2010) and voltage-gated LTCCs that enable calcium entry into the cell upon depolarisation (Gómez *et al.*, 1997). The phosphorylation of these calcium handling proteins causes an increase in calcium mobilization. In particular phosphorylation of PLB increases the activity of SERCA2a resulting in positive lusitropic effects and loading of the SR with greater amounts of calcium (Bokník *et al.*, 2001). A larger SR calcium load is associated with increases in calcium transient amplitude as a consequence of subsequent calcium release from the SR. Abnormalities in cardiac calcium handling protein function can occur in various disease states and the normal interaction within the cardiac signalling pathways

associated with contraction is disrupted and may result in deterioration of cardiac muscle function.

5.1.1 SERCA2a

Upon the depolarisation of cardiac cells, calcium is released from the SR in response to trigger calcium entry via sarcolemmal calcium channels. The transient elevation in intracellular calcium concentration that occurs enables cardiac contraction. SERCA2a is a 100 kDa protein that is vital in this process as it enables cardiac relaxation when it pumps calcium back into the SR thus refilling the SR for the next cardiac contraction event.

The activity of the SR calcium pump is dependent upon the binding of the reversibly phosphorylated PLB (MacLennan and Kranias, 2003). When PLB is dephosphorylated, SERCA2a activity is inhibited. Lower levels of PLB in the heart have been reported to be associated with increases in the levels of activity of SERCA2a and calcium content in the SR (Santana *et al.*, 1997 ; Brittsan and Kranias, 2000). This suggests that basal cardiac contraction and SR calcium content are influenced by the relationship between PLB and SERCA2a. SERCA2a and PLB expression differs between different heart chambers. For example, the abundances of SERCA2a and PLB differ in atria and ventricles of various species (such as mice and rats) with faster relaxation occurring in the basal state in atria due to the increased levels of SERCA2a and lower amounts of PLB found in this tissue (Freestone *et al.*, 1999).

5.1.2 Total and phosphorylated PLB

PLB is a reversible regulator protein of the SR calcium cardiac pump whose function is altered during β-AR activation (MacLennan and Kranias, 2003). When it is in a dephosphorylated state it inhibits the activity of the calcium pump. Following its phosphorylation by PKA or calcium/CaM kinase II, the inhibition exerted by PLB is then relieved and cardiac relaxation is enhanced (MacLennan and Kranias, 2003). Dephosphorylation by PP1 converts PLB back to its native state. PLB has been of great interest due to its regional specific expression in cardiac tissues in human and murine models (Bokník *et al.,* 1999).

However, it is obvious in the existing literature, that there is variability in the current western blotting methods for the detection of PLB in both its native and phosphorylated forms. Studies have reported on the 25 kDa pentameric form of this protein (Bokník *et al.*,1999 ; Lüss *et al.*,1999) and also the 6 kDa monomeric form (Wegener and Jones, 1984; Wientzek and Katz, 1991 ; Fallavollita *et al.*, 1999). The latter was obtained by exposing cardiac tissue homogenates to high temperature (95°C) which aids the denaturing process of the protein structure.

Nevertheless PLB protein abundance has been reported to vary in different chambers of the heart depending on the chamber the tissues have originated from (Bokník *et al.*, 1999). Changes in PLB expression and hence a disturbance to the PLB-SERCA2a interaction has been linked to cardiac pathophysiological conditions such as arrhythmias and HF. A deficiency of PLB

in the heart causes faster relaxation, gradual increase in inotropism and eventually increasing work load upon the heart (Koss and Kranias, 1996).

The phosphorylation of PLB occurs at 2 specific sites namely Ser16 and Thr17 which are triggered by β-adrenergic stimulation (Wegener *et al.*, 1989). Ser16 is phosphorylated by cAMP-dependent PKA whilst Thr17 is phosphorylated by calcium/CaM kinase II. The abundances of PLB and phosphorylated versions of PLB vary between normal hearts and hypertensive hearts (Bokník *et al.*, 1999 ; Mills *et al.*, 2006). However there are inconsistencies in the literature regarding the abundances of phosphorylated PLB in each cardiac chamber under different physiological and pathophysiological conditions. For example, Renna and colleagues (2006) observed that levels of phospho-Ser16 and phospho-Thr17 were higher in WKY ventricular tissues compared to SHR ventricular tissues. On the other hand, Bokník's group (2001) reported no differences in the expression of phospho-Ser16 between these two conditions however the expression of phospho-Thr17 was found to be higher in SHR ventricular tissues compared to WKY normotensive tissues as a result of more active CaM Kinase II in hypertensive rat models.

5.1.3 Total and phosphorylated RyR2

During CICR, an influx of extracellular calcium into the cell causes calcium release from the SR via the calcium release channel (Fabiato and Fabiato, 1978). This calcium channel is RyR2, the 565 kDa cardiac isoform of RyR (Nakai *et al.*, 1990). RyR2 has 3 established phosphorylation sites ; (i) Ser-2808 found in humans and rats is phosphorylated by PKA and CaM kinase II and is dephosphorylated by PP1 (Witcher *et al.*, 1991) ; (ii) Ser-2814 located in cardiac tissues of humans and rodents is phosphorylated by CaM kinase II and dephosphorylated by PP1 and (iii) Ser-2030 which is also located in humans and rat cardiac tissues is phosphorylated by PKA and dephosphorylated by PP1 (Xiao *et al.*, 2006).

The phosphorylation of RyR2 at the Ser-2808 site triggered by an elevation in circulating catecholamines is the main functional cause of enhanced calcium release from the SR via the RyR2 channel (Wehrens *et al.*, 2006 ; Eschenhagen, 2010) resulting in augmented cardiac contraction. However, an alteration of the protein function may cause dysfunctionality in the regulation of calcium flow from the SR during HF (Eschenhagen, 2010). The catecholamines (adrenaline and noradrenaline) which are present at elevated levels in HF cause the RyR2 to be hyperphosphorylated at the Ser-2808 site leading to uncontrolled calcium leakage from the SR which may result in reduced cardiac contractility, cardiac arrhythmias and eventually sudden cardiac death (Laitinen *et al.*, 2001 ; Wehrens *et al.*, 2006 ; Eschenhagen, 2010 ; Shan *et al.*, 2010).

The calcium handling proteins of the heart that have been mentioned, normally work together during EC coupling to enable SR calcium release and the consequent refilling of the SR. However, abnormalities of calcium handling may lead to malfunction in the contraction of the heart and hence contribute to the pathophysiology of cardiac diseases.

5.2 Aim of study

The objective is to investigate whether there are any significant differences in protein levels of the various calcium handling proteins in each of the cardiac chambers of WKY and SHR rats and in tissues derived from a volume overload model of HF (by aorto-caval shunt) and their sham-operated controls.

5.3 Materials

All materials obtained are as described in Chapter 2 with the following addition, the HiMark™ Pre-Stained High Molecular Weight protein standard (Invitrogen) was purchased from Life Technologies Ltd whereas the Precision Plus Protein™ Kaleidoscope™ standard was obtained from BioRad Laboratories, Inc.

5.4 Methods

5.4.1 Animals

WKY, SHR and shunt and sham-operated rats were sacrificed as described in Chapter 2.

5.4.2 Preparation of cardiac tissue homogenates

Cardiac tissues from WKY, SHR and shunt and sham-operated tissues were prepared and homogenised as previously described in Chapter 2.

5.4.3 Gel electrophoresis and western blotting of pure PLB protein

Pure PLB protein was probed using western blotting to show the linearity of this system in terms of signal intensity as described in Chapter 2.

5.4.4 Gel electrophoresis and western blotting of calcium handling proteins in cardiac homogenates

Western blotting was carried out to determine the presence of and to quantify the following calcium handling proteins in rat cardiac tissues; total and phosphorylated versions of PLB, SERCA2a and total and phosphorylated versions of RyR2. Cardiac homogenates were 'boiled' at 95°C initially for 5 mins and for the subsequent experiments the same homogenates were warmed at 37°C for 5 mins. Quantification of the protein of interest for all experiments was carried out using a BioRad densitometer (G-800) and the accompanying QuantityOne software.

5.4.4.1 SERCA2a

A polyacrylamide gel concentration of 9% was used for the detection of SERCA2a (110 kDa). Gel electrophoresis was carried out as previously described. A PVDF membrane which was pre-wetted with methanol was used to transfer the protein samples from the gel body. The blocking solution used was 3% BSA in a 0.1% Tween 20 buffer solution. The primary antibody used was a polyclonal SERCA2a antibody (1 : 5000) and the secondary antibody was a polyclonal anti-rabbit antibody (1 : 1000). SERCA2a was normalised by α-actinin (100 kDa) (1 : 1000). Protein detection and band intensities were quantified as before.

5.4.4.2 PLB recovery when rat ventricular homogenates are subjected to boiling or non-boiling

One group of left and right rat ventricular homogenates were subjected to 95°C and the other group subjected to 37°C for 5 mins before being loaded onto the polyacrylamide gel (15%) which included 6 M urea. The samples were electrophoresed at 200 V before being transferred to a PVDF membrane pre-wetted in methanol. Following the semi-dry transfer of the proteins onto the PVDF membrane, the latter was immersed and incubated with a blocking solution of 5% milk in 0.1% Tween 20 buffer solution. The membrane was incubated at 4°C overnight with a specifically labelled antibody for PLB (1 : 5000) and the secondary antibody was polyclonal IgG anti-mouse (1 : 5000). PLB was normalised by GAPDH (37 kDa) (1 : 1000). Quantification of the protein of interest was carried out as previously described.

5.4.4.3 Total PLB and phosphorylated PLB

The abundance of PLB, phospho-Ser16 and phospho-Thr17 (25 kDa) was analysed by western blotting where a polyacrylamide gel (15%) including 6 M urea was used. The protein samples were loaded and electrophoresed as previously discussed before being transferred to a PVDF membrane pre-wetted in methanol to enable absorption of the transfer buffer. Following the semi-dry transfer of the proteins onto the PVDF membrane, the latter was immersed and incubated with a blocking solution of 5% milk in 0.1% Tween 20 buffer solution for PLB and phospho-Thr17 or 3% BSA in 0.1% Tween 20 buffer solution for phospho-Ser16 on a reciprocating shaker. The membrane was incubated at 4°C overnight with a specifically labelled antibody for PLB (1 : 5000). Phosphorylation specific antibodies, phospho-Thr17 (1 : 5000) and phospho-Ser16 (1 : 5000) were also used in other samples. The secondary antibody used was a polyclonal IgG anti-mouse (1 : 5000) for PLB and a polyclonal IgG anti-rabbit (1 : 1000) for phospho-Ser16 and phospho-Thr17. The labelled antibody was detected by HRP enzyme using a luminol substrate that shows up a signal showing the expression of the protein of interest during the chemiluminescence protein detection process as previously explained in Chapter 2. Total PLB and its phosphorylated proteins were normalised by GAPDH (1 : 1000). Quantification of the protein of interest was carried out as previously described.

5.4.4.4 Total RyR2 and phosphorylated RyR2

The relative abundance of total RyR2 and phosphorylated versions of RyR2 (565 kDa) were determined using a polyacrylamide gel concentration of 4.5%. Separated protein samples were transferred onto methanol pre-wetted PVDF membranes. The membrane blots were pre-incubated in 3% BSA in a 0.1% Tween 20 buffer solution. Protein blots were incubated accordingly with total RyR2 (1 : 1000), RyR2 phospho-Ser2808, RyR2 phospho-Ser2814 and RyR2 phospho-Ser2030 antibodies (1 : 1000). Total RyR2 and its phosphorylated proteins were normalised by α-actinin (1 : 1000). The secondary antibody used was a polyclonal IgG anti-rabbit (1 : 1000). Protein detection and band intensities were quantified as previously described.

5.5 Results

5.5.1 SERCA2a : WKY and SHR atrial and ventricular tissues

SERCA2a abundance in WKY tends to be higher than that of SHR cardiac tissues (Figure 5.1). In terms of chamber specific differences in the expression of SERCA2a, there were no significant differences between WKY left and right atria (1.3 ± 0.14 and 1.2 ± 0.12 respectively ; n = 5 and 4 respectively) and WKY left and right ventricles (1.3 ± 0.05 and 1.0 ± 0.03 respectively ; n = 6). The right ventricle had a similar amount of SERCA2a expressed in normotensive and hypertensive tissue (1.0 ± 0.03 and 1.0 ± 0.01 respectively ; n = 6). There was also no significant difference between WKY and SHR left ventricular homogenates (1.3 ± 0.05 and 1.0 ± 0.05 respectively ; n = 6).

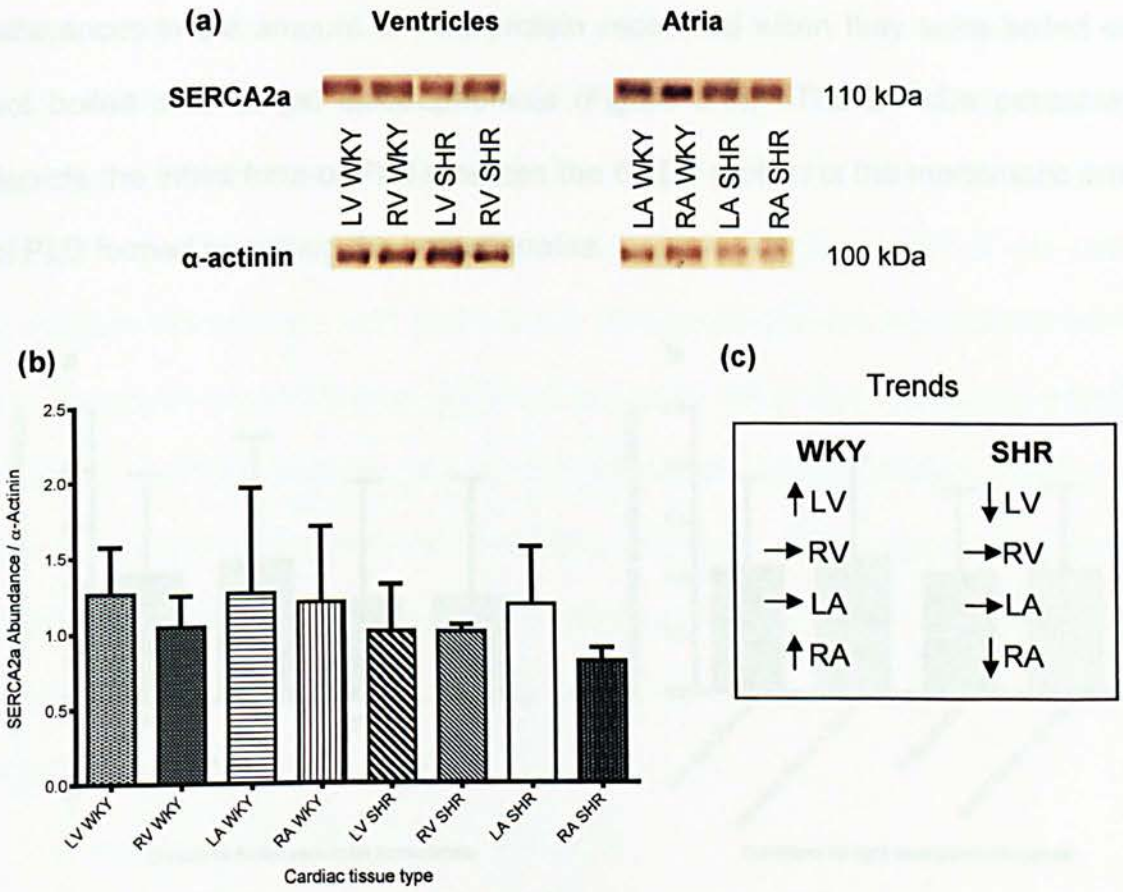

Figure 5.1 Protein expression of SERCA2a in WKY and SHR tissues from all four chambers of the heart. **(a)** and **(b)** representative western blots and chart respectively of SERCA2a in WKY and SHR cardiac tissues. There were no significant differences between the cardiac chambers and the mentioned cardiac conditions (n = 6 for all, except WKY left atrial tissue, n = 5 and right atrial tissue, n = 4). **(c)** Arrows representing trends in the data ; increase (↑), decrease (↓) or no change (→) of protein abundance as comparisons between the two different strains. Combining the atrial samples of both strains and comparing them with the combined ventricular samples would reveal more SERCA2a in atria as previously reported.

5.5.2 Quantification of PLB in boiled and non-boiled cardiac tissue

Both left and right ventricular homogenates showed no significant quantifiable differences in the amount of PLB protein recovered when they were boiled or not boiled prior to gel electrophoresis (Figure 5.3). The 25 kDa pentamer depicts the intact form of PLB whereas the 6 kDa protein is the monomeric unit of PLB formed by boiling the homogenates.

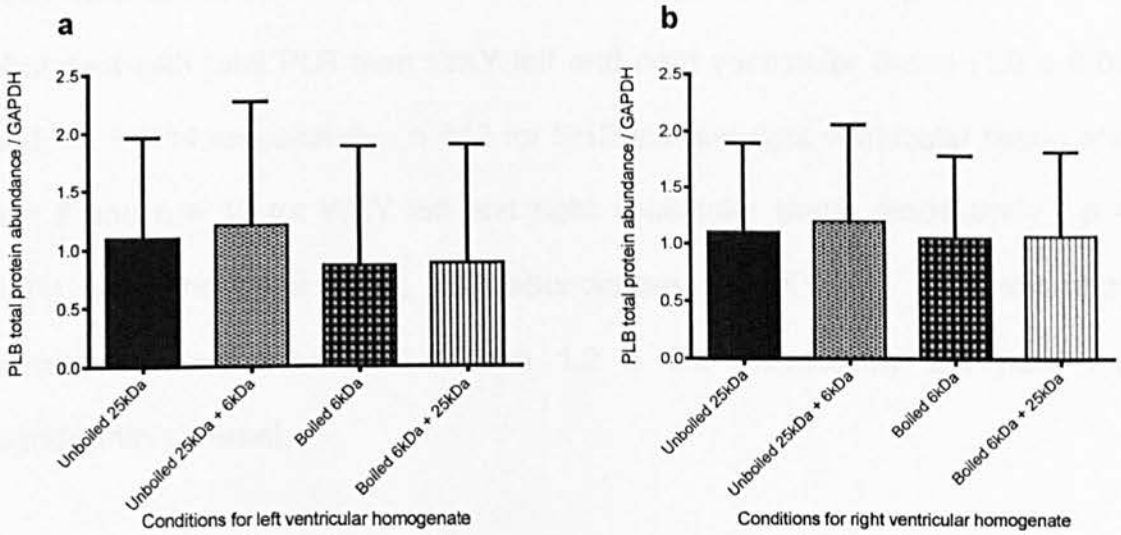

Figure 5.2 Comparison of quantification of PLB in ventricular homogenates subjected to boiling and non-boiling conditions. **(a)** Left ventricular homogenates and **(b)** right ventricular homogenates were treated under boiled and non-boiled conditions and taking into account both monomeric (6 kDa) and pentameric units (25 kDa). There was no significant difference in the amount of PLB protein recovered for both sets of samples.

5.5.3 Total PLB : WKY and SHR atrial and ventricular tissues

The total PLB abundance is elevated in hypertensive tissue (Figure 5.4) compared to normotensive tissue. All PLB bands (25 kDa and if there were 6 kDa) were taken into account. PLB in SHR right atrial homogenate is significantly higher than WKY right atrial homogenate (1.3 ± 0.11 and 0.6 ± 0.14 respectively ; n = 10 and n = 8 respectively ; p = 0.003). SHR left and right ventricular tissue (1.7 ± 0.20 and 1.9 ± 0.19 respectively) are significantly more abundant with total PLB than WKY left and right ventricular tissue (1.0 ± 0.06 and 1.2 ± 0.14 respectively ; n =12 for SHR left and right ventricular tissue and n = 8 and n = 13 for WKY left and right ventricular tissue respectively ; p = 0.01). On the other hand, PLB abundances in WKY and SHR left atrial homogenate were 0.8 ± 0.10 and 1.2 ± 0.2 respectively but were not significantly different.

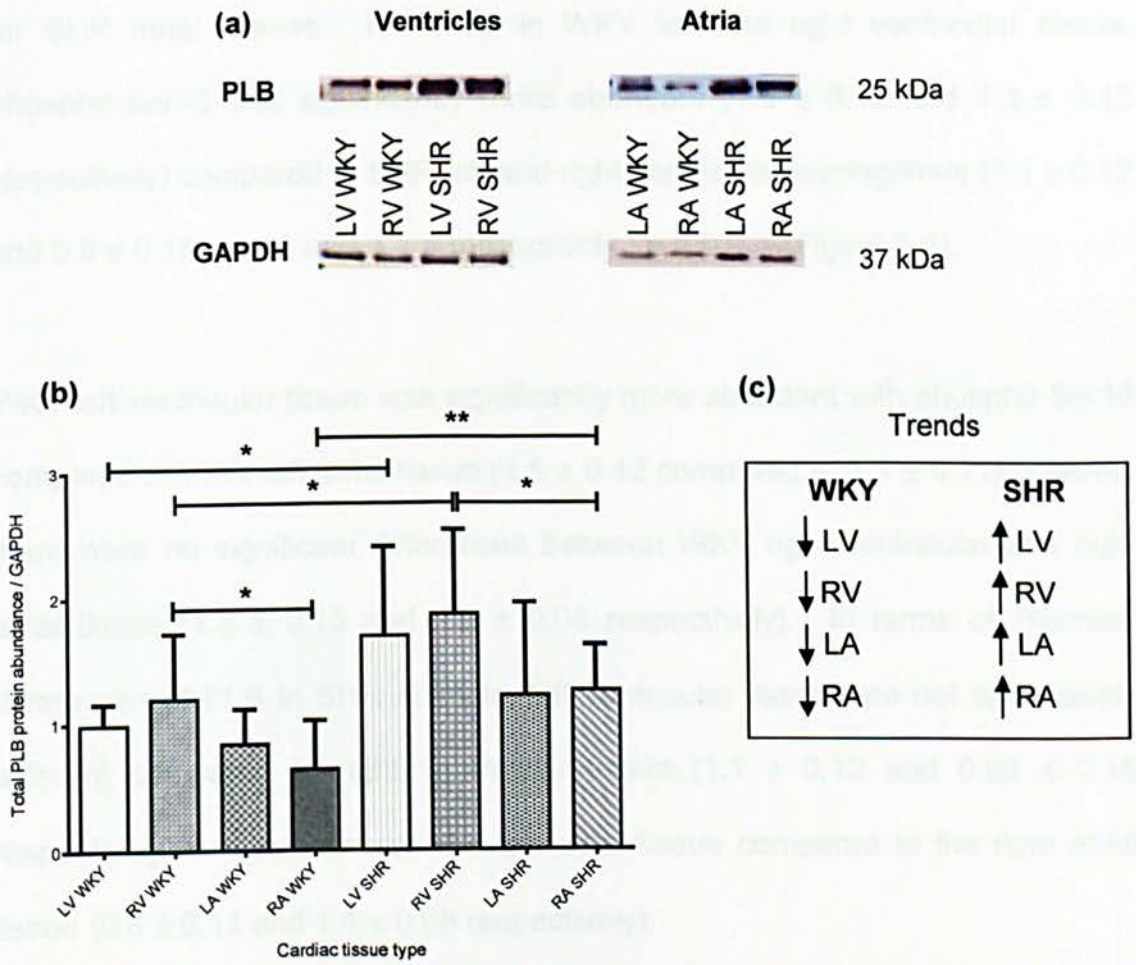

Figure 5.3 Protein expression of total PLB in WKY and SHR tissues from all four chambers of the heart. **(a)** and **(b)** representative western blots and chart respectively of PLB in WKY and SHR cardiac tissues. PLB is more abundant in SHR tissues (n = 12 left and right ventricular homogenates and n = 10 left and right atrial homogenates) compared to WKY tissues (n = 8 and 13 left and right ventricular homogenates respectively and n = 8 left and right atrial homogenates) and in ventricles more than the atria in both rat strains. **(c)** Arrows show trends in the data of protein abundance between the two different strains of rats.

5.5.4 Phospho-Ser16 : WKY and SHR atrial and ventricular tissues

Phospho-Ser16 content in WKY atrial homogenates tended to be higher than for SHR atrial tissues. However, in WKY left and right ventricular tissue, phospho-Ser16 was significantly more abundant (1.5 ± 0.12 and 1.3 ± 0.13 respectively) compared to SHR left and right ventricular homogenate (1.1 ± 0.12 and 0.9 ± 0.16 ; n = 6 and n = 4 respectively ; p = 0.03) (Figure 5.5).

WKY left ventricular tissue was significantly more abundant with phospho-Ser16 compared to WKY left atrial tissue (1.5 ± 0.12 compared to 1.1 ± 0.11) however there were no significant differences between WKY right ventricular and right atrial tissue (1.3 ± 0.13 and 1.2 ± 0.05 respectively). In terms of chamber differences of PLB in SHR animals, left ventricular tissue was not significantly different compared to right ventricular tissue (1.1 ± 0.12 and 0.93 ± 0.18 respectively) and neither was the left atrial tissue compared to the right atrial tissue (0.8 ± 0.11 and 1.1 ± 0.08 respectively).

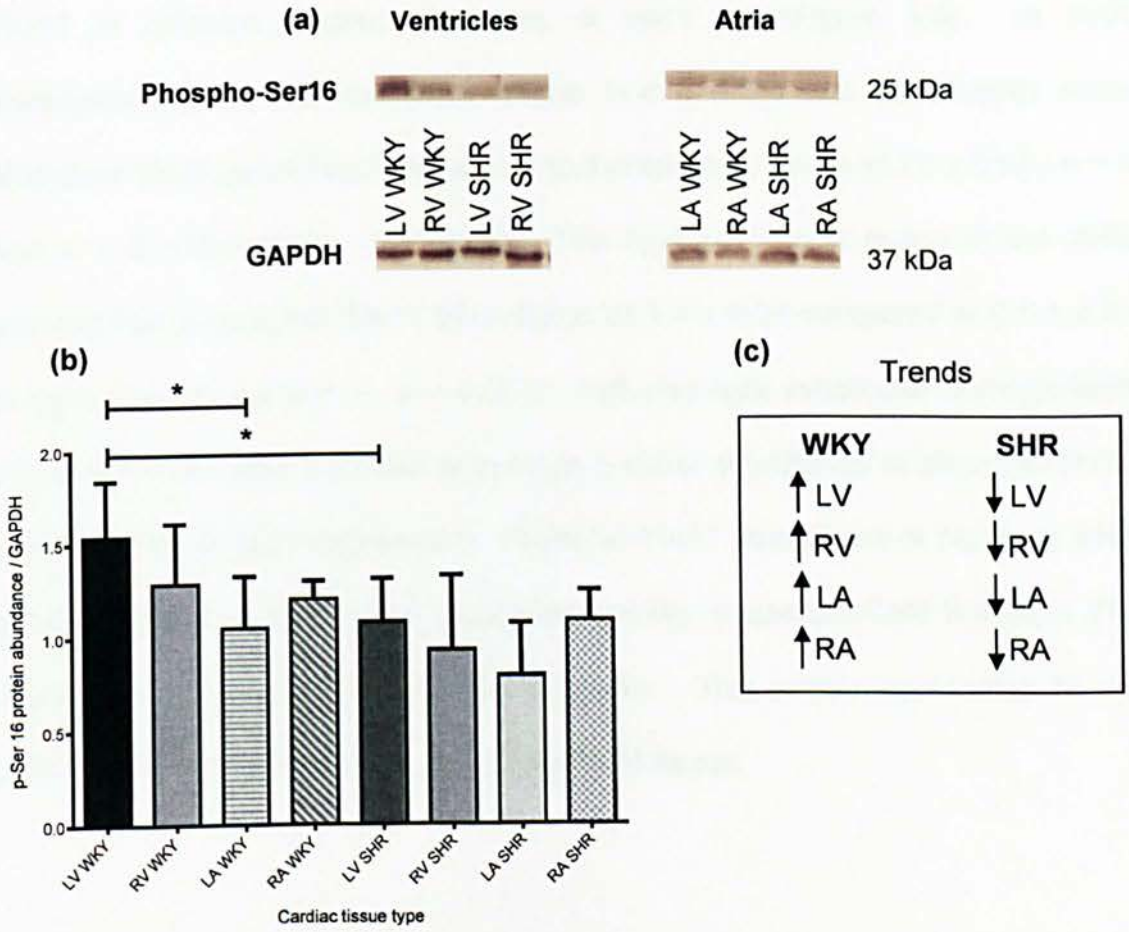

Figure 5.4 Protein expression of phospho-Ser16 in WKY and SHR tissues from all four chambers of the heart. **(a)** and **(b)** representative western blots and chart respectively of phospho-Ser16 in WKY and SHR cardiac tissues. There is a reduction in the expression of phospho-Ser16 in SHR tissues, especially for left ventricular hopmogenate (*$p < 0.1$) because of the inhibition of the protein kinase pathway causing extra tissue growth of the hypertrophied heart. **(c)** Arrows show trends in the data of protein abundance between the two different strains of rats.

5.5.5 Phospho-Thr17 : WKY and SHR atrial and ventricular tissues

There were no significant differences between the abundances of phospho-Thr17 in different cardiac chambers of WKY rat (Figure 5.6). In SHR homogenates, the left ventricular tissue (1.4 ± 0.25) was significantly more abundant in phospho-Thr17 compared to the left atrial tissue (0.76 ± 0.09 ; n = 3 and n = 6 respectively ; p = 0.02). The right ventricular tissue of the SHR animals had a phospho-Thr17 abundance of 1.4 ± 0.08 compared to 0.8 ± 0.01 in right atrial tissue (n = 3 ; p = 0.001). Left and right ventricular homogenates of the WKY rat have a tendency to have a lower abundance of phospho-Thr17 compared to its SHR counterpart. Phospho-Thr17 abundance is higher in SHR ventricular tissues due to the increased activity of calcium/CaM Kinase II that results in an increase in calcium re-uptake. This action contributes to the pathological alterations that occur in the SHR tissue.

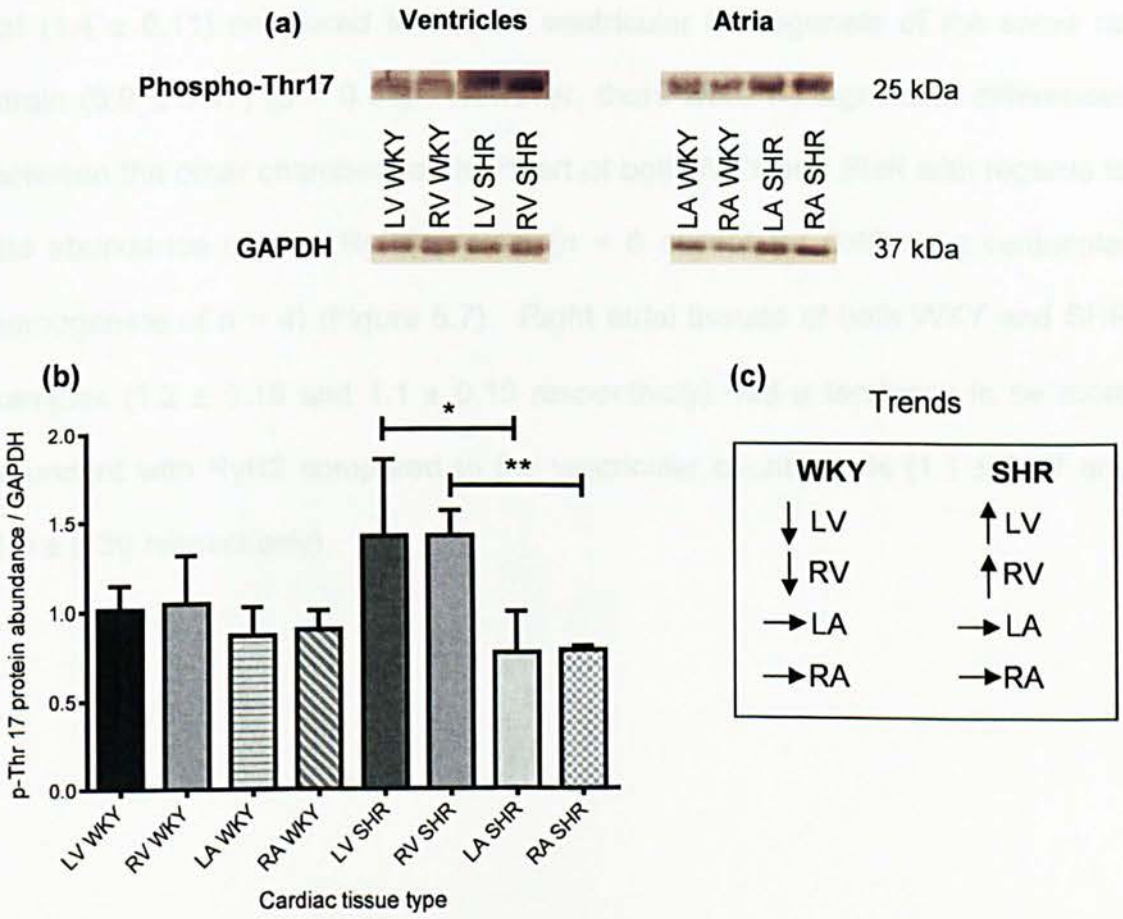

Figure 5.5 Protein expression of phospho-Thr17 in WKY and SHR tissues from all four chambers of the heart. **(a)** and **(b)** representative western blots and chart respectively of phospho-Thr17 in WKY and SHR cardiac tissues. There were no significant differences of phospho-Thr17 abundance in WKY cardiac chambers unlike the SHR homogenates where the right and left ventricles had significantly higher abundance of this protein compared to the right and left atria (**p = 0.001 and *p = 0.02 respectively). This suggests a faster calcium reuptake in SHR tissues. **(c)** Arrows show trends in the data of protein abundance between the two different strains of rats.

5.5.6 Total RyR2 : WKY and SHR atrial and ventricular tissues

Total RyR2 was significantly more abundant in left atrial homogenate of WKY rat (1.4 ± 0.11) compared to the left ventricular homogenate of the same rat strain (0.9 ± 0.17) ($p = 0.04$). However, there were no significant differences between the other chambers of the heart of both WKY and SHR with regards to the abundance of total RyR2 protein ($n = 6$ except for SHR right ventricular homogenate of $n = 4$) (Figure 5.7). Right atrial tissues of both WKY and SHR samples (1.2 ± 0.18 and 1.1 ± 0.18 respectively) had a tendency to be more abundant with RyR2 compared to the ventricular counterparts (1.1 ± 0.17 and 1.0 ± 0.39 respectively).

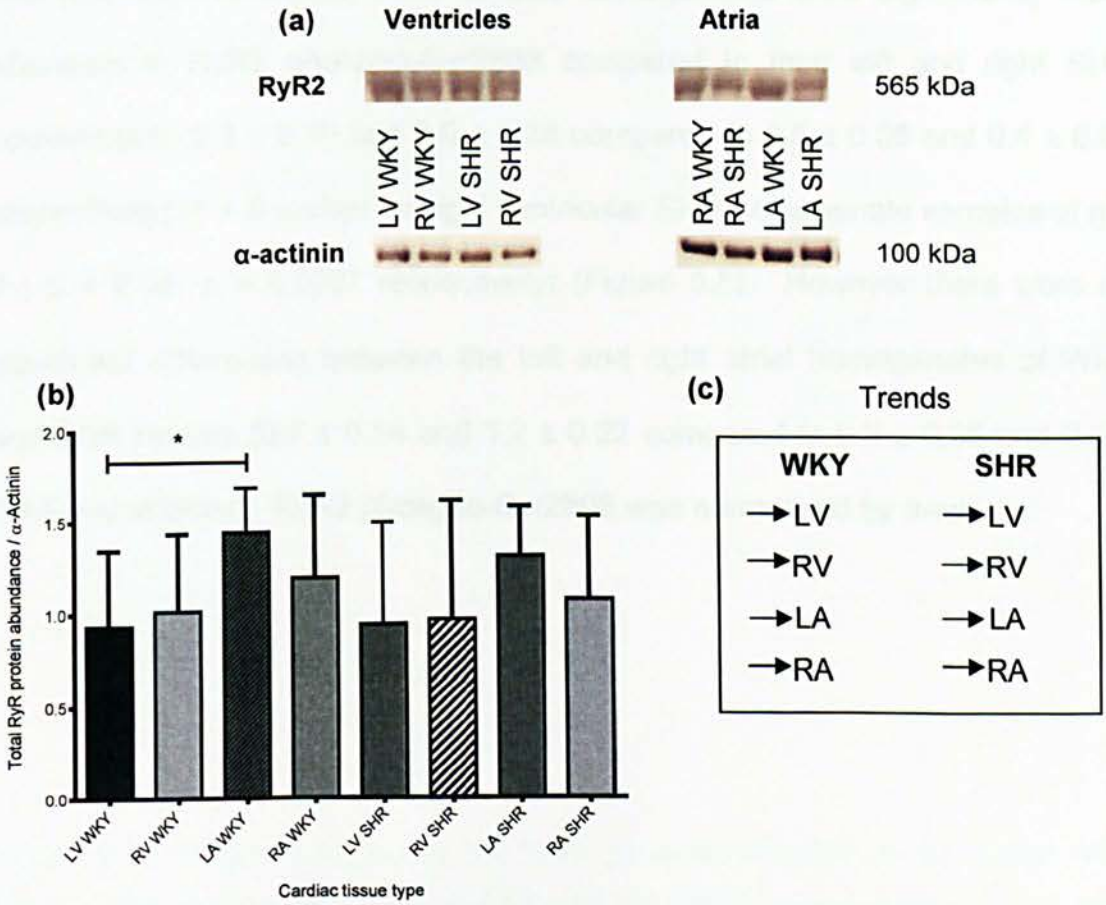

Figure 5.6 Protein expression of total RyR2 in WKY and SHR tissues from all four chambers of the heart. **(a)** and **(b)** representative western blots and chart respectively of RyR2 in WKY and SHR cardiac tissues. RyR2 protein expression between the different heart chambers of WKY and SHR conditions did not differ significantly from one another. **(c)** Arrows show trends in the data of protein abundance between the two different strains of rats.

5.5.7 RyR2 phospho-Ser2808 : WKY and SHR atrial and ventricular tissues

Left and right ventricular WKY cardiac homogenates were significantly more abundant in RyR2 phospho-Ser2808 compared to their left and right SHR counterparts (2.3 ± 0.70 and 2.9 ± 0.38 compared to 0.5 ± 0.05 and 0.4 ± 0.06 respectively) (n = 6 except for right ventricular SHR homogenate samples of n = 4 ; p = 0.04, p = 0.0007 respectively) (Figure 5.8). However there were no significant differences between the left and right atrial homogenates of WKY and SHR tissues (0.7 ± 0.14 and 1.2 ± 0.22 compared to 0.9 ± 0.36 and 0.6 ± 0.12 respectively). RyR2 phospho-Ser2808 was normalised by α-actinin.

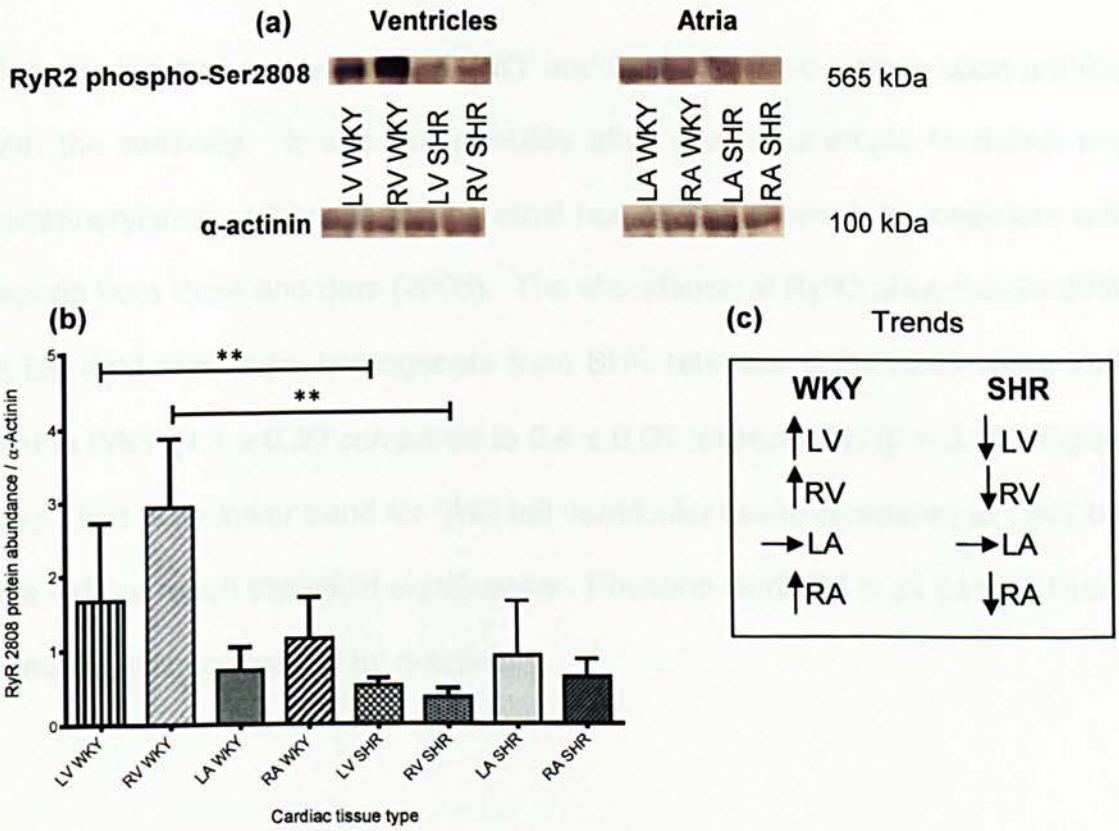

Figure 5.7 Protein expression of RyR2 phospho-Ser2808 in WKY and SHR tissues from all four chambers of the heart. **(a)** and **(b)** representative western blots and chart respectively of RyR2 phospho-Ser2808 in WKY and SHR cardiac tissues. Left and right ventricular WKY homogenates (n =6) contained of the highest amount of RyR2 phospho-Ser2808 whilst the left and right ventricular SHR homogenates (n = 6 and n = 4 respectively) contained of the least amount. **(c)** Arrows show trends in the data of protein abundance between the two different strains of rats.

5.5.8 RyR2 phospho-Ser2030 : WKY and SHR atrial and ventricular tissues

Only ventricular homogenates of WKY and SHR rats gave signals upon probing with the antibody. It was not possible after several attempts to detect any phosphorylation at this site for the atrial homogenates which is consistent with reports from Huke and Bers (2008). The abundance of RyR2 phospho-Ser2030 in the right ventricular homogenate from SHR rats was significantly more than that in WKY (1.1 ± 0.30 compared to 0.4 ± 0.06 respectively) ($p = 0.02$) (Figure 5.9). This is a similar trend for SHR left ventricular tissue compared to WKY but this did not reach statistical significance. Phospho-Ser2030 in all cardiac tissue samples was normalised by α-actinin.

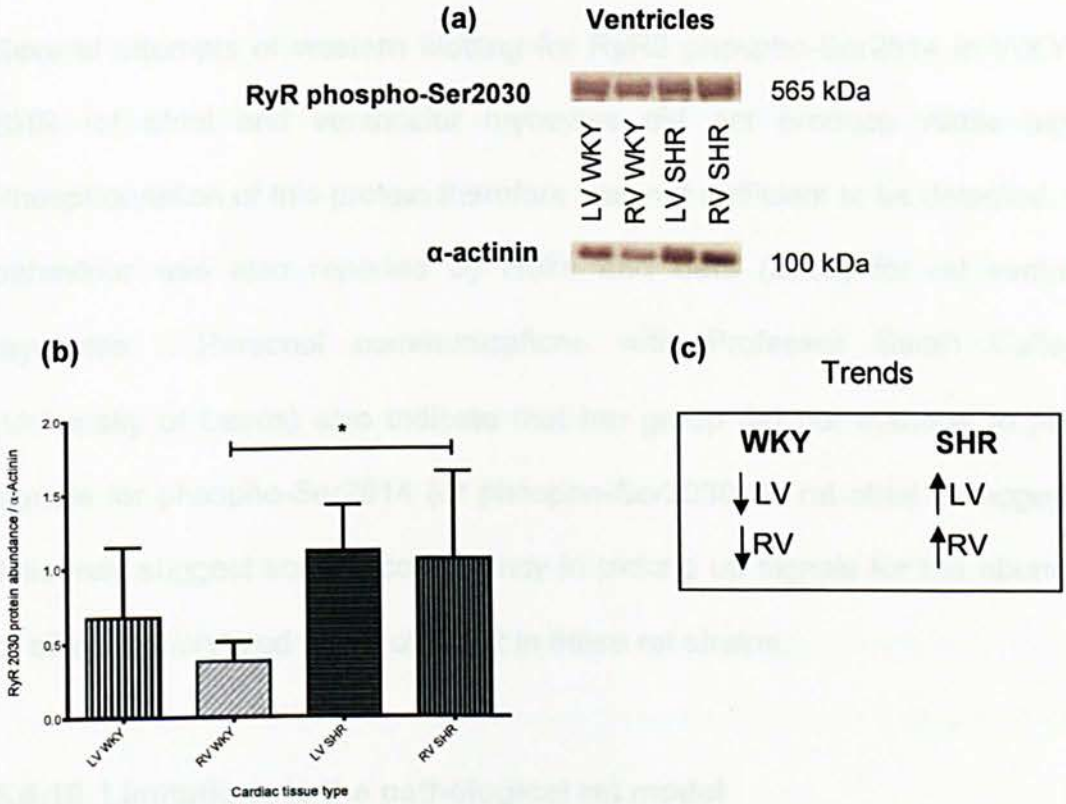

Figure 5.8 Protein expression of RyR2 phospho-Ser2030 in WKY and SHR tissues from all four chambers of the heart. **(a)** and **(b)** representative western blots and chart respectively of RyR2 phospho-Ser2030 in WKY and SHR cardiac tissues. Left ventricular cardiac homogenates (n = 6) tend to be more abundant with RyR2 phospho-Ser2030 compared to the right ventricular homogenates (n = 6). Also, the left and right SHR cardiac tissue (n = 5 and n = 4 respectively) was more abundant with this protein in relation to the WKY counterparts, especially in the case of the right ventricular tissue (*$p < 0.1$). **(c)** Arrows show trends in the data of protein abundance between the two different strains of rats.

5.5.9 RyR2 phospho-Ser2814 : WKY and SHR atrial and ventricular tissues

Several attempts of western blotting for RyR2 phospho-Ser2814 in WKY and SHR rat atrial and ventricular myocytes did not produce viable signals. Phosphorylation of this protein therefore was not sufficient to be detected. This behaviour was also reported by Huke and Bers (2008) for rat ventricular myocytes. Personal communications with Professor Sarah Callaghan (University of Leeds) also indicate that her group did not manage to pick up signals for phospho-Ser2814 (or phospho-Ser2030) in rat atrial homogenates. This may suggest some inconsistency in picking up signals for the abundance of all phosphorylated forms of RyR2 in these rat strains.

5.5.10 Limitations to the pathological rat model

Unfortunately, there was a limitation to the chosen pathological model of the SHR rat since it did not produce the complete set of results for phosphorylated RyR2 proteins (Ser-2030 and Ser-2814). Therefore the volume-overload model of HF rat (shunt) and sham-operated controls (sham) were chosen to further elucidate protein expression and protein phosphorylation differences that may occur in each cardiac chamber in a cardiac disease state. The following results were produced using the same method as for the previous experiments using this experimental model.

5.5.11 SERCA2a : HF atrial and ventricular tissues

The amount of SERCA2a expressed in shunt and sham cardiac tissue as well as between the atria and ventricles did not differ significantly (Figure 5.10). The left and right atria of the sham tissue had an abundance of 1.3 ± 0.18 and 1.1 ± 0.16 respectively whereas the left and right atria of the shunt model had an abundance of 0.7 ± 0.04 and 1.0 ± 0.09 respectively. Left and right atrial sham ventricular tissues had abundances of 1.2 ± 0.02 and 1.0 ± 0.10 respectively compared to their left and right shunt counterparts of 1.1 ± 0.08 and 0.9 ± 0.08 respectively. The order of SERCA2a abundance in the sham tissue chambers was : left atria > left ventricle > right atria > right ventricle whereas in the shunt cardiac tissue it was: left ventricle > right atria > right ventricle > left atria. Combining sham atrial samples and comparing them to pooled sham ventricular samples would show more SERCA2a in atria.

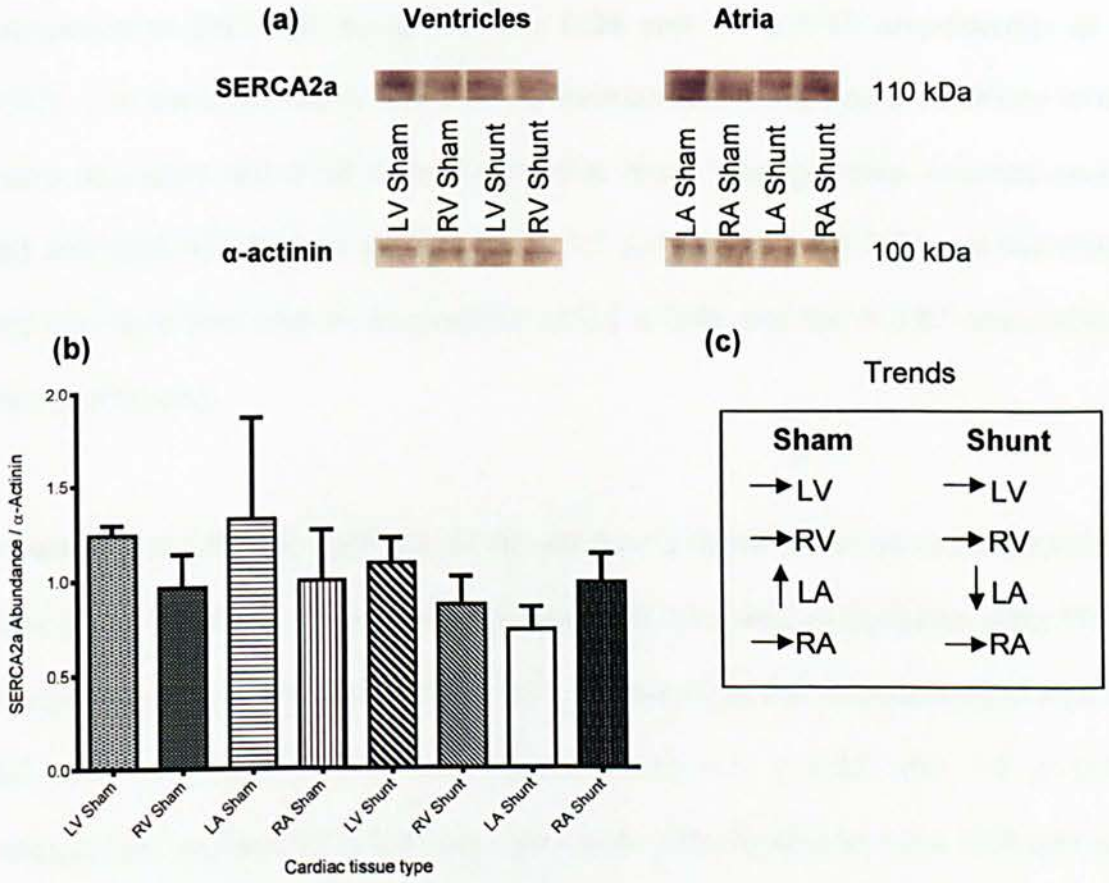

Figure 5.9 Protein expression of SERCA2a in shunt and sham tissues from all four chambers of the heart. **(a)** and **(b)** representative western blots and chart respectively of SERCA2a in shunt and sham cardiac tissues. Sham cardiac tissues were not significantly different to the shunt counterparts (n = 3). **(c)** Arrows show comparisons of protein abundance between tissues of interest.

5.5.12 Total PLB : HF atrial and ventricular tissues

Shunt left ventricular homogenates were significantly more abundant in PLB compared to the sham sample (1.7 ± 0.06 and 1.1 ± 0.15 respectively) ($p < 0.01$). On the other hand, other shunt homogenates only had a tendency to be more abundant with PLB compared to the sham homogenates whereby shunt left and right atria had an abundance of 1.5 ± 0.04 and 1.2 ± 0.23 and the sham left and right atria had an abundance of 0.7 ± 0.40 and 0.6 ± 0.57 respectively (not significant).

However in sham rats, ventricular tissues had a tendency to be more abundant with PLB compared to the atrial tissues and this was comparable with WKY normotensive controls seen previously. For example the abundances of PLB in left and right sham ventricular tissues were 1.1 ± 0.15 and 1.2 ± 0.14 respectively, compared to left and right sham atrial tissues at 1.0 ± 0.34 and 0.9 ± 0.48 respectively. Total PLB abundance in HF atrial tissues was lower in general compared to HF ventricular tissues (Figure 5.11) except for right atrial shunt tissue. PLB was normalised by GAPDH.

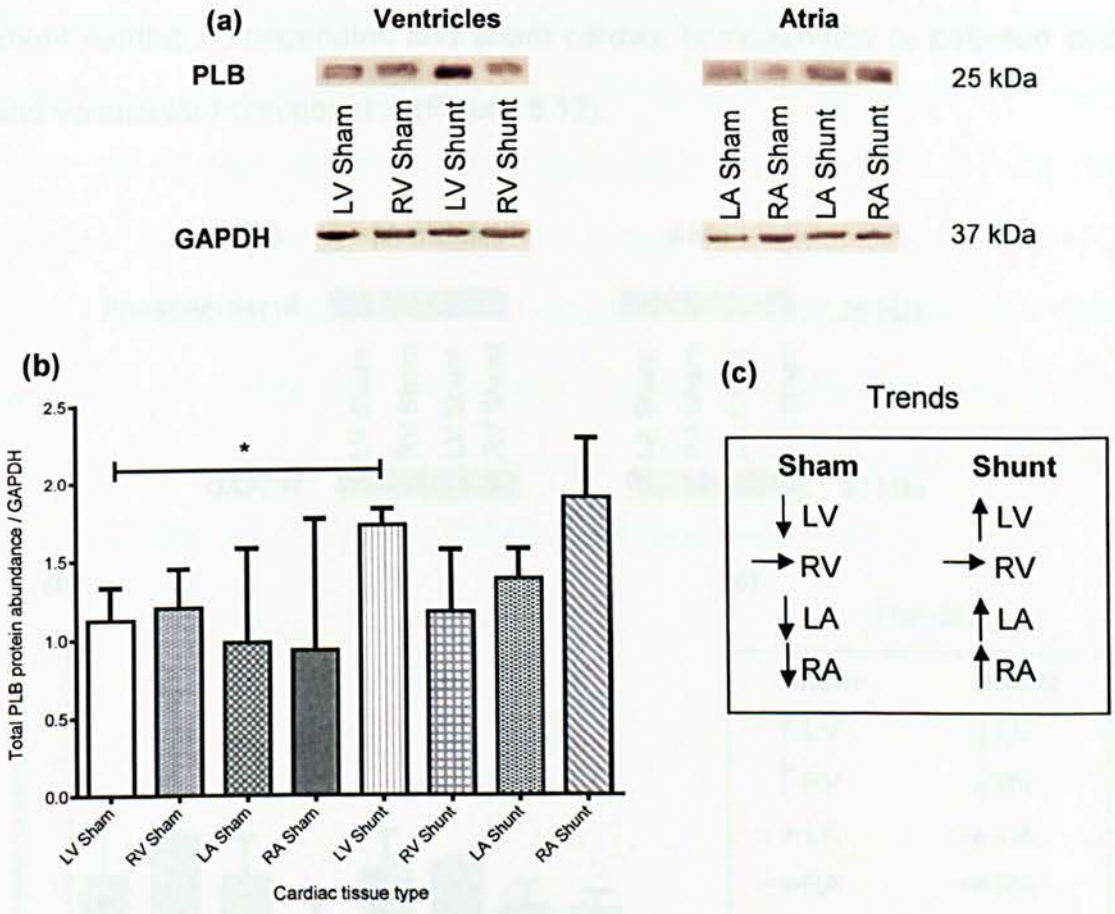

Figure 5.10 Protein expression of total PLB in shunt and sham tissues from all four chambers of the heart. **(a)** and **(b)** representative western blots and chart respectively of PLB in shunt and sham cardiac tissues. Right atrial homogenate subjected to volume-overload HF was the most abundant with PLB whereas the least abundant was right atrial sham tissue (n = 3). **(c)** Arrows show trends in the data of protein abundance between the two different strains of rats.

5.5.13 Phospho-Ser16 : HF atrial and ventricular tissues

There are no significant differences in the abundances of phospho-Ser16 in shunt cardiac homogenates and sham cardiac homogenates or between atrial and ventricular homogenates (Figure 5.12).

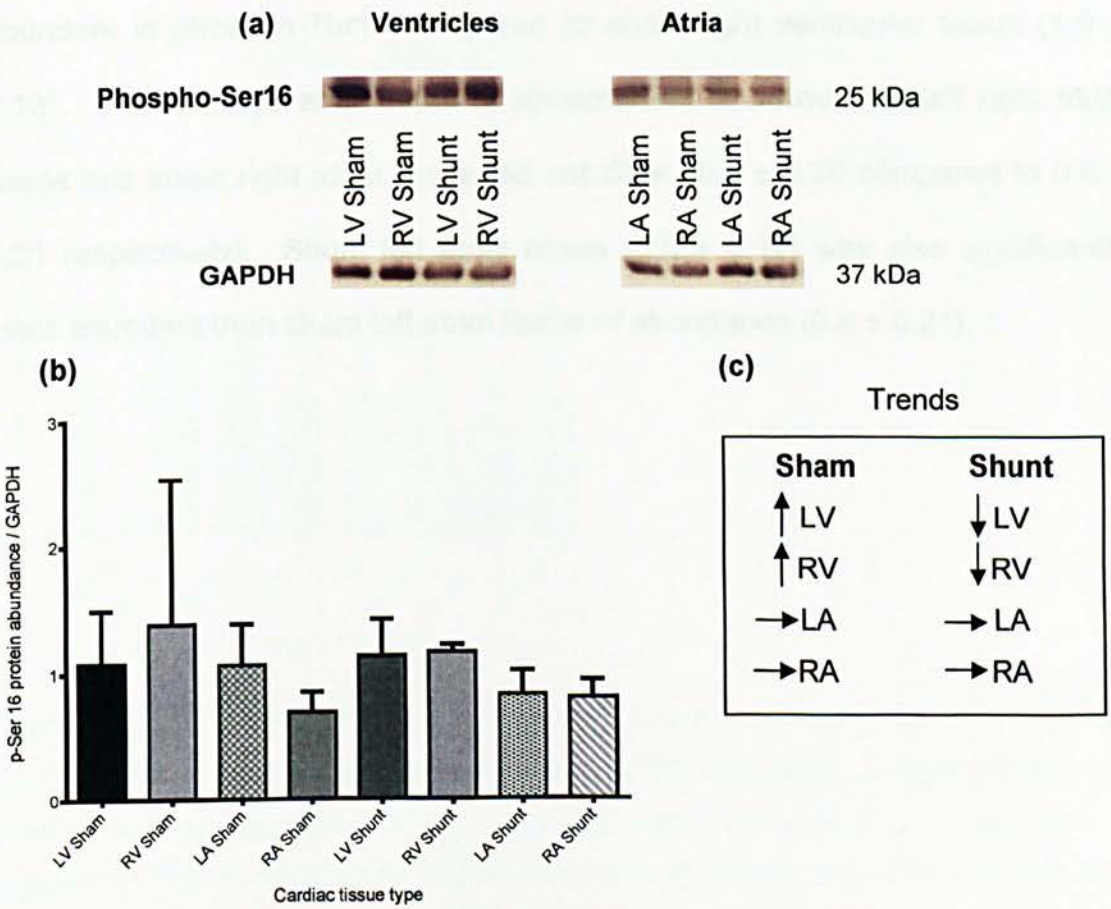

Figure 5.11 Protein expression of phospho-Ser16 in shunt and sham tissues from all four chambers of the heart. **(a)** and **(b)** representative western blots and chart respectively phospho-Ser16 in shunt and sham cardiac tissues. There are no significant differences in phospho-Ser16 between HF and non-HF cardiac tissues (n = 3) **(c)** Arrows show trends in the data of protein abundance between the two different strains of rats.

5.5.14 Phospho-Thr17 : HF atrial and ventricular tissues

The highest abundance of phospho-Thr17 (1.0 ± 0.07) was observed in sham left ventricular tissue whereas the lowest abundance (0.5 ± 0.12) was observed in the shunt left atrial tissue though the difference was not significant (Figure 5.13). Shunt right ventricular tissue (0.6 ± 0.11) had a tendency to be less abundant in phospho-Thr17 compared to sham right ventricular tissue (1.0 ± 0.13). The average abundance of phospho-Thr17 between shunt right atrial tissue and sham right atrial tissue did not differ (0.6 ± 0.28 compared to 0.6 ± 0.21 respectively). Shunt left atrial tissue (0.5 ± 0.12) was also significantly more abundant than sham left atrial tissue of abundance (0.8 ± 0.21).

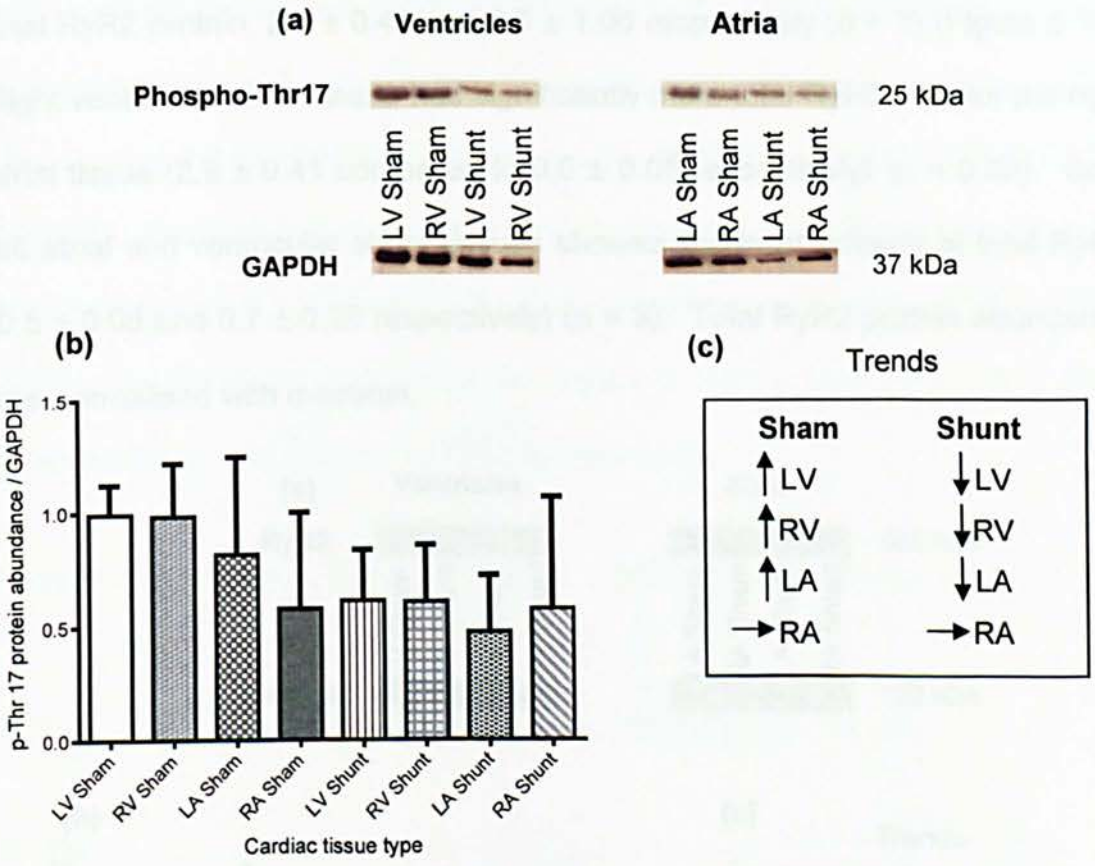

Figure 5.12 Protein expression of phospho-Thr17 in shunt and sham tissues from all four chambers of the heart. **(a)** and **(b)** representative western blots and chart respectively phospho-Thr17 in shunt and sham cardiac tissues. There were no significant differences between the volume-overload tissues (n = 3 for left ventricular and right atrial, n = 5 for right ventricular and n = 4 for left atrial tissues) and sham tissues (n = 3 for left and right ventricular tissues and n = 4 for left and right atrial tissues). **(c)** Arrows show trends in the data of protein abundance between the two different strains of rats.

5.5.15 Total RyR2 : HF atrial and ventricular tissues

The right ventricular and left atrial sham tissues possessed the most abundant total RyR2 protein, 2.9 ± 0.41 and 2.5 ± 1.06 respectively (n = 3) (Figure 5.14). Right ventricular sham tissue had significantly more total RyR2 than for the right atrial tissue (2.9 ± 0.41 compared to 0.6 ± 0.05 respectively) (p = 0.02). Both left atrial and ventricular shunt tissues showed the least amount of total RyR2 (0.5 ± 0.06 and 0.7 ± 0.28 respectively) (n = 3). Total RyR2 protein abundance was normalised with α-actinin.

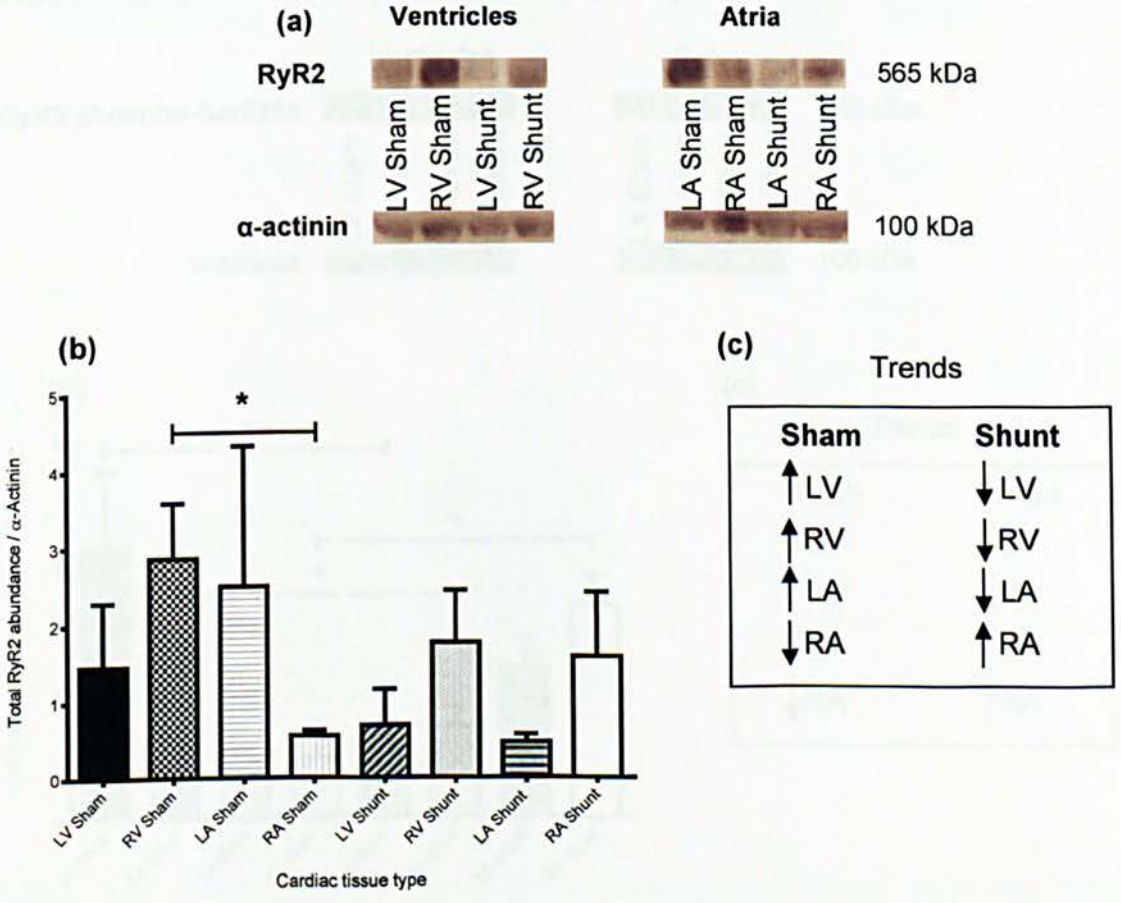

Figure 5.13 Protein expression of total RyR2 in shunt and sham tissues from all four chambers of the heart. **(a)** and **(b)** representative western blots and chart respectively RyR2 in shunt and sham cardiac tissues. Sham right ventricular tissue showed the highest abundance of total RyR2 whereas shunt left atrial tissue had the lowest abundance (n = 3 ; *p < 0.1). **(c)** Arrows show trends in the data of protein abundance between the two different strains of rats.

5.5.16 RyR2 phospho-Ser2808 : HF atrial and ventricular tissues

The highest abundance of this phosphorylated protein was found in sham left ventricular tissue (2.2 ± 0.43) (n = 3) (Figure 5.15). On the other hand, sham right atrial tissue (0.5 ± 0.09) had the lowest abundance of phospho-Ser2808 which is also significantly less than shunt right atrial tissue (1.7 ± 0.14) (n = 3 ; p = 0.002). Both left and right shunt ventricular homogenates were significantly less abundant (0.6 ± 0.04 and 0.7 ± 0.11 respectively) in RyR2 phospho-2808 protein compared to their sham counterparts (2.2 ± 0.43 and 1.5 ± 0.02 respectively) (p = 0.02 and p = 0.003 respectively).

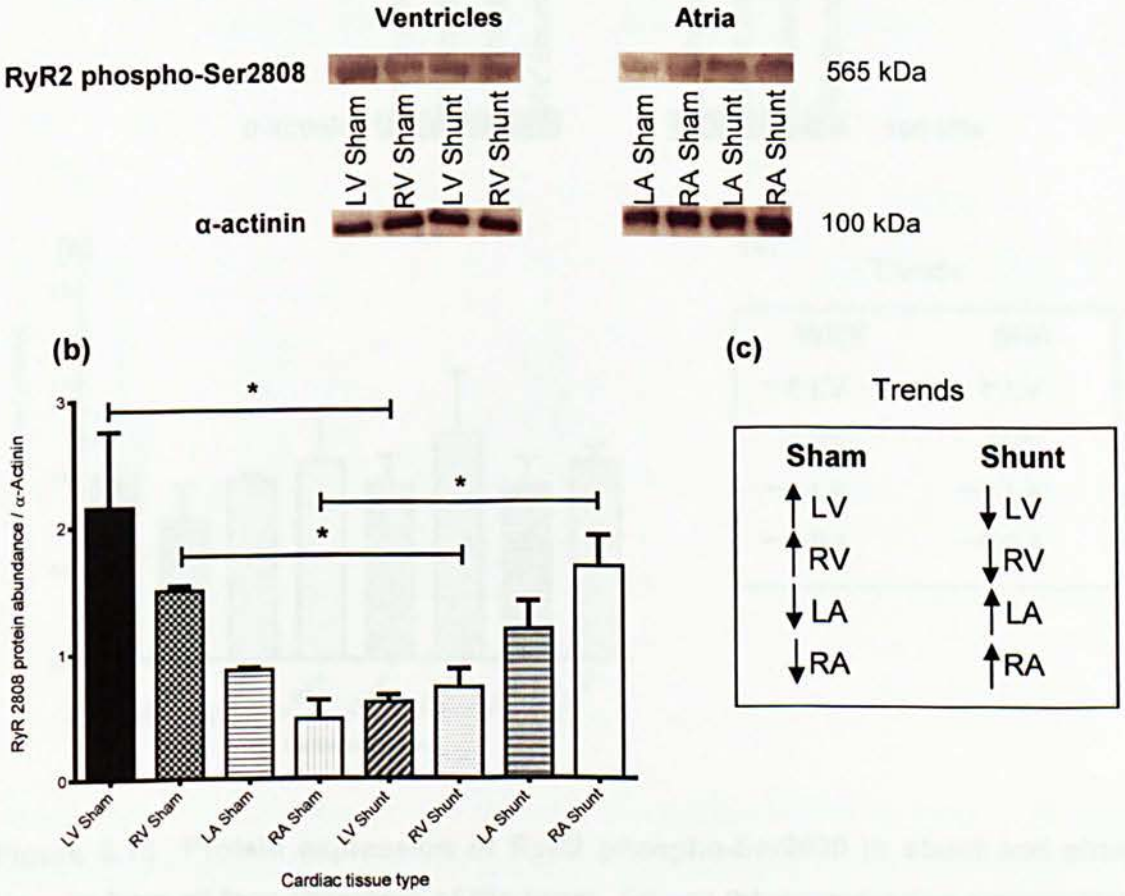

Figure 5.14 Protein expression of RyR2 phospho-Ser2808 in shunt and sham tissues from all four chambers of the heart. **(a)** and **(b)** representative western blots and chart respectively RyR2 phospho-Ser2808 in shunt and sham cardiac tissues. Sham left ventricular tissue was the most abundant with this protein whereas sham right atrial was the least abundant (n = 3 ; *p < 0.1). **(c)** Arrows show trends in the data of protein abundance between the two different strains of rats.

5.5.17 RyR2 phospho-Ser2030 : HF atrial and ventricular tissues

There were no statistically significant differences of RyR2 phospho-Ser2030 abundances between the different chambers of the heart and between the volume overload induced HF and normal tissue conditions (Figure 5.16). Shunt right ventricular tissue showed the highest abundance of phospho-Ser2030 (1.2 ± 0.19) and sham right ventricular tissues showed the lowest abundance (0.8 ± 0.10) (n = 3).

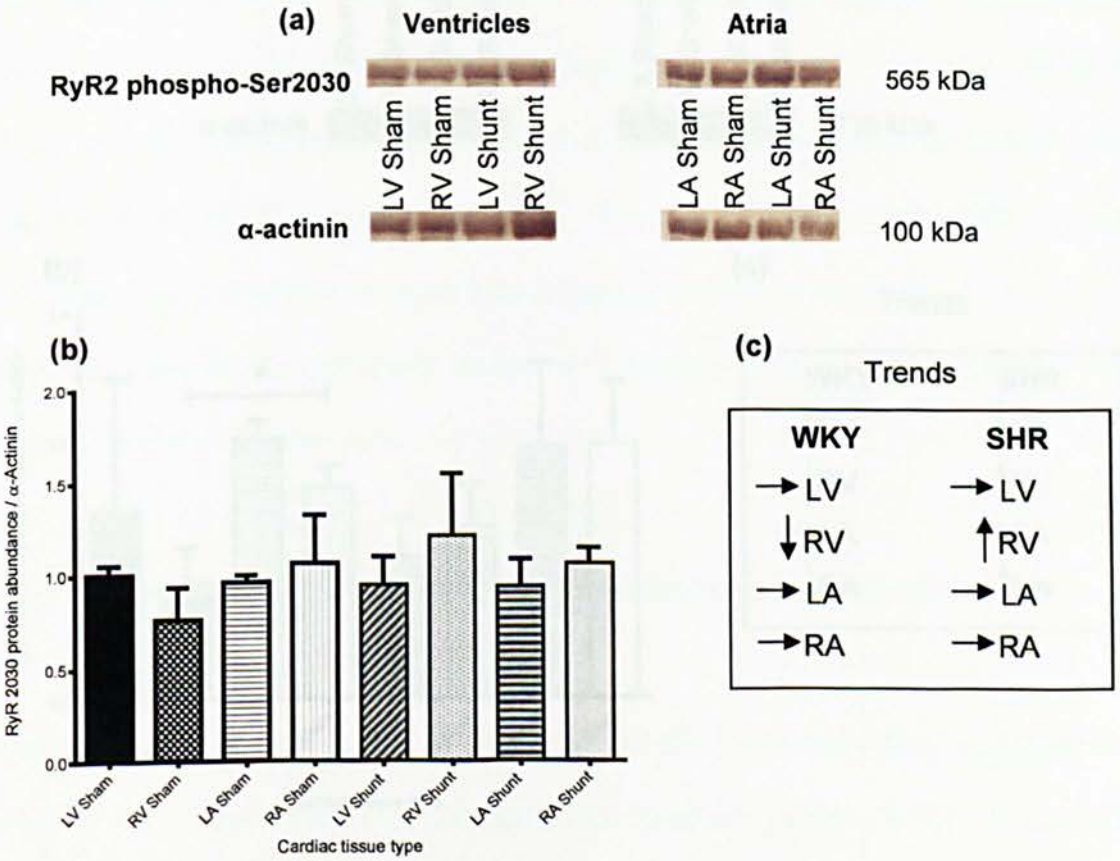

Figure 5.15 Protein expression of RyR2 phospho-Ser2030 in shunt and sham tissues from all four chambers of the heart. (a) and **(b)** representative western blots and chart respectively RyR2 phospho-Ser2030 in shunt and sham cardiac tissues. The distribution of this protein was not significantly different in each cardiac chamber and condition group. **(c)** Arrows show trends in the data of protein abundance between the two different strains of rats.

5.5.18 RyR2 phospho-Ser2814 : HF atrial and ventricular tissues

There were no significant differences between HF and normal left and right atrial and ventricular tissues, except for the sham-operated right atria (0.8 ± 0.05) which had significantly more RyR2 phospho-Ser2814 than the right ventricle (0.5 ± 0.10) (n = 3 ; p = 0.03) (Figure 5.17).

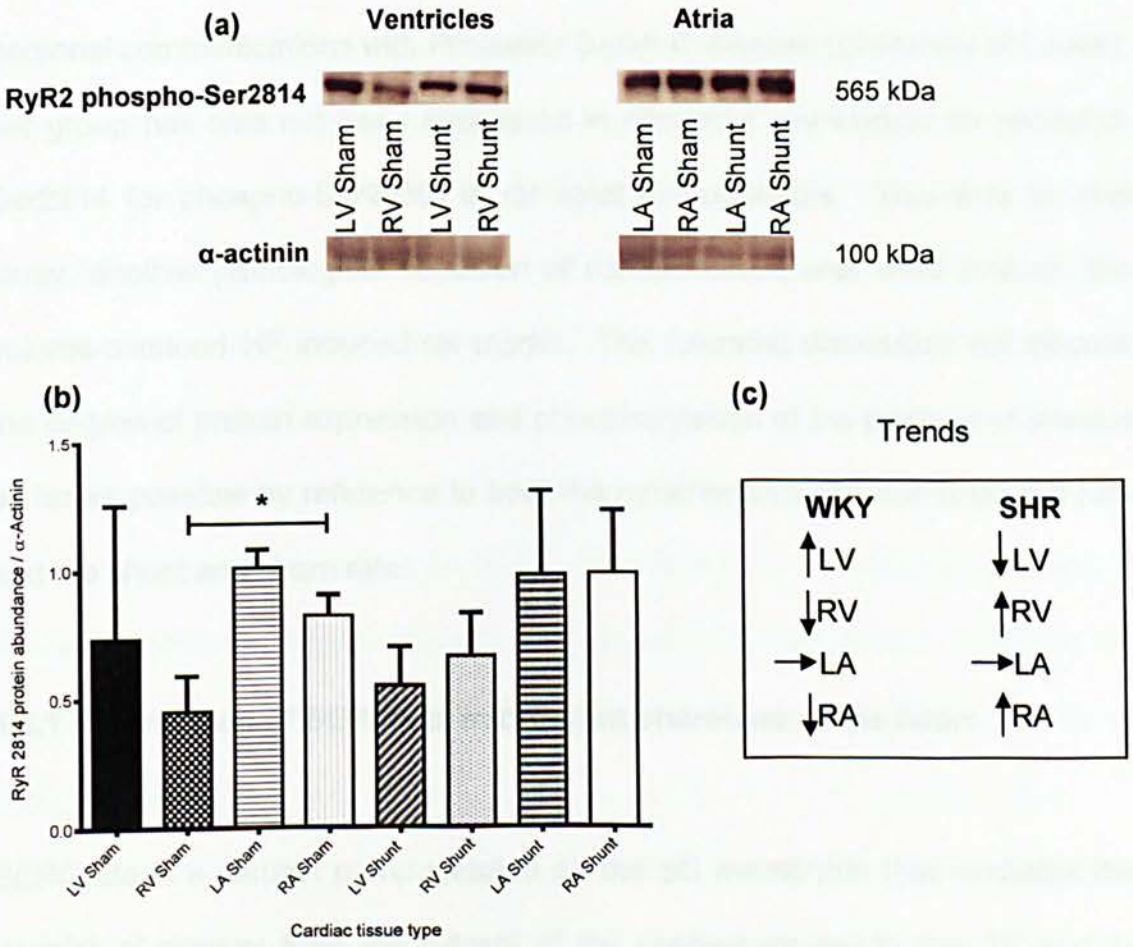

Figure 5.16 Protein expression of RyR2 phospho-Ser2814 in shunt and sham tissues from all four chambers of the heart. **(a)** and **(b)** representative western blots and chart respectively RyR2 phospho-Ser2808 in shunt and sham cardiac tissues. Left atrial homogenates of sham-operated tissue had a tendency to be more abundant with this protein than the left atrial shunt-operated samples. Only the sham-operated right atrial tissue was significantly more abundant with this protein than the right ventricular tissue (n = 3 ; *p < 0.1) **(c)** Arrows show trends in the data of protein abundance between the two different strains of rats.

5.6 Discussion

Initially, WKY and SHR rats were chosen as a means to demonstrate the variability in cardiac protein expression in various heart chambers in health and disease. However, the expression of RyR2 phospho-Ser2030 was detected only for ventricular homogenates of WKY and SHR tissues and in none of the samples for RyR2 phospho-Ser2814 despite several attempts. According to personal communications with Professor Sarah Callaghan (University of Leeds), her group has also not been successful in obtaining any signals for phospho-Ser2814 (or phospho-Ser2030) in rat atrial homogenates. Therefore for this study, another pathological condition of cardiac tissue was used instead, the volume-overload HF induced rat model. The following discussion will discuss the degree of protein expression and phosphorylation of the proteins of interest as far as possible by reference to both the hypertensive and normotensive rats and the shunt and sham rats.

5.6.1 Expression of SERCA2a in different chambers of the heart

SERCA2a is a cardiac pump situated on the SR membrane that mediates the transfer of calcium from the cytosol of the cardiomyocytes to the SR and its activity is inhibited by PLB. SERCA2a thus regulates the rate of calcium removal from the SR and hence cardiac relaxation. The abundances of SERCA2a in all four chambers of the heart may be different due to the various functions or roles each chamber may perform. Research has so far not been undertaken that describes the expression of SERCA2a in each and every chamber of the rat heart of different disease states. Freestone and colleagues

(2000) have shown in their study on WKY rats that SERCA2a abundance was 23% less in ventricular tissue than in atrial tissue. Similarly, in humans, SERCA2a has been reported to be highly expressed in normal atria compared to that in normal ventricles (Bokník *et al.*, 1999 ; Lüss *et al.*, 1999). In mice, SERCA2a abundance was found to be of similar amounts in both atria and ventricles (Bokník *et al.*, 1999).

This study is the only one currently to our knowledge where rat cardiac homogenates (left and right ventricles and left and right atria) from animals with different disease states, such as hypertensive rats and their normotensive controls and volume-overload induced HF rats and their sham-operated controls were used to determine SERCA2a abundances in each chamber of the heart. There were no significant differences in the abundances of SERCA2a between all cardiac chambers in WKY and SHR tissues (however there was a tendency for a lower abundance of the protein in SHR tissues). The present findings of this study are consistent with the work by MacDonnell *et al.*, (2005) in rat ventricular tissue, showing that the level of SERCA2a expression is similar in both WKY and SHR.

SERCA2a is a crucial protein in the removal of calcium during the normal function of the cardiac cycle and hence it may be down-regulated in disease state when the cardiac function is impaired. This could explain the tendency for a lower expression of SERCA2a in SHR homogenates of atria and ventricles. However this might be of significance when left and right SHR atrial homogenates are combined and compared with left and right ventricular homogenates.

In HF patients, SERCA2a in left ventricular tissues has been shown to have a lower amount expressed than in non-failing hearts (Kubo *et al.*, 2001). This is also reported by Meyer and colleagues (1995) in HF cardiac tissue compared to the non-failing myocardium tissues. On the other hand, HF ventricles have been reported to have no differences in the amount of SERCA2a in comparison to patients without HF (Movsesian *et al.*, 1994 ; Bokník *et al.*, 1999). In this study of SERCA2a abundances in all four chambers of the HF rats, the expression of SERCA2a in volume overload rats had a tendency to be less than for the sham-operated rats in the corresponding heart chambers and this may correspond to a perturbation of the SERCA2a proteins in HF. In studies of guinea pigs with induced HF, the dysfunction of the SR calcium re-uptake is related to the decreased levels of SERCA2a protein (Kiss *et al.*, 1995). However, the mechanism regulating the calcium ion movements in and out of SR during HF is still not fully understood.

Bokník's group have also reported higher expressions of SERCA2a protein in normal human atrial tissue compared to ventricular tissues. However in another species, such as mice it was reported that there are no differences in the amount of SERCA2a (Bokník *et al.*, 1999). In this study, for both WKY and sham tissues, left and right atrial tissues have a tendency to be more abundant with SERCA2a compared to the ventricles which corresponds to faster calcium reuptake that is associated with the shorter contraction-relaxation cycle of the atria. Pooling atrial homogenates together and comparing to polled ventricular homogenates would reveal any differences more clearly.

5.6.2 Boiling and not boiling cardiac homogenates when probing for PLB

In the current literature, there is no consistent method for the detection of PLB, the phosphoprotein that regulates the activity of the SERCA2a pump. There have been studies reporting the 25 kDa pentameric form of this protein (Bokník *et al.*, 1999 ; Lüss *et al.*, 1999) as well as the 6 kDa monomeric form (MacDonnell *et al.*, 2005 ; Walden *et al.*, 2009). The 6 kDa form can be obtained by 'boiling' (heating to 95°C) the cardiac homogenates (Fallavollita *et al.*, 1999). Wientzek and Katz (1991) have shown 3 bands (8, 25 and 27 kDa) of the dissociated protein when the rat ventricular sample was not boiled. On the other hand, when the ventricular homogenate was boiled, only a band at 8 kDa was noted. In the studies of PLB and its phosphorylated forms, other bands were observed albeit lighter than the single band at the expected mass. This may be explained by smaller undissociated proteins of PLB suggesting the different phosphorylation sites of the protein, one for cAMP PKA activity and the other CaM Kinase II activity (Wegener and Jones, 1984).

It is worth noting that one of the suppliers of the anti-PLB antibody (Millipore, UK) specifically states that the cardiac samples should not be boiled when western immunoblotting for PLB protein (Most *et al.*, 2003). Upon 'boiling' the cardiac homogenates, the pentameric structure of PLB is denatured (Simmerman and Jones, 1998). It is usually a general practice to 'boil' fresh cardiac preparations (first time use) (MacDonnell *et al.*, 2005 ; Walden *et al.*, 2009) before loading the homogenates into the wells of the gel for any protein detection. The sample buffer contains SDS and β-mercaptoethanol which breaks up the structure of the protein molecule and contributes to the complete

denaturation of the proteins therefore the cardiac homogenates only require warming up to 37°C and vortex agitation for subsequent experiments.

Despite several groups (MacDonnell *et al.*, 2005 ; Connelly *et al.*, 2007) opting to 'boil' their cardiac homogenates to obtain the monomeric form of PLB, according to the results of this study, when the samples were 'boiled', there is a slight tendency for a higher abundance of the monomeric band than pentameric band of PLB compared to when the sample was warmed at 37°C. However, the total quantification of PLB protein abundances normalised with GAPDH showed no significant differences between the samples which were heated to 95°C and those which were heated to 37°C.

5.6.3 Expression of PLB in different chambers of the heart

Up to 90% of the blood arriving at the heart (via the veins) enters the ventricles without any contribution from atrial contraction. To ensure that the remaining blood returning to the atria will enter the ventricles, the atria contract to "top up" the ventricles prior to their contraction. Atrial contraction and relaxation is also notably faster than for the ventricles (Goldman *et al.*, 1984 ; Lüss *et al.*, 1999 ; Freestone *et al.*, 2000 ; Kaasik *et al.*, 2001) which may explain why the PLB expression in the atria is four times less than that in the ventricles (Koss *et al.*, 1996). Freestone *et al.*, (2000) suggested that there was 76% more PLB in ventricular tissues compared to the atrial tissue and additionally, Walden and colleagues (2009) have agreed that PLB content in ventricles is significantly higher than in atria. This pattern is also observed in human and mouse atrial and ventricular tissues (Bokník *et al.*, 1999).

In the present study, there was 50% more PLB in WKY right ventricular tissues compared to the right atria ($p = 0.02$), whereas in the left ventricular tissue, the abundance of PLB had a tendency to be more than in the left atrial tissue. However, when left and right ventricular and atrial tissues were combined together, there was 64% more PLB in WKY ventricular tissues than atrial tissues. This may result in the faster relaxation of the atria compared to the ventricles as reported elsewhere in the literature (Braunwald, 1997 ; Koss *et al.*, 1996).

When comparing total PLB protein abundances in normotensive and hypertensive rat hearts it was observed that there was a higher abundance of PLB in SHR compared with WKY cardiac tissues. PLB was most abundant in the SHR right ventricular homogenate and was significantly more abundant than in the WKY right ventricular homogenate ($p = 0.01$). The pattern was also observed for the left ventricular homogenate where PLB was more abundant in SHR tissue compared to WKY tissue ($p = 0.01$). When comparing right and left atria of SHR and WKY rats, the following PLB expression was noted: SHR right atria > SHR left atria > WKY left atria > WKY right atria. In a study by Li and colleagues (2005), PLB was also shown to be more abundant in whole heart homogenates of the SHR than WKY rats. Raised levels of total PLB in SHR cardiac homogenates may result in decreased calcium re-uptake into the SR of hypertensive cardiac tissues (Bokník *et al.*, 2001). This may cause slower relaxation and less SR calcium loading. To compensate for the increased cardiac inotropy, the ventricles adapt themselves for this task by increasing the thickness of the cardiac muscle.

In terms of HF homogenates, there was no significant difference in PLB in the ventricles except where shunt left homogenate was more abundant with this protein than the sham left homogenate ($p = 0.02$). Kubo and colleagues (2001) studied the abundances of cardiac PLB in patients diagnosed with HF and reported that there was no significant difference between the abundances of PLB in non-failing compared to failing left ventricular tissues.

In this study, there was a noticeable increase of PLB in the shunt atria, especially in the right tissue. The right atrium is the first point of blood return when the volume overload (a mix of arterial oxygenated blood with venous deoxygenated blood due to the aorto-caval shunt) returns to the heart. This suggests that the right atria has an increased amount of PLB to manage the increased SR calcium load and pump the large amount of returning blood into the ventricles.

A similar trend of PLB abundances in each cardiac chamber was noticed between WKY and sham homogenates whereby both strains showed that the right ventricular tissue had the highest abundance of PLB and the right atrial tissue had the lowest amount. This seems feasible since both the "normal" sets of tissues are not experiencing stress as observed in diseased cardiac tissue samples.

5.6.4 Expression of phosphorylated PLB in different chambers of the heart

At least one third of the total PLB found in the ventricles has been reported to exist in the phosphorylated PLB form, phospho-Ser16 and phospho-Thr17 (Kaasik *et al.*, 2001). The phospho-Ser16 site is phosphorylated by PKA whereas the phospho-Thr17 site is phosphorylated by calcium/CaM Kinase II (MacLennan and Kranias, 2003). Phospho-Thr17 has been reported to be more abundant in SHR ventricular tissue than WKY (Bokník *et al.*, 2001 MacDonnell *et al.*, 2005 ; Mills *et al.*, 2006 ; Kolwicz *et al.*, 2007). In addition, a lower abundance of phosphorylated Ser16 has been suggested in SHR left ventricular tissue compared to WKY left ventricular tissue (MacDonnell *et al.*, 2005 ; Renna *et al.*, 2006). This is similar to the findings of this study, whereby both WKY left and right ventricular tissue were more abundant in phospho-Ser16 than their SHR counterparts (significantly so for WKY and SHR left ventricular tissue, $p = 0.03$). Phospho-Thr17 is increased in SHR ventricles compared to WKY similar to the findings of Mills *et al.*, (2006).

The findings suggest that the PKA phosphorylation site of PLB is more abundant in WKY compared to SHR tissues which means there is a reduced relaxation rate of the heart in hypertension under conditions of β-adrenergic stimulation. The reduction in the density of β-ARs during hypertension also means there are less receptor sites being stimulated in the heart (Wang *et al.*, 2004).

The increase of phospho-Thr17 but decrease in phospho-Ser16 in SHR and WKY tissues that occurred in this study is reflective of functional data derived by Freestone *et al.*, (2000) and Mills *et al.*, (2006) which suggests that the two different phosphorylation effects cancel themselves out to result in no change in cardiac relaxation kinetics between WKY and SHR. A decrease in phospho-Ser16 in SHR accounts for this. Furthermore, it seems that in hypertensive tissues, phosphorylation of PLB occurs mainly via calcium/CaM Kinase II and presumably less so by PKA.

In terms of HF cardiac homogenates of different heart chambers, there were no significant differences in the abundances of phospho-Ser16 though there is a tendency for the shunt tissues to have a lower amount of this protein. There is also a tendency for the shunt tissues to have less phospho-Thr17 compared to the sham samples. The results of the present study confirms the findings of Netticadan's (2000) and Mishra's group (2002) whereby left ventricular tissues of HF rats and dogs respectively were found to have reduced amounts of phospho-Thr17. This may be due an increase in phosphatase activity that triggers the dephosphorylation of PLB at CaM Kinase II sites and causes a reduction in calcium uptake and calcium release in HF (Netticadan *et al.*, 2000). Therefore the increase in total PLB and decreased amount of phospho-Thr17 is mainly responsible for the reduction of SR calcium reuptake commonly observed in HF.

5.6.5 Expression of RyR2 and phosphorylated RyR2 in different cardiac chambers

RyR2 is an intracellular calcium channel located on the SR membrane through which calcium flows out of the SR in a process known as CICR (Fabiato and Fabiato, 1978). There are three phosphorylation sites of RyR2, RyR2 phospho-Ser2808 which is phosphorylated by PKA and calcium/CaM Kinase II, RyR2 phospho-Ser2814 which is phosphorylated by CaM Kinase II and RyR2 phospho-Ser2030 which is phosphorylated by PKA. During hypertension, RyR2 phospho-Ser2808 has been reported to be similar in WKY and SHR left ventricular tissues, however the abundance of this protein is increased in SHR right ventricular tissues (Chen-Izu *et al.*, 2007). During HF, RyR2 phospho-Ser2808 becomes hyperphosphorylated and calcium is continuously and uncontrollably being leaked from the SR (Marx *et al.*, 2000). The contraction of the failing heart is subsequently less forceful due to a lower amount of calcium left in the SR as a result of this slow calcium removal (Belevych *et al.*, 2013 ; Meyer *et al.*, 1995 ; Eschenhagen, 2010). Eventually this may result in arrhythmias (Laitinen *et al.*, 2001 ; Eschenhagen, 2010).

In this study, unlike many reports in the current literature, rat cardiac tissues have been deliberately separated out into the four separate chambers. Total RyR2 abundance showed no significant differences between the different heart chambers of WKY and SHR rats or between the cardiac chambers of shunt and sham tissues.

According to Huke and Bers (2008), RyR2808 antibody purchased from Badrilla Ltd was the most reliable for use in western blotting hence it was chosen to be used in this study. With regards to the abundance of RyR2 phospho-Ser2808 between the different heart chambers of the SHR rats, there were no significant differences arising. However, for WKY, the abundance increased for the left ventricular homogenate compared to this tissue in SHR samples. On the other hand, for the shunt rat cardiac samples, there was less of the phosphorylated RyR2 at the Ser-2808 site in left and right ventricular homogenates but more in the left and right atrial tissue. Shunt tissue of the right atria was also more abundant with RyR2 phospho-Ser2808 compared to the sham version of the right atria.

In WKY and SHR cardiac homogenates, the expression of RyR2 phosphorylation at Ser-2030 and Ser-2814 was barely detectable and quantifiable by antibody detection in western blotting. After several attempts, only the WKY and SHR ventricular homogenate probed for RyR2 phospho-Ser2030 managed to be detected by western blot. There were also no significant differences in the abundance of RyR2 phospho-Ser2814 in HF cardiac homogenates compared to sham homogenates. These challenges echoed the views of Huke and Bers (2008) who studied the phosphorylation of RyR2 in rat cardiomyocytes. They reported on the difficulty of detecting phosphorylation of RyR2 at Ser-2814 and also Ser-2030 (Huke and Bers, 2008) compared to Ser-2808. RyR2 phospho-Ser2814 is phosphorylated by calcium/CaM Kinase II and dephosphorylated by PP1 and presumably also by PP2 (Huke and Bers, 2008). This protein might not be easy to detect or be of much significance since RyR2 is mainly phosphorylated by PKA and not CaM

Kinase II (Huke and Bers, 2008). Furthermore, it has been suggested that phosphorylation at Ser2030 has a relatively slow time course (Marx *et al.*, 2000) hence it does not seem to be of functional importance and may explain why the detection of RyR2030 is not always successful.

Surprisingly, signals were detected for shunt and sham homogenates even though there were no detectable signals for the WKY homogenates for RyR2 phospho-Ser2814. There are a few reasons why there might be discrepancies in the detection of this protein considering that the sham homogenates originated from SD rats of normotensive strain and not WKY and this may account for the variable detection of proteins expressed in the different cardiac tissues. Normotensive SD rats have similar blood pressure to SHR rats but not WKY rats, even though WKY rats are genetically more similar to SHR (Mills and Bruckert, 1988). Furthermore, other discrepancies may be the extent of severity of the heart disease and differences in the etiology of rat models. Thus it is possible that some cardiac chambers in some rat strains do not express all versions of the phosphorylated RyR2 protein.

5.7 Conclusion

The study of boiled and non-boiled WKY ventricular samples probed for PLB showed that both conditions did not affect the amount of protein recovered. The results from this study suggests that diseased tissues tend to show lower expression of SERCA2a suggesting a prolonged SR calcium re-uptake hence a longer cardiac cycle. Correspondingly, the high abundance of PLB in these tissues slowed down calcium removal and also slowed the relaxation rate. There is more calcium/CaM Kinase II-mediated phosphorylation in SHR tissues than WKY which explains the higher abundance of phospho-Thr17 and no alteration in phospho-Ser16. However, the increase of phosphatase activity in HF results in decreased calcium uptake and calcium release by increasing the inhibitory activity of PLB on SERCA2a function.

Enhanced PKA phosphorylation of RyR2 is observed in HF tissues which may result in hypersensitivity of the RyR2 channel and a reduction in calcium load. It may be reasonable to suggest as a therapy for HF to counteract the propensity for RyR2 to allow calcium leak causing a reduction of SR calcium load which reduces the efficiency of EC coupling and which may also contribute to arrhythmogenesis.

CHAPTER 6

The role of the novel β_{1L}-AR in spontaneous calcium release in rat atrial myocytes

6.0 The role of the novel β_{1L}-AR in spontaneous calcium release in rat atrial myocytes.

6.1 Introduction

In healthy hearts, cardiac cell contractions are the result of co-ordinated calcium release from the SR. These contractions are initiated at the sarcolemmal membrane by the arrival of an action potential arising from the SA node. Calcium entry via sarcolemmal voltage-dependent LTCCs initiates calcium release via calcium release channels (RyR2) on the SR during CICR resulting in cardiomyocyte contraction. Arrhythmias, on the other hand, are spontaneous cardiac contractions that may be triggered by excess adrenaline and noradrenaline in the heart and are separate to the normal co-ordinated contractions of the cardiac cells. Both atrial and ventricular arrhythmias are quite common in patients diagnosed with CHF (Hynes *et al.*, 2002). A common feature of arrhythmias is spontaneous calcium release from the SR which may cause a calcium wave to propagate from one end of the cell to the other, independent of any electrical stimulation or which may also generate an additional action potential through activation of arrhythmogenic inward current via the sodium/calcium exchanger.

Spontaneous calcium release events come in various forms. Calcium sparks are the fundamental calcium events and they accumulate in time and space to eventually build up to form a propagating whole cell calcium wave or trigger the arrhythmogenic inward current. Intermediate calcium events also occur which are relatively large localised non-propagating calcium release events bigger

than calcium sparks but smaller than calcium waves. They may not necessarily result in cellular contraction and are known as calcium wavelets, or "macrosparks" (Cheng *et al.*, 1993).

6.1.1 Arrhythmogenic events mediated via the novel $\beta1_L$-AR

Sir James Black, a 1988 Nobel Prize laureate pioneered the development of β-blockers (more specifically propranolol) which showed anti-arrhythmic effects (Baker *et al.*, 2011). β-blockers are a class of drugs which serve as one of the most important treatments for arrhythmias and HF. Whilst β-blocking drugs are also favoured in treating hypertension (Pritchard and Gillam, 1969) and angina pectoris (Bianchi *et al.*, 1969), it was suggested that they might also be beneficial in treating ventricular arrhythmias (Podrid and Lown, 1982).

β-blockers function by blocking the ability of catecholamines such as adrenaline and noradrenaline to bind to their receptors and cause cardiostimulation. Paradoxically, in the early 1980s, a specific sub-class of these β-blocking drugs was found not to only inhibit cardiac activity but instead to also cause additional stimulation in particular when at high concentrations. This class of drugs is known as the non-conventional partial agonists and they have subsequently been discovered to work upon a specific β receptor variant, now known as the $\beta1_L$-AR, previously known as the putative β4-AR (Kaumann *et al.*, 1998 ; Kaumann and Molenaar, 2008).

Past evidence showed that the presumed putative β4-AR had strikingly similar pharmacological characteristics to the β3-AR however, stimulatory effects of

CGP12177 were still apparent in β3-AR knockout mice experiments (Kaumann *et al.*, 1998). The same putative β4-AR site also failed to demonstrate the ability to accommodate a selective β3-AR agonist (Kaumann and Molenaar, 1996 ; Malinowska and Schlicker, 1996 ; Sarsero *et al.*, 1999). In β2-AR knockout mice atria, CGP12177 still caused cardiostimulation, however upon deleting the genes for both β1- and β2-AR, cardiostimulation was diminished (Kaumann *et al.*, 2001). This was the first evidence that the putative β4 was actually a variant of the β1-AR.

Drugs such as bucindolol, cyanopindolol and pindolol used in the treatment of HF were found to be clinically ineffective due to their sympathomimetic behaviour presumably mediated by the $\beta1_L$-ARs (Kaumann and Molenaar, 2008). Furthermore, other β-blockers such as atenolol have been shown to shorten survival rates in patients who survive myocardial infarction (Soriano *et al.*, 1997). Pindolol was studied in a clinical investigation of 43 patients with ischaemic HF and was shown to have sympathomimetic activity. Pindolol was reported to lower the heart rate of healthy volunteers during exercise, however in patients with existing heart disease, increasing the concentration of pindolol seemed to encourage further cardiostimulation (Podrid and Lown, 1982). This shows the typical characteristic of a non-conventional partial agonist whereby cardiostimulation occurs at a high concentration however at low concentrations, the characteristics of a β-blocker are observed. Another non-conventional partial agonist and β-AR antagonist is CGP12177, which is similar in structure to pindolol. CGP12177 is a benzimidazolone compound first mentioned in 1983 by Staehelin and colleagues and used as a tool to pharmacologically characterise the $\beta1_L$-AR.

In electrically paced mouse ventricular myocytes, CGP12177 has been shown to be 40 times more potent in causing arrhythmias compared to ISO, a highly potent synthetic analogue of adrenaline and noradrenaline (Freestone *et al.*, 1999). CGP12177 is much more arrhythmogenic than ISO despite it only increasing the intracellular calcium levels by 30% of the amount resulting from administration of ISO (Freestone *et al.*, 1999). CGP12177 was added in the presence of IBMX and propranolol to the mouse ventricular cells. IBMX blocks the phosphodiesterases (PDEs) which normally function to trigger an increase in cAMP levels and PKA activity leading to cardiostimulation via the Gs coupled pathway (Freestone *et al.*, 1999). However, IBMX is not required to show the cardiostimulatory effects in atrial myocytes unlike for the ventricular myocytes (Sarsero *et al.*, 1999) since there presumably is sufficient cAMP to enable cardiostimulation. ISO on the other hand, also causes cardiostimulation in mouse ventricular myocytes but does not cause as many arrhythmogenic events as CGP12177 (Kaumann *et al.*, 1997).

CGP12177 at a low concentration suppresses the stimulatory effects of the catecholamines on the human heart, however when the concentration is increased up to 100 times, the cardiostimulatory effects become apparent (Kaumann, 1989 ; Kaumann and Molenaar, 1997). Lowe and colleagues (1998) have shown in whole ferret hearts perfused with CGP12177 in Langendorff-mode an increase in plateau phase duration of the action potential with shortening of the overall action potential duration more than that observed with noradrenaline acting on conventional β1-ARs. This provides a possible explanation to the arrhythmic responses mediated by the novel β1-AR in the

ferret hearts since the longer action potential plateau suggests there is more calcium entering the cell.

In a study in 2002 by Lowe and colleagues, propranolol did not manage to suppress the pro-arrhythmic effect of CGP12177 in ferret ventricle (Lowe *et al.*, 2002). The cardiostimulatory activity of CGP12177 is therefore propranolol-insensitive (Kaumann, 1989 ; Kaumann *et al.*, 1998 ; Lewis *et al.*, 2004). Furthermore, an investigation in quiescent rat atrial myocytes also supported the propranolol-insensitivity of CGP12177 (Sam *et al.*, 2012). It has been suggested that the active site where propranolol is able to block stimulation of the $\beta1_H$-AR variant is different and separate to the lower affinity β-receptor variant (Walter *et al.*, 1984 ; Sarsero *et al.*, 1998 ; Kaumann *et al.*, 2001). Furthermore, it has been demonstrated in rat atrial myocytes that CGP12177 in the presence of propranolol causes an increase in cAMP levels though less than for ISO (Sarsero *et al.*, 1999). This could possibly lead to a rise in L-type calcium current which may result in arrhythmogenic activity.

6.2 Aim of study

This study aims to investigate spontaneous calcium release from the SR upon the perfusion of a series of cardiostimulatory and cardioinhibitory drugs in quiescent rat atrial cells. ISO and CGP12177 (in the presence of propranolol) were perfused in atrial cells and calcium events compared to their basal conditions. 2-APB, a blocker of IP3R-mediated calcium release was perfused in the presence of CGP12177 to investigate its effect on arrhythmogenic calcium release. Nifedipine, the LTCC receptor blocker (Figure 6.1) was used to

observe its effect on CGP-induced SR calcium release events as well as the RyR2 inhibitor ruthenium red. The agonist BRL37344 was also studied for its effects upon spontaneous SR calcium release to show that a cardioinhibitory effect is possible via β3-AR when other cardiac β-ARs were cardiostimulatory in this model. The frequency of the intracellular spontaneous calcium release events in the form of calcium sparks, wavelets and whole cell calcium waves was obtained by the confocal microscope using whole cell imaging as well as line scanning of the atrial cells.

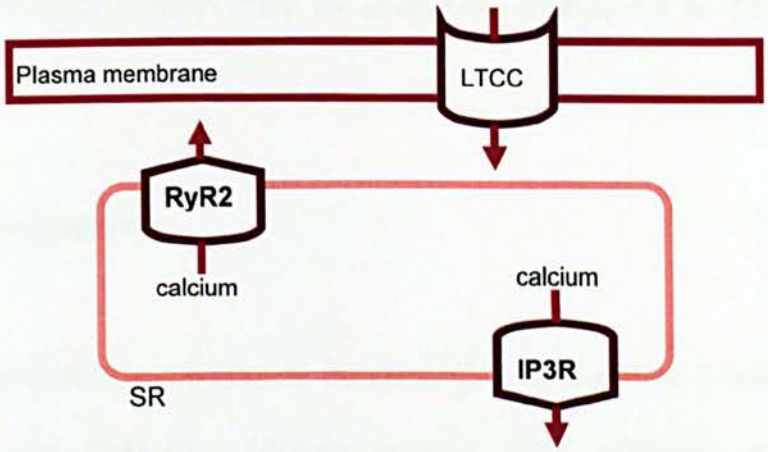

Figure 6.1 Major calcium release channels of the SR in cardiomyocytes. There are two calcium release channels located on the SR, RyR2 and IP3R. Calcium entry into the atrial cell is via the LTCC which is responsible for calcium entry into the cardiomyocyte.

6.3 Materials

All materials used are as previously described in Chapter 2 with the addition of microscope chambers which were made at Kingston University and round glass cover slides (22 mm) which were purchased from VWR International.

6.4 Methods

6.4.1 Animals

Rats used in this study are as described in Chapter 2.

6.4.2 Langendorff method - Perfusing whole rat heart

Male WKY rats were sacrificed and the procedure for whole heart perfusion using the Langendorff method was as previously discussed in the methods section of Chapter 4.

6.4.3 Atrial cell isolation

The atrial cell isolation procedure is as described in Chapter 2 with a slight modification to the method. Minced tissues were manually agitated in collagenase enzyme solution and then Tyrode's solution (0.2 mM calcium) in sessions lasting 5 mins each in the water bath (37°C). After each session, the supernatant was collected and fresh warm enzyme was added to the remaining atrial tissue in the boiling tubes for the last session of manual agitation at 37°C for 15 mins. Any remaining tissue was gently triturated using a Pasteur pipette to aid tissue digestion.

6.4.4 Confocal calcium imaging

Fluo-4AM (4 μM final) solution was made up as previously described in Chapter 2 and added to the cells.

6.4.5 Concentrations of cardiostimulatory and cardioinhibitory drugs

The following were perfused onto the atrial cells in the cell chambers on the confocal microscope using an Eyelar perfusion pump. Cells were exposed to each drug for 6 - 7 mins which enabled equilibrium effects of the drugs to be achieved.

Table 6.1 Experimental procedures for cardiostimulatory and cardioinhibitory drugs perfused in isolated atrial cells for calcium imaging procedures. The above cardiostimulatory and cardioinhibitory experiments were carried out on the confocal microscope by perfusing the described drugs. Calcium imaging videos and line scans were obtained for records of calcium events. Calcium events were obtained in the forms of calcium sparks, wavelets and waves.

	ISO	CGP12177	2-APB	Nifedipine	Bupranolol	BRL37344
Basal conditions	Tyrode's solution	Prop (200nM)	Prop (200nM) + 2-APB (2μM)	Prop (200nM) + Nifedipine (10μM)	Bupranolol (1μM)	Tyrode's Solution
Cardio-active conditions	ISO (100nM)	CGP12177(1μM) + Prop (200nM)	Prop (200nM) + 2-APB (2μM) + CGP12177 (1μM)	Prop (200nM) + Nifedipine (10μM) + CGP12177 (1μM)	Bupranolol (1μM) + CGP12177 (1μM)	BRL37344 (300nM)

**(0.5 mM calcium Tyrode's physiological solution = Basal condition)*
***All drugs were added to the Tyrode's physiological solution to make up the final perfusate.*

6.5 Statistical analysis

Experimental data are presented as mean ± S.E.M. The differences in calcium event frequencies upon administration of cardiostimulatory or cardioinhibitory drugs compared to basal were assessed by means of a paired t-test. Values of $p < 0.05$ were considered as being statistically significant.

6.6 Results

6.6.1 Intracellular calcium release events in atrial myocytes

Upon the perfusion of a cardiostimulatory drug such as CGP12177 in an isolated rat atrial myocyte (Figure 6.2 a) various forms of intracellular calcium events such as calcium sparks (Figure 6.2 b), calcium wavelets (Figure 6.2 c) and calcium waves (Figure 6.2 d) were captured by a confocal microscope.

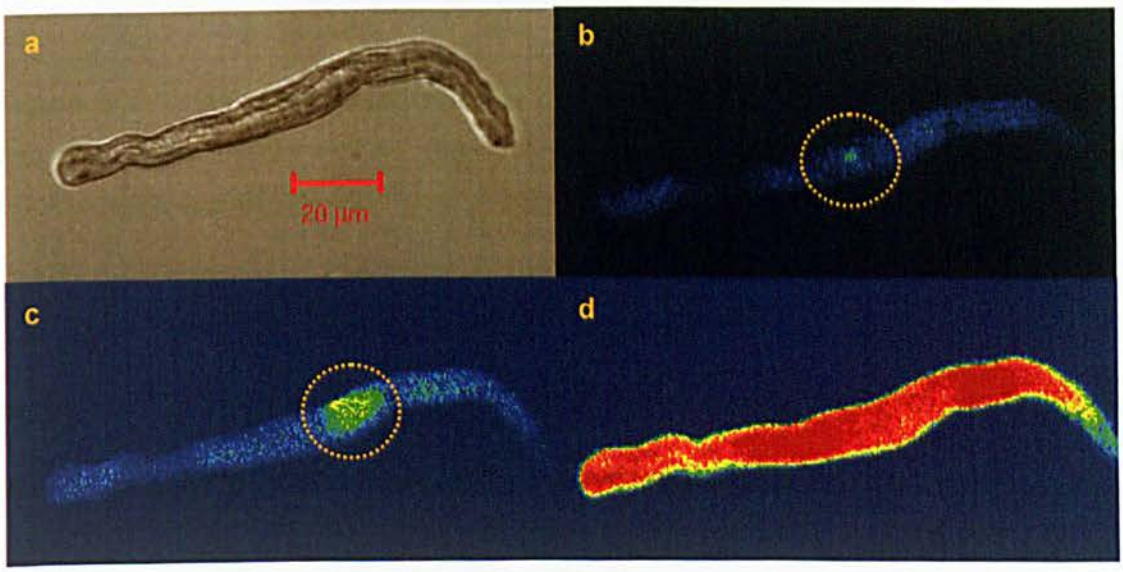

Figure 6.2 Whole cell calcium images of events in a WKY right atrial cell responding to the administration of a cardiostimulatory drug (in this case CGP12177). **(a)** photomicrograph of an isolated rat atrial myocyte **(b)** calcium spark (circled) in a whole cell image **(c)** calcium wavelet (circled) **(d)** whole cell calcium wave. All of the above images of calcium events were taken from the same atrial cell being perfused with CGP12177 in the presence of propranolol.

Calcium events from the perfusion of CGP12177 in a quiescent rat atrial myocyte were also captured in the form of line scans from the confocal microscope (Figure 6.3).

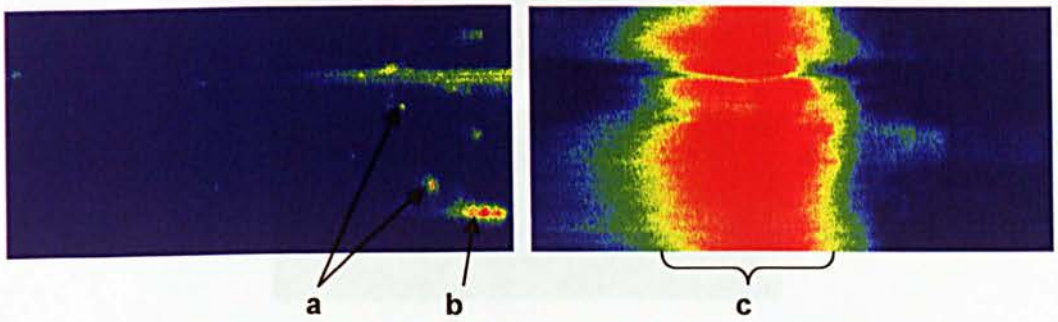

Figure 6.3 Line scan images showing examples of calcium sparks, calcium wavelets and calcium waves. **(a)** calcium sparks **(b)** calcium wavelets **(c)** whole cell calcium wave are all different forms of calcium release activity in a cardiomyocyte.

In this study, frequency analyses of calcium events from the selection of cardioactive drugs involve line scans and whole cell images.

6.6.2 The effect ISO on spontaneous calcium release

During the basal perfusion (Tyrode's physiological solution), the spark frequency in quiescent rat atrial cells was 26.7 ± 4.5 s^{-1} (n = 8). ISO administration (100 nM) resulted in a significant increase (p = 0.04) in spark frequency to 38.7 ± 7.9 s^{-1}, but did not increase the frequency of whole cell calcium waves or wavelets (Figure 6.4 and 6.5).

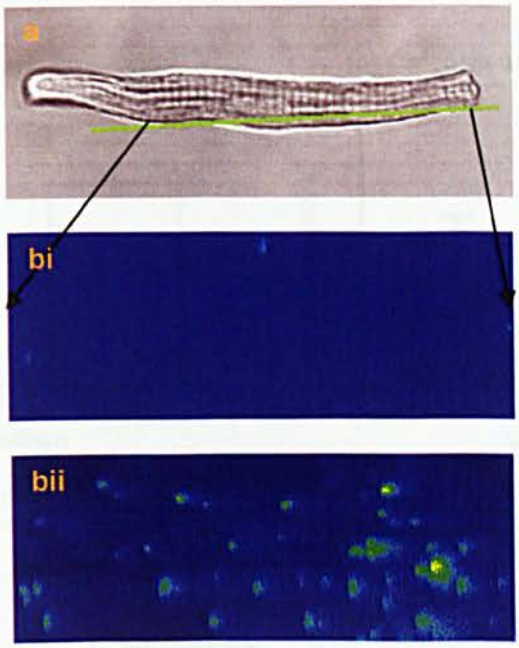

Figure 6.4 Line scan images of quiescent rat atrial cells perfused with ISO. (a) photomicrograph image of a quiescent rat atrial cell. A green line has been selected along the periphery of the cell for the line scan **(bi)** line scan image of the same rat atrial cell being perfused with physiological salt solution **(bii)** line scan image of the calcium events in rat atrial myocytes following perfusion of ISO. Calcium sparks are observed, in yellow/green starting from the left side of the captured line scan image. Calcium wavelets are formed towards the right of the image and are bigger than sparks but are non-propagating.

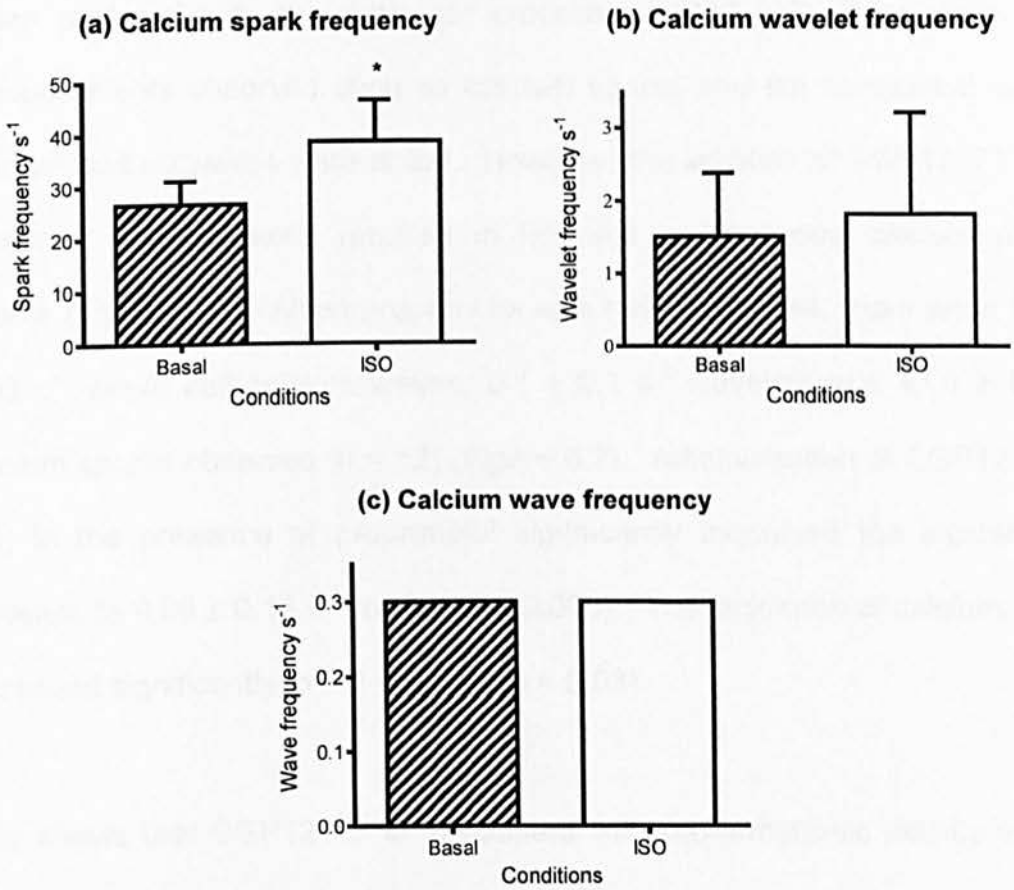

Figure 6.5 Frequency of calcium events upon perfusion of ISO in quiescent rat atrial cells. Bar charts for **(a)** calcium sparks, **(b)** wavelets and **(c)** wave frequency of atrial cells being perfused with ISO (100 nM). Administration of ISO resulted in a significant increase in the frequency of calcium sparks (*p = 0.04). However, there were no significant differences in the number of calcium wavelets or waves in the presence of ISO compared to basal. At basal condition and upon the addition of ISO, 8 cells showed calcium sparks and calcium wavelets, but only one cell showed calcium waves.

6.6.3 The effect of CGP12177 in the presence of propranolol on spontaneous calcium release

When perfused with the β-blocker propranolol (200 nM), there were some calcium events observed such as calcium sparks and the occasional calcium wavelet, but no waves were noted. However, the addition of CGP12177 in the presence of propranolol resulted in frequent spontaneous calcium release events (Figure 6.6). When propranolol was being perfused, there were 0.04 ± 0.03 s^{-1} whole cell calcium waves, 0.4 ± 0.1 s^{-1} wavelets and 41.0 ± 6.7 s^{-1} calcium sparks observed (n = 12) (Figure 6.7). Administration of CGP12177 (1 μM) in the presence of propranolol significantly increased the incidence of wavelets to 0.86 ± 0.17 s^{-1} (n=12 ; p = 0.005). The incidence of calcium waves increased significantly to 0.3 ± 0.1 s^{-1} (p = 0.03).

This shows that CGP12177 is associated with pro-arrhythmic activity even in the presence of a β-blocker. Moreover, in cells which did not show wavelets or waves, CGP12177 increased the incidence of calcium sparks from 45.1 ± 6.69 s^{-1} to 58.6 ± 6.90 s^{-1} (n = 6 ; p < 0.01). Calcium spark activity due to CGP12177 was only increased in the cells showing no wavelets or waves (and not in those showing wavelets or waves) as these events would discharge the SR calcium load resulting in the occurrence of fewer calcium sparks.

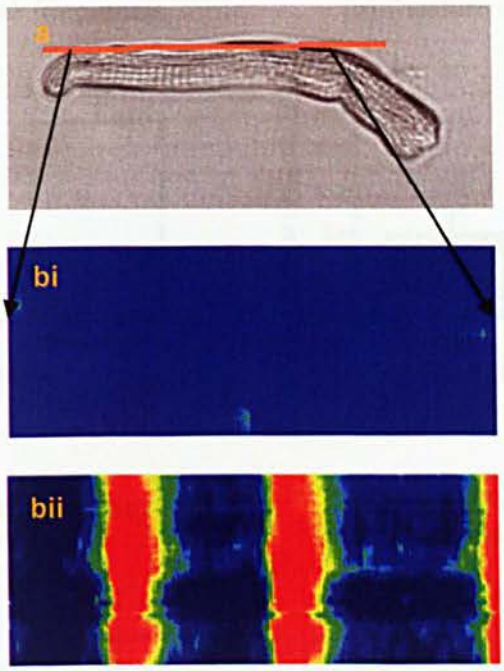

Figure 6.6 Line scan images of quiescent rat atrial cells perfused with CGP12177 in the presence of propranolol. **(a)** photomicrograph image of quiescent rat atrial cell. An orange line has been selected along the periphery of the cell for the line scan **(bi)** line scan image of the same rat atrial cell being perfused with propranolol (200 nM) and only a few calcium sparks are observed **(bii)** line scan image of the calcium events in rat atrial myocytes following perfusion of CGP12177 (1 μM) in the presence of propranolol. The line scan image shows that CGP12177 is highly pro-arrhythmic as observed by the intense calcium activity shown in red. These are calcium waves.

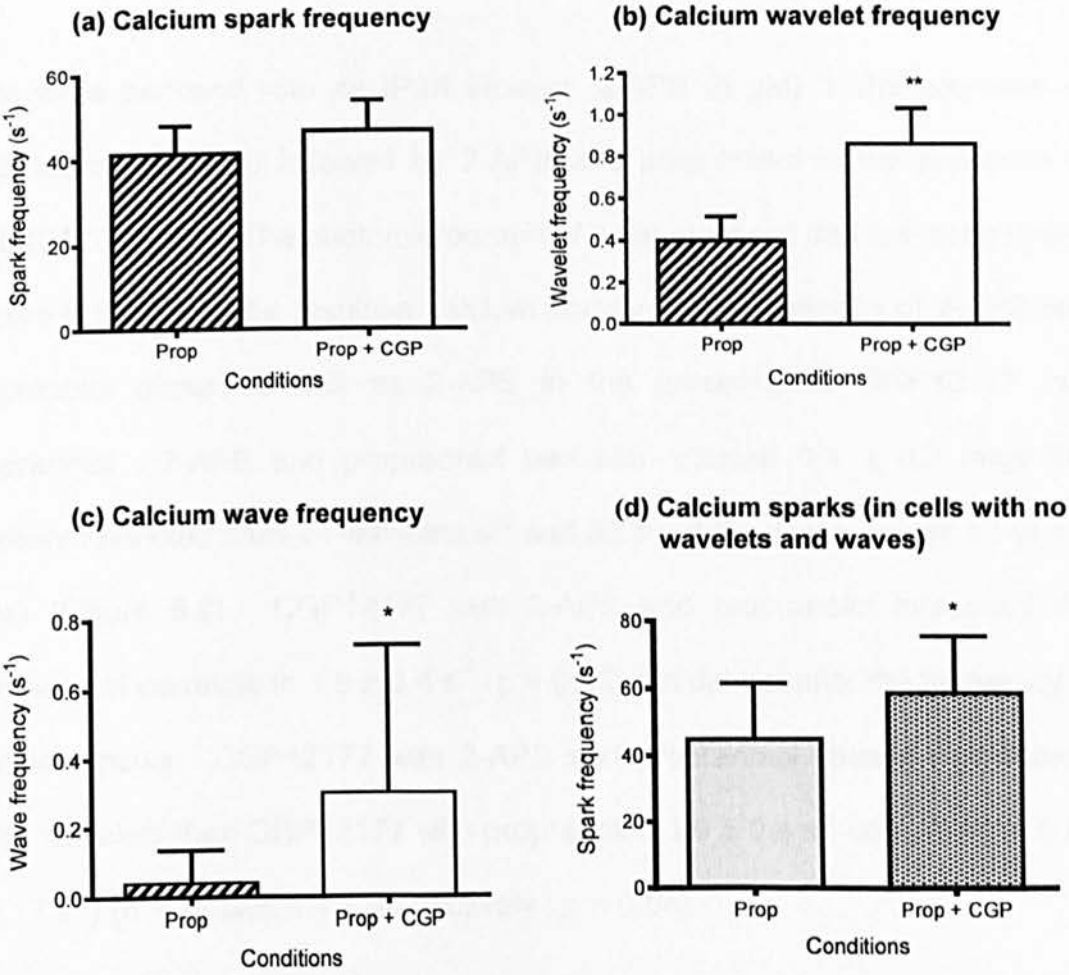

Figure 6.7 Frequency of calcium events upon perfusion of CGP12177 in the presence of propranolol in quiescent rat atrial cells. Bar charts of **(a)** calcium sparks which increased in the presence of CGP12177 and propranolol **(b)** wavelets frequency increased significantly (**p = 0.005) and **(c)** wave frequency of atrial cells in the presence of CGP12177 also increased significantly (*p = 0.03) (1 μM) and propranolol (200 nM) compared to the events under basal conditions **(d)** significant increase in spark frequency in atrial cells which did not produce wavelets or waves when perfused with CGP12177 and propranolol (*p = 0.02). The results suggest the administration of CGP12177 in the presence of a β-blocker still triggered cardiostimulatory activity, hence CGP12177 may be associated with pro-arrhythmogenic effects.

6.6.4 The effect of CGP12177 in the presence of 2-APB and propranolol on spontaneous calcium release

Cells were perfused with an IP3R blocker, 2-APB (5 μM) in the presence of propranolol (200 nM) followed by 2-APB and propranolol in the presence of CGP12177 (1 μM). The photomicrograph of a left atrial cell and line scan image (Figure 6.8) shows the resulting calcium activity in the presence of 2-APB and propranolol alone as well as 2-APB in the presence of CGP12177 and propranolol. 2-APB and propranolol perfusion caused 0.4 ± 0.2 large but spatially restricted calcium wavelets s^{-1} and 30.4 ± 4.3 calcium sparks s^{-1} (n = 7 cells) (Figure 6.9). CGP12177 with 2-APB and propranolol increased the incidence of wavelets to 1.9 ± 0.4 s^{-1} (p = 0.03) but did not alter the frequency of calcium sparks. CGP12177 with 2-APB and propranolol caused significantly more wavelets than CGP12177 with propranolol (1.9 ± 0.4 s^{-1} compared to 0.86 ± 0.17 s^{-1}) (n = 12 and n = 7 respectively ; p = 0.04).

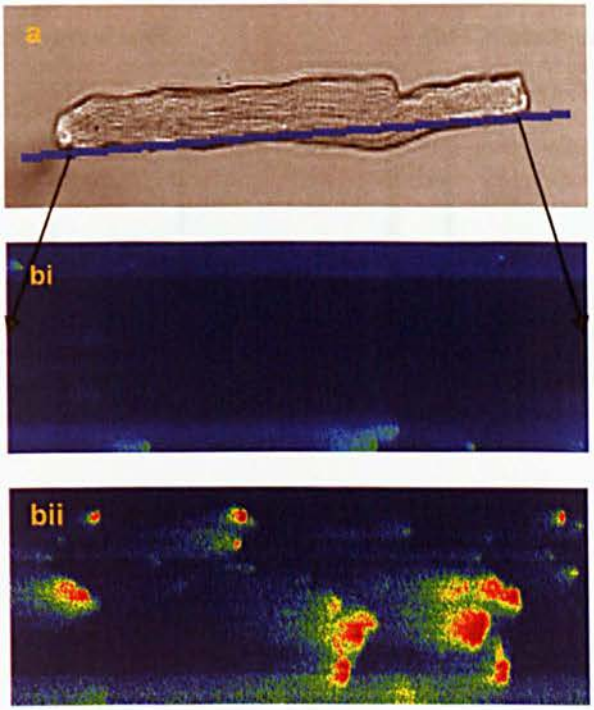

Figure 6.8 Line scan images of quiescent rat atrial cells perfused with CGP12177 in the presence of 2-APB. (a) photomicrograph image of quiescent rat atrial cell. A blue line has been selected along the periphery of the cell for the line scan **(bi)** line scan image of the same rat atrial cell being perfused with 2-APB (5 μM) and propranolol (200 nM) and calcium sparks are observed **(bii)** line scan image of the calcium wavelets in rat atrial myocytes following perfusion of 2-APB (5 μM) in the presence of CGP12177 (1μM) and propranolol (200 nM). 2-APB is an IP3R receptor blocker but as seen in the line scan above, it does not inhibit the calcium efflux from the SR caused by CGP12177 which means that the SR calcium release is likely to be via RyR2.

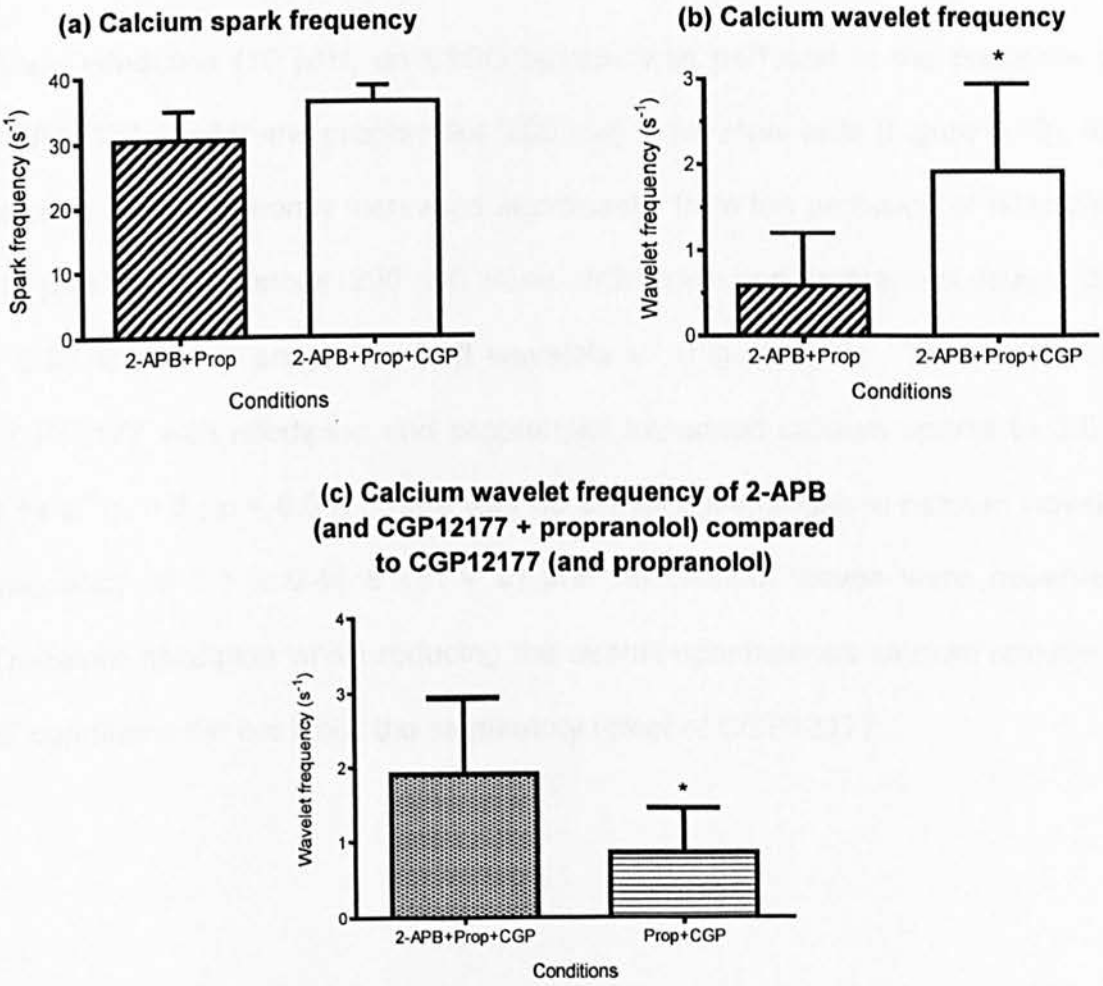

Figure 6.9 Frequency of calcium activity upon perfusion of CGP12177 in the presence of 2-APB in quiescent rat atrial cells. Bar charts for **(a)** calcium sparks and **(b)** significant increase of wavelet frequency of the atrial cells in the presence of CGP12177 (1 μM), 2-APB (5 μM) and propranolol (200 nM) compared to the events under basal conditions. Although larger number of wavelets were observed (*p = 0.03), no waves were recorded. Upon comparison of **(c)** wavelet frequency elicited by 2-APB with CGP12177 with propranolol and CGP12177 (in the presence of propranolol) showed that the latter caused significantly less wavelets than 2-APB with CGP12177 and propranolol (*p = 0.04). The addition of 2-APB does not have any inhibitory effect on CGP12177 mediated SR calcium release in the presence of propranolol but in fact it seems to augment it.

6.6.5 The effect of CGP12177 in the presence of nifedipine and propranolol on spontaneous calcium release

When nifedipine (10 μM), an LTCC blocker was perfused in the presence of CGP12177 (1 μM) and propranolol (200 nM) in rat atrial cells (Figure 6.10), the calcium spark frequency increased significantly from the perfusion of nifedipine (10 μM) and propranolol (200 nM) alone. Nifedipine and propranolol caused 3.0 ± 0.97 sparks s^{-1} and 0.6 ± 0.18 wavelets s^{-1} (Figure 6.11). The addition of CGP12177 with nifedipine and propranolol increased calcium sparks to 5.5 ± 0.84 s^{-1} ($n = 6$; $p = 0.04$). There was no significant increase in calcium wavelet frequency of 1.1 ± 0.44 s^{-1} ($n = 9$) and no calcium waves were observed. Therefore nifedipine whilst reducing the overall spontaneous calcium release in all conditions did not block the stimulatory effect of CGP12177.

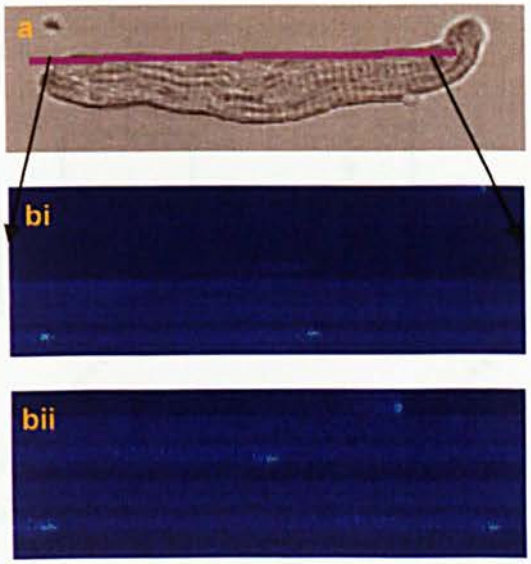

Figure 6.10 Line scan image of quiescent rat atrial cells perfused with CGP12177 in the presence of nifedipine and propranolol. **(a)** photomicrograph image of quiescent rat atrial cell. A purple line has been selected along the periphery of the cell for the line scan **(bi)** line scan image of the same rat atrial cell being perfused with nifedipine (10 μM) and propranolol (200 nM) showing little calcium activity **(bii)** line scan image of an increased frequency of calcium sparks in rat atrial myocytes following perfusion of nifedipine together with CGP12177 and propranolol suggesting that nifedipine might not be completely abolishing the effects of CGP12177 in the presence of propranolol.

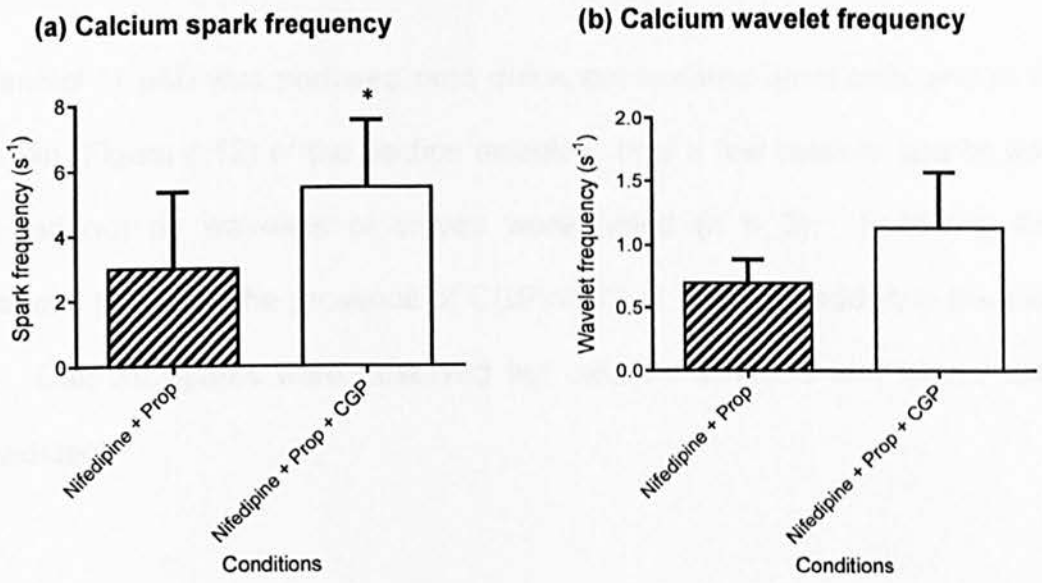

Figure 6.11 Frequency of calcium events upon perfusion of CGP12177 in the presence of nifedipine and propranolol in quiescent rat atrial cells. (a) significant increase in calcium spark frequency during the perfusion of nifedipine (10 μM) with CGP12177 (1 μM) and propranolol (200 nM) compared to nifedipine and propranolol alone (n = 6 ; *p = 0.04). **(b)** wavelet frequency with the perfusion of nifedipine and propranolol (n = 9). The arrhythmogenic effect of CGP12177 is not blocked by inhibition of LTCC. However, there are many fewer calcium events in the presence of nifedipine which indicates that extracellular calcium is the trigger for causing much of the spontaneous SR calcium release.

6.6.6 The effect of CGP12177 in the presence of bupranolol on the spontaneous release of calcium

Bupranolol (1 μM) was perfused onto quiescent isolated atrial cells and in the line scan (Figure 6.12) of the section selected, only a few calcium sparks were observed but no wavelets or waves were noted (n = 5). Following this, bupranolol (1 μM) in the presence of CGP12177 (1 μM) was added to the atrial cells. Calcium sparks were observed but calcium wavelets and waves were non-existent.

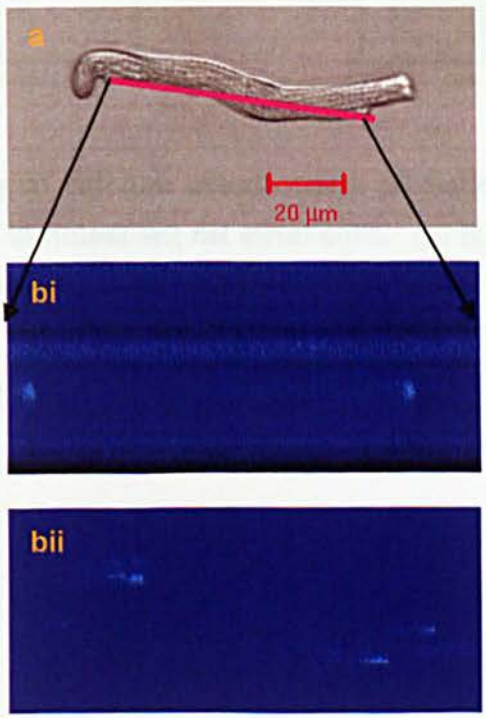

Figure 6.12 Line scan images of quiescent rat atrial cells perfused with CGP12177 in the presence of bupranolol. (a) photomicrograph image of quiescent rat atrial cell. A pink line has been selected along the periphery of the cell for the line scan **(bi)** line scan image of the same rat atrial cell being perfused with bupranolol (1 μM) and a few calcium sparks were observed **(bii)** line scan image of calcium sparks in rat atrial myocytes following perfusion of bupranolol together with CGP12177. Bupranolol antagonises the pro-arrhythmic effect of CGP12177 since the line scan shows no calcium waves, wavelets or as many sparks as observed when CGP12177 was perfused in the presence of propranolol alone.

Bupranolol produced an average of 8.8 ± 2.8 sparks s^{-1} and bupranolol with CGP12177 caused 16.8 ± 5.2 sparks s^{-1} (n = 7) (Figure 6.13). In comparison, for cells not showing wavelets or waves, CGP12177 (with propranolol) caused a significant increase in calcium spark frequency from the perfusion of propranolol alone.

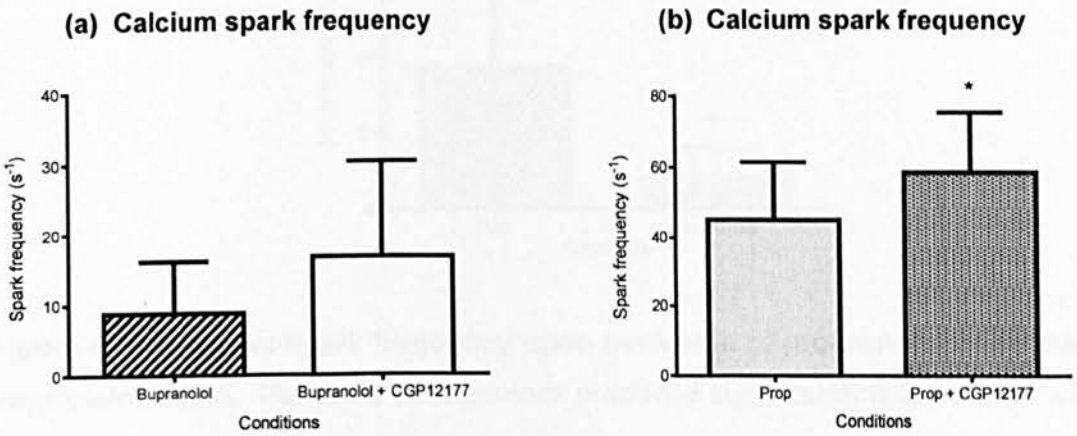

Figure 6.13 Frequency of calcium events upon perfusion of bupranolol in the presence of CGP12177 in quiescent rat atrial cells. **(a)** Bupranolol in the presence of CGP12177 did not significantly increase the calcium spark frequency compared to bupranolol on its own. On the other hand, **(b)** CGP12177 in the presence of propranolol caused a significant increase in spark frequency from its basal conditions (*p = 0.02).

When propranolol (200 nM) alone was perfused in quiescent atrial cells there were 37.2 ± 5.01 calcium sparks s^{-1} (n = 18) (Figure 6.14). However in comparison to the perfusion of bupranolol (1 μM) alone, the frequency of sparks was significantly less at 8.8 ± 2.79 s^{-1} (n = 7 ; p = 0.002).

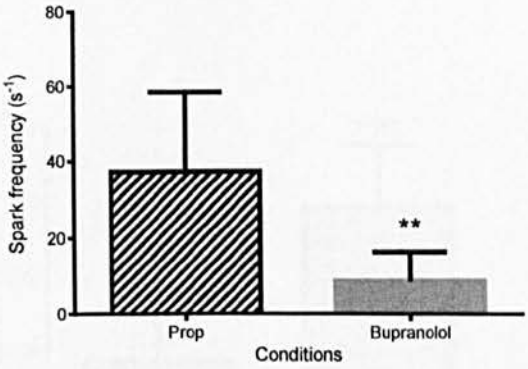

Figure 6.14 Calcium spark frequency upon perfusion of propranolol compared to bupranolol alone. Perfusion of bupranolol produced significantly less calcium sparks compared to propranolol suggesting an inverse agonism revealed by bupranolol blockage of $\beta 1_L$-AR (**p = 0.002).

For cells not exhibiting waves or wavelets, CGP12177 in the presence of propranolol produced 58.6 ± 6.90 calcium sparks s^{-1} ($p = 0.02$) which was significantly more than those produced during the perfusion of bupranolol and CGP12177 which caused only 16.8 ± 5.2 sparks s^{-1} ($n = 6$ and 7 respectively ; $p = 0.0004$) (Figure 6.15) but produced no waves or wavelets.

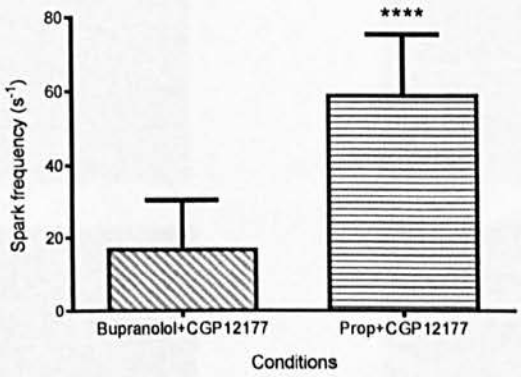

Figure 6.15 Comparing calcium spark frequency upon perfusion of CGP12177 and bupranolol with CGP12177 and propranolol. In cells (which showed no waves or wavelets) perfused with CGP12177 in the presence of propranolol there were significantly more calcium sparks than when CGP12177 is being perfused in the presence of bupranolol (****$p = 0.0004$). This experiment proves that CGP12177's effects are mediated by a β-AR different to the classical β1-AR.

6.6.7 The effect of BRL37344 on spontaneous calcium release

Upon addition of the β3-AR agonist - BRL37344 (300 nM) no calcium waves or wavelets were observed from the calcium imaging videos. The line scan image taken from the blue line drawn upon the micrograph of the left atrial cell (Figure 6.16) shows BRL37344 causing no calcium events whether it is being perfused alone or with propranolol. The mean frequency of calcium sparks at basal

conditions decreased significantly upon the perfusion of BRL37344 on its own from 22.0 ± 2.72 s^{-1} to 14.5 ± 2.19 s^{-1} (n = 5 ; p = 0.04) (Figure 6.17). BRL37344 in the presence of propranolol yielded an average frequency of calcium sparks of 15.4 ± 3.25 s^{-1} which was significantly lower than during the perfusion of propranolol alone at 29.3 ± 3.25 s^{-1} (n = 6 respectively ; p = 0.04).

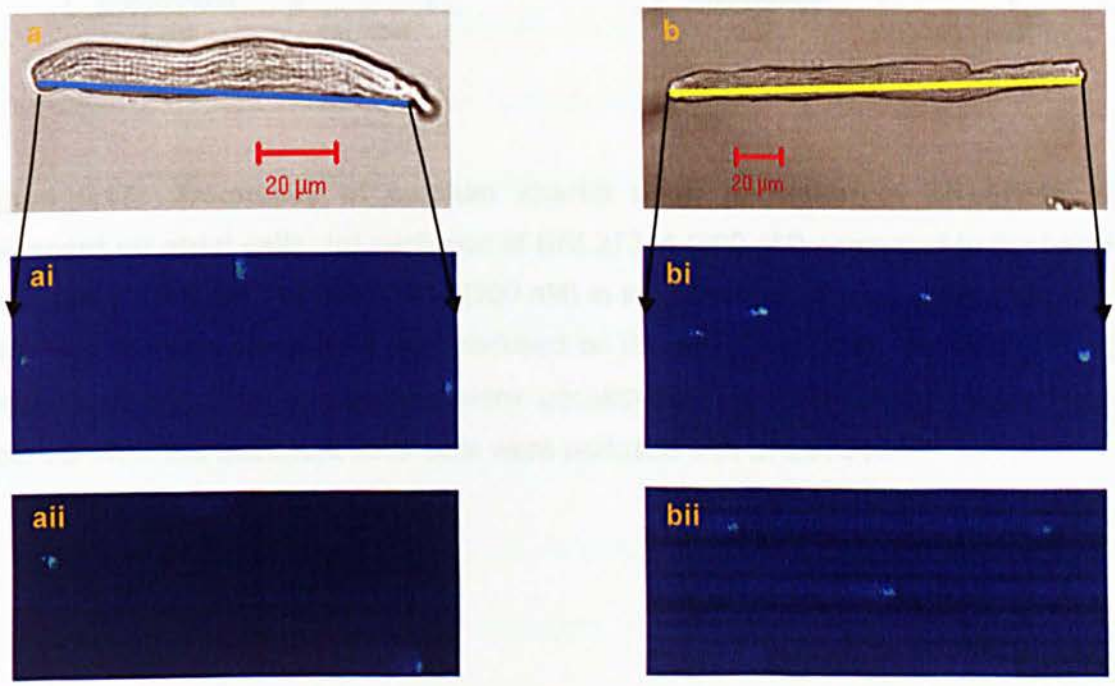

Figure 6.16 Line scan image of quiescent rat atrial cells perfused with BRL37344. (a) and (b) photomicrograph images of quiescent rat atrial cells. A line has been selected along the periphery of the cell for line scan **(ai)** line scan image of the rat atrial cell under basal conditions **(aii)** line scan image of a lack of calcium activity in rat atrial cell in the presence of BRL37344 (300 nM) **(bi)** line scan image of rat atrial cell under the conditions of propranolol perfusion **(bii)** line scan image of rat atrial cell when BRL37344 is perfused with propranolol.

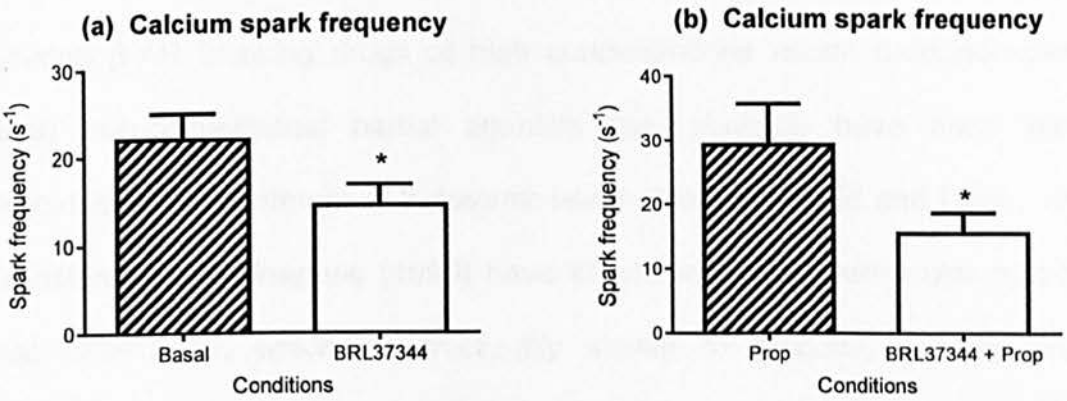

Figure 6.17 Frequency of calcium sparks upon perfusion of BRL37344 in quiescent rat atrial cells **(a)** perfusion of BRL37344 (300 nM) compared to the basal conditions (*p = 0.04) **(b)** BRL37344 (300 nM) in the presence of propranolol (200 nM) compared to when propranolol was perfused on its own (*p = 0.04). Furthermore, at basal conditions calcium wavelets were occasionally observed though none were reported when the quiescent atrial cells were perfused with BRL37344.

6.7 Discussion

Several β-AR blocking drugs at high concentrations cause cardiostimulation. Such non-conventional partial agonists (eg. pindolol) have been contra-indicated in the treatment of ischaemic heart disease (Podrid and Lown, 1982). Freestone and colleagues (1999) have shown in mouse ventricular myocytes that CGP12177, which is structurally similar to pindolol, causes smaller increases in intracellular calcium concentration, but is 40-fold more pro-arrhythmic than ISO which is the most potent sympathomimetic agonist. The aim of this study was to study the behaviour of various cardioactive drugs on the spontaneous calcium release in quiescent rat atrial myocytes thus providing a clearer understanding of the reported arrhythmogenic effects that occur.

This study has demonstrated that CGP12177 administration in isolated quiescent adult rat atrial myocytes caused many more spontaneous calcium release events than ISO. This agrees with previous findings that have described pro-arrhythmic effects of CGP12177 in electrically stimulated rat atrial and ventricular myocytes (Sarsero *et al.*, 1999) as well as mouse ventricular myocytes (Freestone *et al.*, 1999). Live videos of whole cell calcium activities and line-scan images from confocal microscopy confirmed that cardiostimulation caused by CGP12177 was insensitive to the presence of propranolol by exhibiting high calcium activity in the form of calcium sparks, wavelets and waves in both left and right atrial cells. Calcium activity analyses however have been carried out in whole cell calcium imaging mode.

6.7.1 Cardiostimulatory activity by ISO

ISO administration in isolated rat atrial myocytes caused an increase in calcium spark frequency compared to basal, however there was no significant increase in the frequency of whole cell calcium waves or wavelets. This may be due to the SR being depleted of its calcium store resulting from the initial increase in calcium release in the form of sparks (Cheng *et al.*, 1993).

6.7.2 Pro-arrhythmogenic activity of CGP12177

Administration of CGP12177 in the presence of propranolol significantly increased the incidence of wavelets and waves compared to the perfusion of propranolol alone. The increase of calcium activity in terms of calcium wavelets and waves signify and confirm the pro-arrhythmogenicity of CGP12177, even in the presence of propranolol. CGP12177 also increased the incidence of calcium sparks in those cells not exhibiting wavelets or waves ($p < 0.01$) and therefore not subject to a decreased calcium load.

Interestingly, CGP12177 at lower concentrations (100 nM and 10 nM) also caused increases in spontaneous SR calcium release (data not shown). This study outcome agrees with previous findings whereby it has been shown in electrically stimulated mouse ventricular myocytes and rat ventricular and atrial cells respectively that while CGP12177 causes much smaller increases in intracellular calcium levels than ISO, it is also much more pro-arrhythmic than ISO (Freestone *et al.*, 1999 ; Sarsero *et al.*, 1999). CGP12177 was more potent than noradrenaline, acting on conventional β1-ARs in ferret heart at eliciting

action potential shortening but plateau prolongation (Lowe *et al.*, 1998). It is therefore possible that arrhythmias caused by stimulation of the novel β_{1L}-AR are disconnected from the global intracellular calcium levels (Sam *et al.*, 2012). The mechanism for this effect remains to be elucidated.

In 2001, Kaumann and colleagues stated that the arrhythmogenic effect of CGP12177 is supposedly mediated via the high affinity state of the β1-AR (Kaumann *et al.*, 2001). However, considering that CGP12177 is added with propranolol at a concentration that completely blocks the stimulatory effect of ISO, this assertion seems to be incorrect. Unfortunately, this misinterpretation is also evident in the work of Lewis *et al.*, 2004. Perfusion of ruthenium red (10 μM) and CGP12177 produced no cardiostimulatory events suggesting that ruthenium red has inhibited the spontaneous calcium release caused by CGP12177 confirming that CGP12177 exhibits its pro-arrhythmogenic effects via the RyR2 (data not shown).

6.7.3 Stimulatory effect of CGP12177 in the presence of 2-APB and propranolol on spontaneous calcium release

Previously, arrhythmias in rat atrial cells have been observed in the presence of endothelin due to calcium efflux via the IP3R (Li *et al.*, 2005). In this study, 2-APB (a membrane permeable antagonist of the IP3R) was perfused in quiescent single isolated rat atrial cells to investigate the effect of this IP3R blocker on arrhythmogenic SR calcium release caused by CGP12177. As shown previously for mouse ventricular myocytes, (Freestone *et al.*, 1999) CGP12177 is associated with potent arrhythmogenic effects in rat atrial cells.

This effect of CGP12177 on rat atrial myocytes is not affected by the addition of 2-APB. This has previously been suggested to be effective in controlling the spontaneous calcium release which might contribute to the development of calcium-mediated atrial arrhythmias (Zima and Blatter, 2004). However, results obtained from this study contradict those of Zima and Blatter (2004) since 2-APB did not block CGP-induced spontaneous calcium release. There were more calcium events with 2-APB and CGP12177 with propranolol compared to CGP12177 with propranolol. This might be due to the fact that blocking the IP3R loads up the SR with more calcium increasing the frequency of SR calcium release via RyR2. Therefore it seems likely that the arrhythmic events mediated by the β_{1L}-AR are not the result of calcium release via IP3R.

6.7.4 Nifedipine reduces overall spontaneous calcium release but does not block the stimulatory effect of CGP12177

LTCCs are located on the plasma membrane of the cardiac myocyte and can be blocked by nifedipine. Upon the opening of these channels, the RyR2 calcium channel readily allows the release of calcium ions from the SR (Poláková *et al.*, 2008). The addition of CGP12177 with nifedipine in the presence of propranolol (200 nM) did not result in an increase in calcium wavelet frequency from nifedipine and propranolol alone. No calcium waves were observed. In terms of calcium sparks, there was a significant increase in frequency compared to its basal conditions. The results suggest that nifedipine has drastically though not completely abolished the cardiostimulatory effect produced by CGP12177 in the presence of propranolol and calcium sparks are dependent largely on calcium current through LTCC. The findings of this study

agree with the work of Santana's group (1996) in rat ventricular myocytes, whereby nifedipine inhibited calcium release activity by delaying the re-opening of the LTCCs. Additionally, Zhang and colleagues (2013) reported that cardiac stem cell spontaneous beating rate was reduced by 61% due to nifedipine administration.

6.7.5 Inhibition of the effect of CGP12177 by bupranolol

Perfusion of the non-selective β-blocker, bupranolol in the presence of CGP12177 blocked the stimulatory effect of CGP12177 on spontaneous calcium release from the SR. There were no calcium waves or wavelets occurring and the frequency of calcium sparks was lower compared to CGP12177 in the presence of propranolol.

Therefore, the $\beta1_L$-ARs through which the cardiostimulatory effects of CGP12177 are mediated in rat atrial cells, are insensitive to propranolol but are completely blocked by bupranolol. It has been also postulated that the chronotropic effect of CGP12177 on the right atria of the mouse was insensitive to propranolol, however upon the addition of bupranolol the effect of CGP12177 was moderately blocked (Kaumann *et al.*, 1998). This supports the data presented here. Furthermore bupranolol has been shown to cause more of an inverse agonistic effect in quiescent atrial cells via $\beta1_L$-ARs compared to propranolol which only blocks $\beta1_H$-AR and β2-ARs. Hence bupranolol reveals a significant amount of intrinsic activity being mediated via the $\beta1_L$-AR.

6.7.6 Decrease in the occurrence of spontaneous SR calcium release events due to addition of BRL37344

BRL37344 was used in this study as a tool to show that negative effects can also be observed in the isolated atrial cells and not only positive stimulatory activities as with ISO and CGP12177. The β3-AR of human ventricular myocytes mediates negative inotropic effects (Gauthier *et al.*, 1998 ; Michel *et al.*, 2011) and has been shown to be upregulated during HF as a cardio-protective measure (Moniotte *et al.*, 2001). A β3 agonist such as BRL37344 couples with Gi proteins of the cardiomyocytes and activates the Gi intracellular signalling pathway. This results in an increase in cGMP levels and a decrease in the force and rate of contraction of the cardiac cells of the heart (Rozec *et al.*, 2000).

This study performed on quiescent rat atrial cells is consistent with the negative inotropism suggested by Gauthier *et al.*, 1998 in their work on the β3-AR agonist on the human heart. BRL37344 in the presence of propranolol caused a statistically significant decrease in the average spark frequency compared to when propranolol was perfused on its own. BRL37344 on its own perfused in rat atrial cells caused a decrease in the average frequency of calcium sparks from basal conditions. Basal conditions showed other calcium events such as wavelets, but no calcium waves were observed. However, perfusion of BRL37344, only caused calcium sparks and no wavelets or waves were seen. This is due to the stimulation of β3-AR inhibiting cardiac contractility via the release of NO in the Gi protein pathway. The reduction in calcium activity observed with the addition of BRL37344 therefore was due to β3-ARs

stimulation, mediated by a PKG-dependent pathway. This present work confirms the negative inotropic effect of BRL37344 mediated by β3-ARs in rat atrial myocytes.

6.8 Conclusion

- Isoprenaline showed cardiostimulatory activity however it was not as arrhythmogenic as CGP12177 in the presence of propranolol.

- 2-APB showed no effect on reducing the frequency of calcium events despite being an IP3R blocker.

- The addition of nifedipine alone significantly reduced spontaneous calcium release from the SR though CGP12177 was able to still cause a significant increase in SR calcium release even in the presence of nifedipine.

- The pro-arrhythmogenic activity of CGP12177 was completely blocked by bupranolol.

- Arrhythmogenic effects caused by CGP12177 are mediated by β1-AR and unusually this occurs in an environment where there is low calcium mobilisation and low levels of cAMP and PKA than the usual classical β1-AR.

CHAPTER 7

Final Discussion

Atrial and ventricular arrhythmias are commonly observed in people with HF. A large number of experimental studies have focussed mainly upon ventricular arrhythmias possibly due to the relatively difficult task of obtaining viable single isolated rat atrial myocytes compared to ventricular myocytes. More recently, a surge of interest has been initiated in the study of atrial arrhythmias in single quiescent atrial myocytes. The research incorporated into this thesis has been based largely on the specific morphology of left and right rat atrial myocytes and how their features correlate with calcium spark initiation sites during EC coupling, the pathophysiology of calcium handling proteins that interrupts the normal EC-coupling process, and the role of the low affinity β1-AR in spontaneous arrhythmogenic calcium release in rat atrial myocytes.

A pilot study was carried out on cultured chick embryonic ventricular myocytes to determine and classify the pharmacology of the four cardiac β-ARs and to confirm the actions of the various cardiostimulatory and cardioinhibitory drugs that act upon the different receptors. Cardiostimulatory effects triggered by ISO (100 nM) via the Gs protein signalling pathway at the $\beta1_H$/β2-ARs increased the mean spontaneous cardiac contraction rate from the basal contraction rate. This observation is supported by Lands *et al.*, (1969) Sperelakis, (1978), Marvin *et al.*, (1979). Propranolol (at 200 nM; a concentration shown to block the stimulatory effects of 100 nM ISO), a $\beta1_H$/β2 antagonist, was introduced to chick embryonic ventricular cells where it caused a significant decrease in the mean spontaneous contraction rate from basal rate. This demonstrates the phenomenon of inverse agonism. The concomitant addition of the non-conventional partial agonist CGP12177 (1 μM; a concentration previously shown to exert maximal cardiostimulatory effects in a variety of cardiac tissues)

increased the contraction rate. The cardiostimulatory effect of CGP12177 confirms the presence of $\beta 1_L$-AR in chick ventricular myocytes. On the other hand, BRL37344 (600 nM) confirmed the presence of β3-AR in chick ventricular cells by stimulating the Gi pathway of the cardiomyocytes resulting in a negative chronotropic effect. It would have been logical to retrieve chick embryonic atrial cells for this study since the work of this thesis focuses mainly on atrial cells. However, the initial interest here remains to only confirm the pharmacology of the different β-ARs in cardiac cells. The specific contributions of all β-ARs have been confirmed in this preliminary pilot study by the pharmacological responses of the cardio-active drugs (negatively chronotropic by β3-AR stimulation and positively chronotropic with the other remaining β-ARs) in chick embryonic ventricular cells.

It is of importance to study the specific morphology of left and right atrial cells since there seems to be a relationship regarding this and the calcium release sites that contribute to the initiation of cell contraction in normal EC coupling. The left and right mammalian atrial cell dimensions differ slightly from each other and there appears to be a relationship between cell width and the presence (or absence) of the t-tubules in each atrial chamber (reported by a number of groups such as Smyrnias *et al.*, 2010 ; Dibb *et al.*, 2009). During CICR, the small initial extracellular calcium influx eventually results in large intracellular calcium release from the SR. Atrial cell widths seem to determine the sites of origin of calcium sparks which contribute to the generation of whole cell calcium transients and cell contraction. This study showed evidence of some t- tubules (or TATS) in the left atrial cells but none for the right atrial cells. It has also been confirmed that the wider atrial cells on average were left atrial

cells and this is probably due to the fact that the left atrium generates more pressure during contraction than the right.

The wider left atrial cells had more calcium sparks originating from the centre of the cell and this supports the fact that more TATs exist in left atrial cells rather than right atrial cells. In the narrower right atrial cells there were no TATS found and calcium sparks were largely restricted to the sub-sarcolemmal space at the periphery of the cell. The atrial cell widths from this study were consistent with the average width measurements of atrial cells from work done by others (Kirk *et al.*, 2003 ; Dibb *et al.*, 2009 ; Smyrnias *et al.*, 2010) however these groups did not separate out the left and right rat atrial cells. Impaired t-tubular structures (either due to pathophysiology or experimental disruption) in atrial cells promotes dysregulation of normal calcium propagation in EC-coupling and CICR which may contribute to poor contractility, leading to AF, often observed in HF.

Cardiac contractility is modulated by intracellular signalling pathways triggered by a ligand binding to β-ARs. These include mobilization of cAMP and activation of cAMP-dependent protein kinase. This kinase phosphorylates important calcium handling proteins such as PLB, SERCA2a and the cardiac RyR2. The calcium handling protein expression has been found to vary in the different chambers of the mammalian heart and in different cardiac disease states. PLB and SERCA2a are proteins that control calcium uptake into the SR and therefore regulate cell relaxation. Western blotting of rat tissue homogenates enabled the protein expression in these tissues to be studied.

It was observed that there was a higher abundance of total PLB at 25kDa in SHR cardiac homogenates (more specifically in left ventricular homogenate) compared to WKY cardiac tissues. This is consistent with the study by Li and colleagues (2005) whereby PLB was shown to be more abundant in whole heart homogenates of the SHR than WKY rats. SERCA2a removes calcium during the normal cardiac cycle, but it is less abundant in the impaired cardiac homogenates of the SHR. This results in a prolonged intracellular calcium release period from the SR and a decrease in systolic contraction (in a setting of higher systolic blood pressure). Furthermore, this study reveals that SERCA2a is less abundant in HF cardiac homogenates compared to normal cardiac homogenates and this may result in impaired SERCA2a pump function in the failing heart.

In WKY cardiac tissue, PLB was most abundant in the (right) ventricular homogenate and was the least abundant in atrial tissue homogenates. This result in the shorter contraction period of the atria compared to the ventricles. PLB phosphorylation occurs at two sites, Ser16 and Thr17 and both are triggered by β-adrenergic stimulation (Wegener *et al.*, 1989). In normal rats, the abundance of phospho-Thr17 is higher in ventricular homogenates compared to atrial homogenates whereas there is no alteration between these chambers for phospho-Ser16. Thr17 phosphorylated by calcium/CaM kinase II is increased in SHR ventricles since the phosphorylation of PLB occurs mainly via mediation by calcium/CaM Kinase II and less so by PKA in hypertension (Mills *et al.*, 2006). Furthermore, the PKA phosphorylation site is more phosphorylated in WKY due to a reduction in β-ARs in the SHR strain which results in less stimulation (ie phosphorylation events) in the heart.

An impairment of the cardiac SR calcium release channel, RyR2, that regulates the calcium release from the SR may be responsible for the uncontrolled leakage of calcium that is a common feature in HF. This is due to dysfunction of the phosphorylated cardiac RyR2 protein that contributes to less efficient cardiac contraction and susceptibility to arrhythmias.

In this study, the shunt and sham rat models were considered as a pathological models since the SHR homogenates did not yield quantifiable results for the phosphorylated versions of the RyR2 protein. HF cardiac homogenates (except right atrial sample) had lower abundances of total RyR2 compared to non-HF. It has been established that RyR2 is phosphorylated mainly via the PKA pathway and phospho-RyR2808 has been reported to cause abnormal calcium release from the SR during HF (Marx *et al.*, 2000). Shunt right atrial homogenates showed a higher abundance of phospho-RyR2808 compared to the ventricles possibly due to the right atria being the first recipient of blood before the ventricles. Also, it may be fair to suggest that some discrepancies may be unavoidable in this study since there might be genetic differences in the origin of animal models used (eg. WKY and normal SD rats) as well as extent of the disease of the rats used.

Having seen that the expression of calcium handling proteins differs in atrial and ventricular tissue and normal and diseased hearts, an investigation into a specific situation where arrhythmias have been reported to occur in isolated single cells was undertaken.

This involved the pharmacology of the propranolol-insensitive novel $\beta1_L$-AR and atrial arrhythmias in quiescent atrial cells. It was investigated whether the addition of the non-conventional partial agonist, CGP12177 to quiescent rat atrial myocytes in the presence of propranolol resulted in an increase in spontaneous calcium release events which may cause cardiac contractions independent of SA node activity. This study has shown that the administration of CGP12177 in isolated quiescent adult rat atrial myocytes caused a significant increase in arrhythmic events compared to ISO even though the latter causes a larger increase in intracellular calcium than CGP12177. This agrees with previous findings which have described the pro-arrhythmic effect of CGP12177 in rat atrial and ventricular myocytes (Sarsero *et al.*, 1999) and mouse ventricular myocytes (Freestone *et al.*, 1999). It is possible therefore that arrhythmias caused by the stimulation of the novel $\beta1_L$-AR are disconnected from the global intracellular calcium levels.

On the other hand, the administration of 2-APB which is an antagonist of IP3R, in the presence of CGP12177 was studied in quiescent rat atrial cells to see whether it reduces the frequency of spontaneous SR calcium release as suggested previously by Zima and Blatter (2004). These authors suggested that 2-APB was successful in controlling the spontaneous calcium release which would otherwise lead to atrial arrhythmias. Furthermore, Proven and colleagues (2006) have also shown similar results to Zima and Blatter (2004) whereby spontaneous calcium release in rat ventricular myocytes caused by endothelin-1 were completely terminated by the introduction of 2-APB. In this study however, the pro-arrhythmogenic effect of CGP12177 was still observed with 2-APB through the observation of calcium activity in the forms of calcium

sparks, wavelets and waves in rat atrial myocytes. It is clear therefore that the arrhythmic events triggered by $\beta1_L$-AR are not due to calcium efflux via IP3R but via RyR2 instead.

Previously it has been suggested that bupranolol, a non-selective β-blocker, hinders the $\beta1_L$-AR with moderate potency in mice (Kaumann *et al.*, 1998) and hence inhibits the pro-arrhythmic effects caused by CGP12177. This study has shown that $\beta1_L$-AR is propranolol-insensitive however the cardiostimulatory effect of CGP12177 was blocked by bupranolol. Bupranolol in the presence of CGP12177 in quiescent rat atrial myocytes did not cause a significant increase in calcium spark frequency compared to bupranolol on its own. Furthermore, no calcium wavelets or waves were produced upon the perfusion of bupranolol alone or bupranolol in the presence of CGP12177. On the other hand, in rat atrial cells which did not exhibit waves or wavelets (in which the SR calcium store was therefore not depleted), CGP12177 (in the presence of propranolol) increased the incidence significantly of calcium sparks. The calcium spark frequency of bupranolol with CGP12177 was thus lower than the calcium spark frequency of CGP12177 in the presence of propranolol. Also $\beta1_L$-AR seems to possess significant intrinsic activity because when bupranolol binds, it causes more inverse agonism in quiescent atrial cells than propranolol that blocks $\beta1_H$-AR and β2-AR.

The mechanistic pathway of how the pro-arrhythmogenic effects caused by CGP12177 binding to the $\beta1_L$-AR occur and how the highly arrhythmogenic effects can be controlled if not blocked is still yet to be understood. However the novel finding of arrhythmogenic effects being preferentially mediated by

activation of a specific sub-type of the β1-AR ($\beta1_L$-AR) has been confirmed here. The fact that this occurs in an intracellular environment in which there is less calcium, cAMP and PKA being mobilised compared to classical β1-AR binding events only adds to the noteworthiness of this data.

REFERENCES

Anderson R.H., and Cook A.C., The structure and components of the atrial chambers. *Europace* 2007 ; **9** : vi 3-vi 9.

Amos W.B., White J.G., How the confocal laser scanning microscope entered biological research. *Biology of the Cell* 2003 ; **95** : 335-342.

Baker J.G., Hall I.P., Hill S.J., Agonist and inverse agonist actions of β-blockers at the human β2-adrenoceptor provide evidence for agonist-directed signalling. *Molecular Pharmacology* 2003 ; **64** (6) : 1357-1369.

Baker J.G., The selectivity of β-adrenoceptor agonists at human β1, β2 and β3-adrenoceptors. *British Journal of Pharmacology* 2005 ; **144** (3) : 317-322.

Baker J.G., Hill S.J., Summers R.J., Evolution of β-blockers : from anti-anginal drugs to ligand-directed signalling. *Trends in Pharmacological Sciences* 2011 ; **32** (4) : 227-234.

Bartel S., Krause E-G., Wallukat G., Karczewski P., New insights into β2-adrenoceptor signalling in the adult rat heart. *Cardiovascular Research* 2003 ; **57** : 694 – 703.

Bauml M.A., Underwood D.A., Left ventricular hypertrophy : An overlooked cardiovascular risk factor. *Cleveland Clinic Journal of Medicine* 2010 ; **77** (6) : 381-387.

Belevych A.E., Radwański P.B., Carnes C.A., Györke S., 'Ryanopathy' : causes and manifestations of RyR2 dysfunction in heart failure. *Cardiovascular Research* 2013 ; **98** : 240-247.

Bell D., Kelso E.J., Argent C.C.H., Lee G.R., Allen A.R., McDermott B.J., Temporal characteristics of cardiomyocyte hypertrophy in the spontaneously hypertensive rat. *Cardiovascular Pathology* 2004 ; **13**(2) : 71-78.

Benham C.D., Bolton T.B., Spontaneous transient outward currents in single visceral and vascular smooth muscle cells of the rabbit. *Journal of Physiology* 1986 ; **381** : 385-406.

Benjamin E.J., Wolf P.A., D'Agostino R.B., Silbershatz H., Kannel W.B., Levy D., Impact of atrial fibrillation on the risk of death : The Framingham heart study. *Circulation* 1998 ; **98** : 946-952.

Bernstein D., Fajardo G., Zhao M., Urashima T., Powers J., *et al.*, Differential cardioprotective/cardiotoxic effects mediated by β-adrenergic receptor subtypes. *American Journal of Physiology* 2005 ; **289** : H2441-H2449.

Bers D.M., Cardiac excitation-contraction coupling. *Nature* 2002 ; **415** ; 198-205.

Bers D.M., Ryanodine receptor S2808 phosphorylation in heart failure : Smoking gun or red herring? *Circulation Research* 2012 ; **110** : 796-799.

Bhattacharya S., Hall S.E., Li H., Vaidehi N., Ligand stabilized conformational states of the human β2-adrenergic receptor: insight into G-protein coupled receptor activation. *Biophysical Journal* 2008 ; **94** : 2027-2042.

Black A.H., Cardiac conditioning in curarized dogs : The relationship between heart rate and skeletal behaviour. In *Classical Conditioning : A symposium* ed 1995; W.F. Prokasy 20-47. New York: Appleton-Century-Crofts 421pp

Bokník P., Unkel C., Kirchhefer U., Kleideiter U., Klein-Wiel O., *et al.*, Regional expression of phospholamban in the human heart. *Cardiovascular Research* 1999 ; **42** : 67-76.

Bokník P., Heinroth-Hoffmann I., Kirchhefer U., Knapp J., Linck B., *et al.*, Enhanced protein phosphorylation in hypertensive hypertrophy. *Cardiovascular Research* 2001 ; **51** : 717-728.

Bolton T.B., Gordienko D.V., Confocal imaging of calcium release events in single smooth muscle cells. *Acta Physiologica Scandinavica* 1998 ;**164** : 567-575.

Boyett M.R., Honjo H., Kodama I., The sino-atrial node, a heterogenous pacemaker structure. *Cardiovascular Review* 2000 ; **47** : 658-687.

Braunwald E., Cardiovascular medicine at the turn of the millennium : Triumphs, concerns and opportunities. *New England Journal of Medicine* 1997 ; **337** : 1360-1369.

Brette F., Orchard C., T-tubule function in mammalian cardiac myocytes. *Circulation Research* 2003 ; **92** : 1182-1192.

Brette F., Orchard C., Resurgence of cardiac t-tubule research. *Physiology* 2007 ; **22** (3) : 167-173.

Brette F., Sallé L., Orchard C.H., Quantification of calcium entry at the t-tubules and surface membrane in rat ventricular myocytes. *Biophysical Journal* 2006 ; **90**:381-389.

Bristow M.R., Ginsburg R., Umans V., Fowler M., Minobe W., *et al.*, β1- and β2-adrenergic receptor subpopulations in nonfailing and failing human ventricular myocardium : coupling of both receptor subtypes to muscle contraction and selective β1-adrenoceptor down-regulation in heart failure. *Circulation Research* 1986 ; **59** : 297-309.

Brittsan A.G., Kranias E.G., Phospholamban and cardiac contractile function. *Journal of Molecular and Cellular Cardiology* 2000 ; **32** : 2131-2139.

Brodde O-E., β1 and β2-adrenoceptors in the human heart : Properties, function and alterations in chronic heart failure. *Pharmacological reviews* 1991 ; **43** (2) : 203-242.

Brodde O., Michel M.C., Adrenergic and muscarinic receptors in the human heart. *Pharmacological Reviews* 1999 ; **51** (4) : 651-690.

Burrows M.T., Rhythmical activity of isolated heart muscle cells in vitro. *Science* 1912 ; **3** : 90-92.

Bustamante J.O., Watanabe T., Murphy D.A., McDonald T.F., Isolation of single atrial and ventricular cells from the human heart. *Canadian Medical Association Journal* 1982 ; **126** (7) : 791-793.

Chen F., Mottino G., Klitzner T.S., Philipson K.D., Frank J.S., Distribution of the Na^+/Ca^{2+} exchange protein in developing rabbit myocytes. *American Journal of Physiology* 1995 ; **268** : 1126-1132.

Cheng H., Lederer W.J., Cannell M.B., Calcium sparks: elementary events underlying excitation-contraction coupling in heart muscle. *Science* 1993 ; **262** (5134) : 740-744.

Cheng H., Lederer W.J., Calcium sparks. *Physiological Reviews* 2008 ; **88** : 1491-1545.

Cheng H-J., Zhang Z-S., Onishi K., Ukai T., Sane D.C., Cheng C-P., Upregulation of functional β3-Adrenergic receptor in the failing canine myocardium. *Circulation Research* 2001 ; **89** : 599-606.

Chen-Izu Y., Xiao R-P., Izu L.T., Cheng H., Kuschel M., *et al.,* G(i)-dependent localization of β2-adrenergic receptor signalling to L-type Ca^{2+} channels. *Biophysical Journal* 2000 ; **79** (5) : 2547-2556.

Chidiac P., Hebert T.E., Valquette T., Dennis M., Bouvier M., Inverse agonist activity of β-adrenergic antagonists. *Molecular Pharmacology* 1994 ; **45** (3) :490-499.

Chopra N., Knollmann B.C., Cardiac calsequestrin : The new kid on the block in arrhythmias. *Journal of Cardiovascular Electrophysiology* 2009 ; **20** (10) : 1179-1185.

Communal C., Singh K., Sawyer D.B., Colucci W.S., Opposing effects of β1- and β2-adrenergic receptors on cardiac myocyte apoptosis : role of a pertussis toxin-sensitive G protein. *Circulation* 1999 ; **100** : 2210-2212.

Connelly K.A., Kelly D.J., Zhang Y., Prior D.L., Martin J., *et al.*, Functional, structural and molecular aspects of diastolic heart failure in the diabetic (mRen-2)27 rat. *Cardiovascular Research* 2007 ; **76** : 280-291.

Creazzo T.L., Burch J., Godt R.E., Calcium buffering and excitation-contraction coupling in developing avian myocardium. *Biophysical Journal* 2004 ; **86** (2) : 966-977.

DeHann R.L., Regulation of spontaneous activity and growth of embryonic chick heart cells in tissue culture. *Developmental Biology* 1967 ; **16** (3) : 216-249.

De Young M.B., Scarpa A., ATP receptor-induced Ca^{2+} transients in cardiac myocytes: sources of mobilized Ca^{2+}. *American Journal of Physiology Cell Physiology* 1989 ; **257** (4) : C750-C758.

Dibb K.M., Clarke J.D., Horn M.A., Richards M.A., Graham H.K., *et al.*, Characterization of an extensive transverse tubular network in sheep atrial myocytes and its depletion in heart failure. *Circulation Heart Failure* 2009 ; **2** : 482-489.

Dobrev D., Teos L.Y., Lederer W.J., Unique atrial myocyte Ca^{2+} signalling. *Journal of Molecular and Cellular Cardiology* 2009 ; **46** (4) : 448-451.

Dulhunty A.F., Beard N.A., Hanna A.D., Regulation and dysregulation of cardiac ryanodine receptor (RyR2) open probability during diastole in health and disease. *The Journal of General Physiology* 2012 ; **140** (2) : 87-92.

Dzimiri N., Regulation of β-adrenoceptor signaling *in cardiac function and* disease. *Pharmacological Reviews* 1999 ; **51** (3) : 465-501.

Eliška O., Purkynje fibers of the heart conduction system - history and the present time. *Casopís Lékařů Českých* 2006 ; **145** : 329-335.

Emorine L.J., Marullo S., Briden –Sutren M-M., Patey G., Tate K., *et al.*, Molecular characterization of the human β3-adrenergic receptor. *Science* 1989 ; **245** (4922) : 1118-1121.

Eschenhagen T., Is ryanodine receptor phosphorylation key to the fight or flight response and heart failure? *The Journal of Clinical Investigation* 2010 ; **120** (12) : 4197-4203.

Fabiato A., Fabiato F., Effects of pH on the myofilaments and the sarcoplasmic reticulum of skinned cells and cardiac and skeletal muscles. *Journal of Physiology* 1978 ; **276** :233-255.

Fabiato A., Simulated calcium current can both cause calcium loading in and trigger calcium release from the sarcoplasmic reticulum of a skinned canine cardiac purkinje cell. *Journal of General Physiology* 1985 ; **85** : 291-320.

Fallavollita J.A., Jacob S., Young R.F., Canty J.M., Jr, Regional alterations in SR Ca^{2+}-ATPase, phospholamban and HSP-70 expression in chronic hibernating myocardium. *American Journal of Physiology : Heart Circulation Physiology* 1999 ; **277** : H1418-H1428.

Fechner S., Busch C., Oppitz M, Drews U., Meyer-Wittkopf M., The chick embryo as a model for intrauterine ultrasound-guided heart intervention. *Ultrasound in Obstetrics and Gynaecology* 2008 ; **31** : 277-283.

Ford L.E., Heart Size. *Circulation Research* 1976 ; **39** : 297-303.

Franzini-Armstrong C., Protasi F., Ramesh V., Shape, size and distribution of Ca^{2+} release units and couplons in skeletal and cardiac muscles. *Biophysical Journal* 1999 ; **77** : 1528-1539.

Freestone N., Singh J., Krause E.G., Vetter R., Early postnatal changes in sarcoplasmic reticulum calcium transport function in spontaneously hypertensive rats. *Molecular and Cellular Biochemistry* 1996 ; **163-164** : 57-66.

Freestone N.S., Heubach J.F., Wettwer E., Ravens U., Brown D., Kaumann AJ., β4-adrenoceptors are more effective than β1-adrenoceptors in mediating arrhythmic Ca^{2+} transients in mouse ventricular myocytes. *Naunyn-Schmiedebergs Archive Pharmacology* 1999 ; **360** : 445-456.

Freestone N.S., Ribaric S., Scheuermann M., Mauser U., Paul M., Vetter R., Differential lusitropic responsiveness to β-adrenergic stimulation in rat atrial and ventricular myocytes. *Pflügers Archiv : European Journal of Physiology* 2000 ; **441** (1) :78-87.

Freestone N.S., Jahangiri M., Kaminski Y., Bolton T., Gordienko D., Human atrial cell morphology is linked to heterogeneous distribution of Ca^{2+}sparks. *Proceedings of the Physiological Society* (poster communication) 2007.

Frey N., Katus H. A., Olson E. N., Hill J.A., Hypertrophy of the heart. A new therapeutic target? *Circulation* 2004 ; **109** : 1580-1589.

Frielle T., Daniel K., Caron M.G., Lefkowitz R.J., Structural basis of β-adrenergic receptor subtype specificity studied with chimeric β1 - β2-adrenoceptors. *Proceedings of the National Academy of Sciences of the United States of America* 1988 ; **85** : 9494-9498.

Gauthier C., Tavernier G., Charpentier F., Langin D., Le Marec H., Functional β3-AR in the human heart. *The Journal of Clinical Investigation* 1996 ; **98** (2) : 556-562.

Gauthier C., Leblais V., Kobzik L., Trochu J.N., Khandoudi N., *et al.,* The negative inotropic effect of β3-adrenoceptor stimulation is mediated by activation of a nitric oxide synthase pathway in human ventricle. *The Journal of Clinical Investigation* 1998 ; **102** (7) : 1377-1384.

Gelebart P., Opas M., Michalak M., Calreticulin a Ca^{2+}-binding chaperone of the endoplasmic reticulum. *The International Journal of Biochemistry and Cell Biology* 2005 ; **37** : 260-266.

Goldman S., Olajos M., Morkin E., Comparison of the left atrial and left ventricular performance in conscious dogs. *Cardiovascular Research* 1984 ; **18** : 604-612.

Gómez A.M., Valdivia H.H., Cheng H., Lederer M.R., Santana L.F., *et al.*, Defective excitation-coupling in experimental cardiac hypertrophy and heart failure. *Science* 1997 ; **276** (5313) : 800-806.

Gradman A.H., Alfayoumi F., From left ventricular hypertrophy to congestive heart failure : Management of hypertensive heart disease. *Progress in Cardiovascular Disease* 2006 ; **48** (5) : 326-341.

Hamburger V., Hamilton H.L., A series of normal stages in the development of the chick embryo. *Journal of Morphology* 1951 ; **88** (1) : 49-92.

Hasenfuss G., Meyer M., Schillinger W., Preuss M., Pieske B., Just H., Calcium handling proteins in the failing human heart. *Basic Research in Cardiology* 1997 ; **92** (1) : 87-93.

Ho S.Y., Anderson R.H., Sánchez-Quintana D., Atrial structure and fibres: morphologic bases of atrial conduction. *Cardiovascular Research* 2002 ; **54** : 325-336.

Huke S., Bers D.M., Ryanodine receptor phosphorylation at Serine 2030, 2808 and 2814 in rat cardiomyocytes. *Biochemical and Biophysical Research Communications* 2008 ; **376**(1) : 80-85.

Hume J.R., Uehara A., Ionic basis of the different action potential configurations of single guinea-pig atrial and ventricular myocytes. *Journal of Physiology* 1985 ; **368** : 525-544.

Hüser J., Lipsius S.L., Blatter L.A., Calcium gradients during excitation-contraction coupling in cat atrial myocytes. *Journal of Physiology* 1996 ; **494** (3) : 641-651.

Huxley H.E., Hansen J., Changes in the cross-striations of muscle during contraction and stretch and their structural interpretation. *Nature* 1954 ; **173** : 973-976.

Huxley A.F., Niedergerke R., Structural changes in muscle during contraction : Interference microscopy of living muscle fibres. *Nature* 1954 ; **173** : 971-973.

Hynes B.J, Luck J.C., Wolbrette D.L., Boehmer J., Naccarelli G.V., Arrhythmias in patients with heart failure. *Current treatment options in Cardiovascular Medicine* 2002 ;**4** (6) : 467-485.

Johnson M., Molecular mechanisms of β2-adrenergic receptor function, response and regulation. *Journal of Allergy and Clinical Immunology* 2006 ; **117** (1) : 18-24.

Johnson W.D., Ganjoo A.K., Stone C.D., Srivyas R.C., Howard M., The left atrial appendage : our most lethal human attachment! Surgical implications. *European Journal of Cardiothoracic Surgery* 2000 ; **17** : 718-722.

Kaasik A., Paju K., Minajeva A., Ohisalo J., Decreased expression of phospholamban is not associated with lower β-adrenergic activation in rat atria. *Molecular and Cellular Biochemistry* 2001 ; **223** : 109-115.

Katz A.M., Zile M.R., New molecular mechanisms in diastolic heart. *Circulation* 2006 ; **113** : 1922-1925.

Kaumann A.J., Is there a third heart β-adrenoceptor? *Trends in Pharmacological Sciences* 1989 ; **10** : 316-320.

Kaumann A.J., Molenaar P., Differences between the third cardiac β-adrenoceptor and the colonic β3-adrenoceptor in the rat. *British Journal of Pharmacology* 1996 ; **118** (8) : 2085-2098.

Kaumann A.J., Lynham J.A., Stimulation of cyclic AMP-dependent protein kinase in rat atria by (-) CGP12177 through an atypical β-adrenoceptor. *British Journal of Pharmacology* 1997 ; **129** : 1187-1189.

Kaumann A.J., Molenaar P., Modulation of human cardiac function through β-adrenoceptor populations. *Naunyn-Schmiedebergs Archive Pharmacology* 1997; **255** : 667-681.

Kaumann A.J., Preitner F., Sarsero D., Molenaar P., Revelli J-P., Giacobino J.P., (-)-CGP 12177 causes cardiostimulation and binds to cardiac putative β4-adrenoceptors in both wild-type and β3-adrenoceptor knockout mice. *Molecular Pharmacology* 1998 ; **53** : 670-675.

Kaumann A.J., Engelhardt S., Hein L., Molenaar P., Lohse M., Abolition of (-)-CGP12177-evoked cardiostimulation in double β1/β2-adrenoceptor knockout mice. Obligatory role of β1-adrenoceptors for putative β4-adrenoceptor pharmacology. *Naunyn-Schmiedebergs Archive Pharmacology* 2001 ; **363** : 87-93.

Kaumann A.J., Molenaar P., The low-affinity site of the β_1-adrenoceptor and its relevance to cardiovascular pharmacology. *Pharmacology and Therapeutics* 2008 ; **118** : 303-336

Kenakin T., Principles : receptor theory in pharmacology. *Trends in Pharmacological Sciences* 2004 ; **25** (4): 186-192.

Kirk M.M., Izu L.T., Chen-Izu Y., McCulle S.L., Wier G.W *et al.,* Role of transverse-axial tubule system in generating calcium sparks and calcium transients in rat atrial myocytes. *Journal of Physiology* 2003 ; **547** : 441-451.

Kiss E., Ball N.A., Kranias E.G., Walsh R.A., Differential changes in cardiac phospholamban and sarcoplasmic reticular Ca^{2+}-ATPase protein levels. Effects on Ca^{2+} transport and mechanics in compensated pressure-overload hypertrophy and congestive heart failure. *Circulation Research* 1995 ; **77** : 759-764.

Kiss E., Edes I., Sato Y., Luo W., Liggett S.B., Kranias E.G., β-adrenergic regulation of cAMP and protein phosphorylation in phospholamban-knockout mouse hearts. *American Journal of Physiology* 1997 ; **272** (2) : H785-H790.

Koch W.J., Lefkowitz R.J., Rockman H.A., Functional consequences of altering myocardial adrenergic receptor signalling. *Annual Reviews of Physiology* 2000 ; **62** : 236-260.

Kolwicz S.C., Seqqat R., Renna B.F., Rafiq K., Houser S.R., *et al.*, Exercise training attenuates apoptosis in the spontaneously hypertensive rat. *Federation of American Societies for Experimental Biology Journal* 2007 ; **21** : 765.24.

Konkar A.A., Zhai Y., Granneman J.G., β1-adrenergic receptors mediate β3-adrenergic-independent effects of CGP12177 in brown adipose tissue. *Molecular Pharmacology* 2000 ; **57** : 252-258.

Korecky B., Michael L.H., Regional differences in contractions of mammalian hearts. *Recent advances in studies on cardiac structure and metabolism* 1974 ; **4**: 77-87.

Koss K.L., Ponniah S., Jones W.K., Grupp I.L., Kranias E.G., Differential phospholamban gene expression in murine cardiac compartments. Molecular and physiological analyses. *Circulation Research* 1995 ; **77** (2) : 342-353.

Koss K.L., Kranias E.G., Phospholamban : a prominent regulator of myocardial contractility. *Circulation Research* 1996 ; **79** : 1059-1063.

Koss K.L., Grupp I.L., Kranias E.G., The relative phospholamban and SERCA2a ratio : A critical determinant of myocardial contractility. *Basic Research in Cardiology* 1997 ; **92** (1) : 17-24.

Kubo H., Margulies K.B., Piacentino V., III., Gaughan J.P., Houser S.R., Patients with end-stage congestive heart failure treated with β-adrenergic receptor antagonists have improved ventricular myocyte calcium regulatory protein abundance. *Circulation* 2001 ; **104** : 1012-1018.

Kushnir A., Marks A.R., The ryanodine receptor in cardiac physiology and disease. *Advances in Pharmacology* 2010 ; **59** :1-30.

Laitinen P.J., Brown K., Piippo K., Swan H., Devaney J.M., et al., Mutations of the cardiac ryanodine receptor (RyR2) gene in familial polymorphic ventricular tachycardia. *Circulation* 2001 ; **103** (4) : 485-490.

Lands A.M., Arnold A., McAuliff J.P., Luduena F.P., Brown T.G. Jr., Differentiation of receptor systems activated by sympathomimetic amines. *Nature* 1967 ; **214** (5088) : 597-598.

Lands A.M., Luduena F.P., Buzzo H.J., Adrenotrophic β-receptors in the frog and chicken. *Life Sciences* 1969 ; **8** (7) : 373-382.

Lanner J.T., Georgiou D.K., Joshi A.D., Hamilton S.L., Ryanodine receptors : Structure, expression, molecular details, and function in calcium release. *Cold Spring Harbor Perspectives in Biology* 2010 ; **2** : 1-21.

Leeson T.S., T-tubules, couplings and myofibrillar arrangements in rat atrial myocardium. *Acta Anatomica* 1980 ; **108** : 374-388

Levick J.R., An introduction to Cardiovascular Physiology 5th Edition 2012 ; Hodder Education : ISBN 1444166476

Levitzki A., Signal transduction in hormone-dependent adenylate cyclase. *Cell Biophysics* 1988 ; **12** (1) : 133-143.

Lewis C.J., Gong H., Brown M.J., Harding S.E., Overexpression of β1-adrenoceptors in adult rat ventricular myocytes enhances CGP12177A cardiostimulation : implications for 'putative' β4-adrenoceptor pharmacology. *British Journal of Pharmacology* 2004 ; **141** : 813-824.

Li S-Y., Golden K-L., Jiang Y., Wang G.J., Privratsky J.R., *et al.,* Inhibition of sarco(endo)plasmic reticulum Ca^{2+}-ATPase differentially regulates contractile function in cardiac myocytes from normotensive and spontaneously hypertensive rats. *Cell Biochemistry and Biophysics* 2005 ; **42** : 1-12.

Li X., Zima A.V., Sheikh F., Blatter L.A, Chen J., Endothelin-1-induced arrhythmogenic Ca^{2+} signalling is abolished in atrial myocytes of Inositol-1,4,5-Triphosphate (IP3)-receptor type 2-deficient mice. *Circulation Research* 2005 ; **96** : 1274-1281.

Lindner E., Die submikroskopische Morphologie des Herzmuskels. *Zeitschrift Zellforsch* 1956 ; **45** : 702-746.

Lipp P., Niggli E., Ratiometric confocal Ca^{2+} measurements with visible wavelength indicators in isolated cardiac myocytes. *Cell Calcium* 1993 ; **14** : 359-372.

Lipp P., Schwaller B., Niggli E., Specific inhibition of Na-Ca exchange function by antisense oligodeoxynucleotides. *Federation of European Biochemical Societies* 1995 ; **364** (2) 198-202.

Lohse M.J., Engelhardt S., Eschenhagen T., What is the role of β-adrenergic signalling in heart failure? *Circulation Research* 2003 ; **93** : 896-906.

Lo H.M., Lin F.Y., Lin J.L., Hsu K.L., Chiang F.T., Tseng C.D., Tseng Y.Z., Impaired cardiac performance relating to delayed left atrial activation after atrial compartment operation for chronic atrial fibrillation. *Pacing Clinical Electrophysiology* 1999 ; **22** : 379-381.

Louch W.E., Sejersted O.M., and Swift F., There goes the neighbourhood: Pathological alterations in t-tubule morphology and consequences for cardiomyocyte Ca^{2+} handling. *Journal Biomedicine and Biotechnology* 2010 ; Article ID 503906, 17 pgs.

Lowe M.D., Grace A.A., Vandenberg J.I., Kaumann A.J., Action potential shortening through the putative β_4-adrenoceptor in ferret ventricle : comparison with β_1 and β_2-adrenoceptor-mediated effects. *British Journal of Pharmacology* 1998 ; **124** : 1341-1344.

Lowe M.D., Lynham J.A., Grace A.A., Kaumann A.J., Comparison of the affinity of β-blockers for two states of the β_1-adrenoceptor in ferret ventricular myocardium. *British Journal of Pharmacology* 2002 ; **135** (2) ; 451-461.

Lüss I., Boknik P., Jones L.R., Kirchhefer U., Knapp J., et al., Expression of cardiac calcium regulatory proteins in atrium v ventricle in different species. *Journal of Molecular and Cellular Cardiology* 1999 ; **31** : 1299-1314.

MacDonnell S.M., Kubo H., Crabbe D.L., Renna B.F., Reger P.O., *et al.*, Improved myocardial β-adrenergic responsiveness and signalling with exercise training in hypertension. *Circulation* 2005 ; **111** : 3420-3428.

Mackenzie L., Bootman M.D., Berridge M.J., Lipp P., Predetermined recruitment of calcium release sites underlies excitation-contraction coupling in rat atrial myocytes. *Journal of Physiology* 2001 ; **530** (3) : 417-429.

MacLennan D.H., Wong P.T.S., Isolation of calcium-sequestering protein from sarcoplasmic reticulum. *Proceedings of the National Academy of Sciences of the United States of America* 1971 ; **68** (6) : 1231-1235.

MacLennan D.H., Kranias E.G., Phospholamban : A crucial regulator of cardiac contractility. *Nature Reviews Molecular Cell Biology* 2003 ; **4** : 566-577.

Maisel W.H., Stevenson L.W., Atrial fibrillation in heart failure : epidemiology, pathophysiology and rationale for therapy. *American Journal of Cardiology* 2003; **91** (6A) : 2D-8D.

Malinowska B., Schlicker E., Mediation of the positive chronotropic effect of CGP12177 and cyanopindolol in the pithed rat by atypical β-adrenoceptors, different from β3-adrenoceptors. *British Journal of Pharmacology* 1996 ; **117**(5) : 943-949.

Marks A.R., Reiken S., Marx S.O., Progression in heart failure : Is Protein Kinase A hyperphosphorylation of the ryanodine receptor a contributing factor? *Circulation* 2002 : **105** : 272-275.

Marvin W.J., Robinson R.B., Hermsmeyer K., Functional and morphological properties of cultured cardiac and vascular muscle cells. *Circulation Research* 1979 ; **45** : 528-540.

Marx S.O., Reiken S., Hisamatsu Y., Jayaraman T., Burkhoff D., et al., PKA phosphorylation dissociates FKBP12.6 from the calcium release channel (ryanodine receptor) : defective regulation in failing hearts. *Cell* 2000 ; **101** : 365-376.

McCrossan Z.A., Billeter R., White E., Transmural changes in size, contractile and electrical properties of SHR left ventricular myocytes during compensated hypertrophy. *Cardiovascular Research* 2004 ; **63** : 283-292.

McCain E.R., McLaughlin J.S., Developmental and physiological aspects of the chicken embryonic heart. *Proceedings of the 20th Workshop/Conference of the Association for Biology Laboratory Education (ABLE)* 1999 ; **20** : 85-100.

McGraw D.W., Liggett S.B., Molecular mechanisms of β2-adrenergic receptor function, response and regulation. *Proceedings of the American Thoracic Society* 2005 ; **2** (4) : 292-296.

Meyer M., Schillinger W., Pieske B., Holubarsch C., Heilmann C., *et al.*, Alterations of sarcoplasmic reticulum proteins in failing human dilated cardiomyopathy. *Circulation* 1995 ; **92** : 778-784.

Michalak M., Corbett E.F., Mesaeli N., Nakamura K., Opas M., Calreticulin : one protein, one gene, many functions. *Biochemical Journal* 1999 ; **344** : 281-292.

Michel M.C., Harding S.E., Bond R.A., Are there functional β3-adrenoceptors in the human heart? *British Journal of Pharmacology* 2011 ; **162** (4) : 817-822.

Mills E., Bruckert, J.W., Pressor mechanisms linked obligatorily to spontaneous hypertension in the rat. *Hypertension* 1988 ; **11** : 427-432.

Mills G.D., Kubo H., Harris D.M., Berretta R.M., Piacentino III V., *et al.*, Phosphorylation of phospholamban at threonine-17 reduces cardiac adrenergic contractile responsiveness in chronic pressure overload – induced hypertrophy. *American Journal of Physiology - Heart and Circulatory Physiology* 2006 ; **291** : H61-H70.

Minsky M., Memoir on inventing the confocal scanning microscope. *Scanning* 1988 ; **10** : 128-138.

Mishra S., Sabbah H.N., Jain J.C., Gupta R.C., Reduced Ca^{2+}-calmodulin-dependent protein kinase activity and expression in left ventricular myocardium of dogs with heart failure. *American Journal of Physiology : Heart and Circulatory Physiology* 2003 ; **284** : H876-H883.

Molenaar P., Parsonage W.A., Fundamental considerations of β-adrenoceptor subtypes in human heart failure. *Trends in Pharmacological Sciences* 2005 ; **26**:368-375.

Molenaar P., Chen L., Semmler A., Parsonage W., Kaumann A., Human heart β-adrenoceptors : β1-adrenoceptor diversification through "affinity states" and polymorphism. *Clinical and Experimental Pharmacology and Physiology* 2007 ; **34** (10) : 1020-1028.

Moniotte S., Kobzik L., Feron O., Trochu J.N., Gauthier C., Balligand J.L., Upregulation of β(3)-adrenoceptors and altered contractile response to inotropic amines in human failing myocardium. *Circulation* 2001 ; **103** (12) 1649-1655.

Most P., Remppis A., Pleger S.T., Löffler E., Ehlermann P., *et al.*, Transgenic overexpression of the Ca^{2+}-binding protein S100A1 in the heart leads to increased *in vivo* myocardial contractile performance. *The Journal of Biological Chemistry* 2003 ; **278** (36) : 33809-33817.

Movsesian M.A., Karimi M., Green K., Jones L.R., Ca^{2+}-transporting-ATPase phospholamban and calsequestrin levels in nonfailing and failing human myocardium. *Circulation*. 1994 ; **90** : 653-657.

Müller O.J., Lange M., Rattunde H., Lorenzen H.P., Müller M., *et al.*, Transgenic rat hearts overexpressing SERCA2a show improved contractility under baseline conditions and pressure overload. *Cardiovascular Research* 2003; **59** :380-389.

Naga Prasad S.V., Nienaber J., Rockman H.A., β-adrenergic axis and heart disease. *Trends in Genetics* 2001 ; **17** (10) : S44-S49.

Nakai J., Imagawa T., Hakamat Y., Shigekawa M., Takeshima H., Numa S., Primary structure and functional expression from cDNA of the cardiac ryanodine receptor/calcium release channel. *Federation of European Biochemical Societies Letters* 1990 ; **271** : 169-177.

Nakamura K., Robertson M., Liu G., Dickie P., Nakamura K., *et al.*, Complete heart block and sudden death in mice overexpressing calreticulin. *The Journal of Clinical Investigation* 2001 ; **107** (10) : 1245-1253.

Napp A., Brixius K., Pott C., Ziskoven C., Boelck B., Effects of the β3-adrenergic agonist BRL 37344 on endothelial nitric oxide synthase phosphorylation and force of contraction in human failing myocardium. *Journal of Cardiac Failure* 2009 ; **15** (1) : 57-67.

Netticadan T., Temsah R.M., Kawabata K., Dhalla N.S., Sarcoplasmic reticulum Ca^{2+}-calmodulin dependent protein kinase is altered in heart failure. *Circulation Research* 2000 ; **86** : 596-605.

Noguchi K., Takahashi K., Higuchi S., In-vitro negative chronotropic and inotropic effects of a novel dihydropyridine derivative, CD-832 in the guinea-pig : comparison with calcium-channel antagonists. *Journal of Pharmacy and Pharmacology* 1998 ; **50** : 329-334

Orchard C., Brette F., T-tubules and sarcoplasmic reticulum function in cardiac ventricular myocytes. *Cardiovascular Research* 2008 ; **77** : 237-244.

Orchard C.H., Bryant S.M., James A.F., Do t-tubules play a role in arrhythmogenesis in cardiac ventricular myocytes? *The Journal of Physiology* 2013 ; symposium review :1-7.

Ostwald T.J., MacLennan D.H., Isolation of a high affinity calcium-binding protein from sarcoplasmic reticulum. *The Journal of Biological Chemistry* 1974 ; **3** : 974-979.

Parker I., Zang W-J., Wier W.G., Ca^{2+} sparks involving multiple Ca^{2+} release sites along Z-lines in rat heart cells. *Journal of Physiology* 1996 ; **497** : 31-38.

Pedro de Magalhães J., From cells to ageing : a review of models and mechanisms of cellular senescence and their impact on human ageing. *Experimental Cell Research* 2004 : **300** : 1-10.

Podrid P.J., Lown B., Pindolol for ventricular arrhythmia. *American Heart Journal* 1982 ; **104** (2) : 491-496.

Poláková E., Zahradníková A. Jr., Pavelková J., Zahradník I., Zahradníková A., Local calcium release activation by DHPR calcium channel openings in rat cardiac myocytes. *Journal of Physiology* 2008 ; **586** : 3839-3854.

Polontchouk L., Haefliger J.A., Ebelt B., Schaefer T., Stuhlmann D., *et al.*, Effects of chronic atrial fibrillation on gap junction distribution in human and rat atria. *Journal of American College of Cardiology* 2001 ; **38** : 883-891.

Porchiatti F., Pelzmann B., Cerbai E., Schaffer P., Pino R., *et al.*, The pacemaker current I-f in single human atrial myocytes and the effect of beta-adrenoceptor and A(1) adenosine receptor stimulation. *British Journal of Pharmacology* 1997 ; **122** (5) : 963-969.

Pritchard B.N.C., Gillam P.M.S., Treatment of hypertension with propranolol. *British Medical Journal* 1969 ; **1** (5635) : 7-16.

Proven A., Roderick L.H., Conway S.J., Berridge M.J., Horton J.K., *et al.*, Inositol 1,4,5-triphosphate supports the arrhythmogenic action of endothelin-1 on ventricular cardiac myocytes. *Journal of Cell Science* 2006 ; **119** (16) : 3363-3375.

Rabkin S.W., Freestone N.S., Quamme G.A., Nifedipine does not alter the increased cytosolic free magnesium during inhibition of mitochondrial function in isolated cardiac myocytes. *General Pharmacology* 1994 ; **25** : 1481-1491.

Rabkin S.W., Sunga P., The effect of doxorubicin (adriamycin) on cytoplasmic microtubule system in cardiac cells. *Journal of Molecular and Cellular Cardiology* 1987 ; **19** (11) : 1073-1083.

Renna B.F., Kubo H., Macdonnell S.M., Crabbe D.L., Reger P.O., *et al.*, Enhanced acidotic myocardial Ca^{2+} responsiveness with training in hypertension. *Medicine and Science in Sports and Exercise* 2006 ; **38**(5) : 847-855.

Richards M.A., Clarke J.D., Saravanan P., Voigt N., Dobrev D., *et al.,* Transverse tubules are a common feature in large mammalian atrial myocytes including human. *American Journal of Physiology Heart Circulation Physiology* 2011 ; **301** : H1996-H2005.

Robbins J., Dorn II G.W., Listening for hoof beats in heartbeats. *Nature Medicine* 2000 ; **6** : 968-970.

Rohrer D.K., Chruscinski A., Schauble E.H., Bernstein D., Kobilka B.K., Cardiovascular and metabolic alterations in mice lacking both β1- and β2-adrenergic receptors. *Journal of Biological Chemistry* 1999 ; **274** (24) : 16701-16708.

Rozec B., Gauthier C., β3-adrenoceptor in the cardiovascular system : putative roles in human pathologies. *Pharmacological Therapeutics* 2006 : **11** : 652-673.

Ruijtenbeek K., De Mey J.G.R., Blanco C.E., The chicken embryo in developmental physiology of the cardiovascular system : A traditional model with new possibilities. *American Journal of Physiology - Regulatory, Integrative and Comparative Physiology* 2002 ; **283** : R549-R551.

Sam C.L.S., Bolton T.B., Gordienko D., Piper I.T., Freestone N.S., Is there a relationship between calcium spark initiation sites and cell morphology in rat atrial myocytes? *Physiological Society Main Meeting, Manchester, UK,* 2009 ; **Poster Communication**.

Sam C.L.S., Bolton T.B., Piper I.T., Freestone N.S., A novel mechanism for the genesis of arrhythmias? The role of the low affinity β1-adrenergic receptor and CGP12177 in spontaneous calcium release in rat atrial myocytes. *Proceedings (P717) of the 6th European Congress of Pharmacology.* 2012 ; Medimond International Proceedings.

Santana L.F., Cheng H., Gómez A.M., Cannell M.B., Lederer W.J., Relation between the sarcolemmal Ca^{2+} current and Ca^{2+} sparks and local control theories for cardiac excitation-contraction coupling. *Circulation Research* 1996 ; **78** (1) : 166-171.

Santana L.F., Kranias E.G., Lederer W.J., Calcium sparks and excitation-contraction coupling in phospholamban-deficient mouse ventricular myocytes. *Journal of Physiology* 1997 ; **503** : 21-29.

Sarsero D., Molenaar P., Kaumann A.J., Validity of (-)-[^{3}H]-CGP 12177A as a radioligand for the 'putative β4-adrenoceptor' in rat atrium. *British Journal of Pharmacology* 1998 ; **123** (3) : 371-380.

Sarsero D., Molenaar P., Kaumann A.J., Freestone N.S., Putative β4-adrenoceptors in rat ventricle mediate increases in contractile force and cell Ca^{2+}: comparison with atrial receptors and relationship to (-)-[^{3}H]-CGP 12177 binding. *British Journal of Pharmacology* 1999 ; **128** : 1445-1460.

Savio-Galimberti E., Frank J., Inoue M., Goldhaber J.I., Cannell M., Novel features of the rabbit tranverse tubular system revealed by quantitative analysis of three-dimensional reconstructions from confocal images. *Biophysical Journal* 2008 ; 95 (4) : 2053-2062.

Scheuermann-Freestone M., Freestone N.S., Langenickel T., Höhnel K., Dietz R., Willenbrock R., A new model of congestive heart failure in the mouse due to chronic volume overload. *European Journal of Heart Failure* 2001 ; **3** : 535-543.

Schwinger R.H., Böhm M., Schmidt U., Karczewski P., Bavendiek U., *et al.*, Unchanged protein levels of SERCA II and phospholamban but reduced Ca^{2+} uptake and Ca(2+)-ATPase activity of cardiac sarcoplasmic reticulum from dilated cardiomyopathy patients compared with patients with non-failing hearts. *Circulation* 1995 ; **92** (11) : 3220-3228.

Seifert R., Wenzel-Seifert K., Constitutive activity of G-protein-coupled receptors : cause of disease and common property of wild-type receptors. *Naunyn Schmiedeberg's Archives of Pharmacology* 2002 ; **366** (5) : 381-416.

Semwogerere D., Weeks E.R., Confocal microscopy. *Encyclopedia of Biomaterials and Biomedical Engineering* 2005 : 1-10.

Shan J., Kushnir A., Betzenhauser M.J., Reiken S., Li J., *et al.,* Phosphorylation of the ryanodine receptor mediates the cardiac fight or flight response in mice. *The Journal of Clinical Investigation* 2010 ; **120** (12) : 4388-4398.

Shen J.B., Pappano A.J., Liang B.T., Extracellular ATP-stimulated current in wild-type and P2X4 receptor transgenic mouse ventricular myocytes : implications for a cardiac physiologic role of P2X4 receptors. *Federation of American Societies for Experimental Biology Journal* 2006 ; **20** (2) : 277-284.

Shirikova N., González A., Kirsch W.G., Ríos E., Pizarro G., *et al.*, Calcium sparks : release packets of uncertain origin and fundamental role. *Journal of General Physiology* 1999 ; **113** : 377-384.

Shorofsky S.R., Aggarwal R., Corretti M., Baffa J.M., Strum J.M., Al-Seikhan B.A., Kobayashi Y.M., Jones L.R., Wier W.G., Balke C.W., Cellular mechanisms of altered contractility in the hypertrophied heart : Big hearts, big sparks. *Circulation Research* 1999 ; **84** : 424-434.

Simmerman H.K.B., Jones L.R., Phospholamban: Protein structure, mechanism of action and role in cardiac function. *Physiology Reviews* 1998 ; **78** : 921-947.

Smyrnias I., Mair W., Harzheim D., Walker S.A., Roderick H.L., Bootman M.D., Comparison of the T-tubule system in adult rat ventricular and atrial myocytes, and its role in excitation-contraction coupling and inotropic stimulation. *Cell Calcium* 2010 ; **47** (3) : 210-233.

Soeller C., Cannell M.B., Two-photon microscopy : Imaging in scattering samples and three-dimensionally resolved flash photolysis. *Microscopy Research and Technique* 1999 ; **47** :182-195.

Solaro R.J., Rarick H.M., Troponin and tropomyosin : Proteins that switch on and tune in the activity of cardiac myofilaments. *Circulation Research* 1998 ; **83** : 471-480.

Song W., Lu X., Feng Q., Tumor necrosis factor-alpha induces apoptosis via inducible nitric oxide synthase in neonatal mouse cardiomyocytes. *Cardiovascular Research* 2000 ; **45** : 595-602.

Sonnenberg H., Milojevic S., Chong C.K., Veress A.T., Atrial natriuretic factor: reduced cardiac content in spontaneously hypertensive rats. *Hypertension* 1983 ; **5** :672-675.

Soriano J.B., Hoes A.W., Meems L., Grobbee D.E., Increased survival with β-blockers : importance of ancillary properties. *Progress in Cardiovascular Diseases* 1997 ; **39**(5) :445-456.

Sperelakis N., Cultured heart cells reaggregate model for studying cardiac toxicology. *Environmental Health Perspectives* 1978 ; **26** : 243-267.

Staehelin M., Simons P., Jaeggi K., Wigger N., CGP-12177 a hydrophilic β-adrenergic receptor radioligand reveals high affinity binding of agonists to intact cells. *Journal of Biological Chemistry* 1983 ; **258** : 3496-3502.

Taira C.A., Carranza A., Mayer M., Di Verniero C., Opezzo J.A.W., Höcht C., Therapeutic implications of β-adrenergic receptor pharmacodynamic properties. *Current Clinical Pharmacology* 2008 ; **3** (3) : 174-184.

Tavernier G., Galitzky J., Bousquet-Melou A., Montastruc J.L., Berlan M., The positive chronotropic effect induced by BRL 37344 and CGP 12177, two β3-adrenergic agonists, does not involve cardiac β-adrenoceptors but baroflex mechanisms. *The Journal of Pharmacology and Experimental Therapeutics* 1992; **263** (3) : 1083-1090.

Tidball J.G., Cederdahl J.E., Bers D.M., Quantitative analysis of regional variability in the distribution of transverse tubules in rabbit myocardium. *Cell Tissue Research* 1991 ; **264** : 293-298.

Towbin H., Staehelin T., Gordon J., Electrophoretic transfer of proteins from polyacrylamide gels to nitrocellulose sheets: procedure and some applications. *Proceedings of the National Academy of Sciences of the United States of America* 1979 ; **76** (9) :4350-4354.

Tunwell R.E.A., Wickenden C., Bertrand B.M.A., Shevchenko V.I., Walsh M.B., *et al.,* The human cardiac muscle ryanodine receptor - calcium release channel : identification, primary structure and topological analysis. *The Biochemical Journal* 1996 ; **318** : 477-487.

Ursino M.G., Vasina V., Raschi E., Crema F., De Ponti F., The β3-adrenoceptor as a therapeutic target : current perspectives. *Pharmacological Research* 2009 ; **59** (4) : 221-234.

Venetucci L.A., Trafford A.W., O'Neill S.C., Eisner D.A., The sarcoplasmic reticulum and arrhythmogenic calcium release. *Cardiovascular Research* 2008 ; **77** ; 285-292.

Walden A.P., Dibb K.M., Trafford A.W., Differences in intracellular calcium homeostasis between atrial and ventricular myocytes. *Journal of Molecular and Cellular Cardiology* 2009 ; **46** : 463-473.

Walter M., Lemoine H., Kaumann A.J., Stimulant and blocking effects of optical isomers of pindolol on the sinoatrial node and trachea of guinea pig. Role of β-adrenoceptor subtypes in the dissociation between blockade and stimulation. *Naunyn Schmiedeberg's Archives of Pharmacology* 1984 ; **327** : 159-175.

Wang W., Zhu W., Wang S., Yang D., Crow M.T., *et al.*, Sustained β1-adrenergic stimulation modulates cardiac contractility by Ca^{2+}/calmodulin kinase signalling pathway. Circulation Research 2004 ; **95** :798-806.

Weaver D., Cardiac cells beating in culture : A laboratory exercise. *American Biology Teacher* 2007 ; **69** (7) : 407-410.

Wegener A.D., Jones L.R., Phosphorylation-induced mobility shift in phospholamban in sodium dodecyl sulphate polyacrylamide gels. *The Journal of Biological Chemistry* 1984 ; **259** : 1834-1841.

Wegener A.D., Simmerman H.K., Lindemann J.P., Jones L.R., Phospholamban phosphorylation in intact ventricles. Phosphorylation of serine 16 and threonine 17 in response to β-adrenergic stimulation. *The Journal of Biological Chemistry* 1989 ; **264** : 11468-11474.

Wehrens X.H., Lehnart S.E., Marks A.R., Intracellular calcium release and cardiac disease. *Annual Review of Physiology* 2005 ; **67** : 69-98.

Wehrens X.H.T., Lehnart S.E., Reiken S., Vest J.A., Wronska A., Marks A.R., Ryanodine receptor/calcium release channel PKA phosphorylation : A critical mediator of heart failure progression. *Proceedings of the National Academy of Sciences of the United States of America* 2006 ; **103** (3) : 511-518.

Wientzek M., and Katz S., Isolation and characterization of purified sarcoplasmic reticulum membranes from isolated adult rat ventricular myocytes. *Journal of Molecular and Cellular Cardiology* 1991 ; **23** : 1149-1163.

Williams J.C., Armesilla A.L., Mohamed T.M.A., Hagarty C.L., McIntyre F.H., The sarcolemmal calcium pump α-1 syntrophin and neuronal nitric-oxide synthase are parts of a macromolecular protein complex. *The Journal of Biological Chemistry* 2006 ; **281** (33) : 23341-23348.

Witcher D.R., Kovacs R.J., Schulman H., Cefali D.C., Jones L.R., Unique phosphorylation site on the cardiac ryanodine receptor regulates calcium channel activity. *The Journal of Biological Chemistry* 1991 ; **266** : 11144-11152.

Woo S-H., Cleemann L., Morad M., Ca^{2+} current-gated focal and local Ca^{2+} release in rat atrial myocytes: evidence from rapid 2-D confocal imaging. *Journal of Physiology* 2002 ; **543** : 439-453.

Woo S-H., Cleemann L., Morad M., Spatiotemporal characteristics of junctional and nonjunctional focal Ca^{2+} release in rat atrial myocytes. *Circulation Research* 2003 ; **92** : 1-11.

Woo S-H., Cleemann L., Morad M., Diversity of atrial local Ca^{2+} signalling: evidence from 2-D confocal imaging in Ca^{2+} buffered rat atrial myocytes. *The Journal of Physiology* 2005 ; **567** : 905-921.

Xiao B., Zhong G., Obayashi M., Yang D., Chen K., *et al.*, Ser-2030, but not Ser-2808, is the major phosphorylation site in cardiac ryanodine receptors responding to protein kinase A activation upon β-adrenergic stimulation in normal and failing hearts. *Biochemical Journal* 2006 ; **396** : 7-16.

Xiao R.P., Zhang S.J., Chakir K., Avdonin P., Zhu W., *et al.*, Enhanced Gi signalling selectively negates β2-adrenergic receptor (AR)- but not β1-AR-mediated positive inotropic effect in myocytes from failing rat hearts. *Circulation* 2003 ; **108** : 1633-1639.

Xiao R.P., Zhu W., Zheng M., Chakir K., Bond R., *et al.*, Subtype-specific β-adrenoceptor signaling pathways in the heart and their potential clinical implications. *Trends in Pharmacological Sciences* 2004 ; **25** (7) :358-365.

Zhang G.Q., Wei H., Lu J., Wong P., Shim W., Identification and characterisation of calcium sparks in cardiomyocytes derived from human induced pluripotent stem cells. *Public Library of Science* 2013 ; **8**(2) :1-11.

Zhang H., Makarewich C.A., Kubo H., Wang W., Duran J.M., *et al.*, Hyperphosphorylation of the cardiac ryanodine rec eptor at Serine 2808 is not involved in cardiac dysfunction after myocardial infarction. *Circulation Research* 2012 ; **110** : 831-840.

Zheng M., Zhu W., Han Q., Xiao R.P., Emerging concepts and therapeutic implications of β-adrenergic receptor subtype signalling. *Pharmacology and Therapeutics* 2005 ; **108** (3) : 257-268.

Zhu W., Zeng X., Zheng M., Xiao R-P., The enigma of β2-adrenergic receptor Gi signalling in the heart : The good, the bad and the ugly. *Circulation Research* 2005 ; **97** : 507-509.

Zima A.V., Blatter L.A., Inositol-1,4,5-triphosphate-dependent Ca^{2+} signalling in cat atrial excitation-contraction coupling and arrhythmias. *Journal of Physiology* 2004 ; **555** (3) : 607-615.

List of Presentations at National and International Conferences

1) **Sam C.L.S.,** Bolton T.B., Feldheiser A., Piper I.T., Freestone N.S., (2013) Chamber-specific expression of sarcoplasmic reticulum Ca^{2+}-ATPase in healthy and diseased rat hearts. *International Union of Physiological Sciences, Birmingham, UK*, **Poster Communication.**

2) **Sam C.L.S.,** Bolton T.B., Piper I.T., Al-Jobarah M., Freestone N.S., (2013) Bupranolol blocks the cardiostimulatory effect of CGP12177 in rat atrial myocytes mediated via the low affinity β1-adrenoceptor. *International Union of Physiological Sciences, Birmingham, UK*, **Poster Communication.**

3) **Sam C.L.S.,** Bolton T.B., Piper I.T., Freestone N.S., (2013) The β3 agonist BRL37344 mediates a negative inotropic effect in rat atrial cells. *International Union of Physiological Sciences, Birmingham, UK*, **Poster Communication.**

4) **Sam C.L.S.,** Bolton T.B., Piper I.T., Al-Jobarah M., Freestone N.S., (2013) Bupranolol blocks the cardiostimulatory effect of CGP12177 in rat atrial myocytes mediated via the low affinity β1-adrenoceptor. *International Early Careers Symposium : Clinical and Translational Physiology, University of Birmingham, UK,* **Poster Communication.**

5) **Sam C.L.S.,** Bolton T.B., Piper I.T., Freestone N.S., (2013) Atrial myocyte physiology and pharmacology. *Kingston University School of Pharmacy and Chemistry Research Day 2013, UK.* **Oral Communication*. (Second prize award)**

6) **Sam C.L.S.,** Bolton T.B., Piper I.T., Freestone N.S., (2013) Atrial myocyte physiology and pharmacology. *Kingston University Staff Research and Development Day, UK.* **Invited Oral Communication*.**

7) **Sam C.L.S.,** Bolton T.B., Piper I.T., Freestone N.S., (2012) Inositol 1, 4, 5-triphosphate receptors are not involved in spontaneous calcium release from the sarcoplasmic reticulum triggered by the low affinity β_1-adrenoceptor stimulation in rat atrial myocytes. *Academy of Pharmacological Sciences, Nottingham, UK,* **Poster Communication.**

8) **Sam C.L.S.,** Bolton T.B., Piper I.T., Freestone N.S., (2012). The effect of nifedipine mediated via the low affinity β1- adrenoceptor, *Physiological Society Cardiac and Respiratory Themed Meeting, Manchester, UK*, **Oral Communication and Poster Communication.**

9) **Sam C.L.S.,** Bolton T.B., Piper I.T., Freestone N.S., (2012) A novel β-1 adrenoceptor mediates arrhythmogenic effects in rat atrial myocytes. *6th European Pharmacological Congress 2012, Granada, Spain,* **Oral Communication**.

10) **Sam C.L.S**., Alhakem H, Patel K, Read C, Piper I.T., Freestone N.S., (2012) Pharmacological evidence for four separate β-adrenoceptors in chick embryo ventricular cardiac myocytes, *6th European Pharmacological Congress, Granada Spain*, **Poster Communication.**

11) **Sam C.L.S.,** Bolton T.B., Piper I.T., Freestone N.S., (2012) Spontaneous calcium release from the sarcoplasmic reticulum mediated by the low affinity β_1-adrenoceptor in rat atrial myocytes does not occur via inositol 1, 4, 5-triphosphate receptors. *Physiological Society Main Meeting 2012, Edinburgh, UK,* **Poster Communication**.

12) **Sam C.L.S**., Alhakem H, Patel K, Read C, Piper I.T., Freestone N.S (2011) Pharmacological evidence for four distinct β-adrenoceptor sites in chick embryo ventricular myocytes. *Academy of Pharmacological Sciences 2011, Nottingham, UK,* **Poster Communication.**

*13)***Sam C.L.S.,** Bolton T.B., Piper I.T., Freestone N.S., (2011) Chamber-specific expression of sarco(endo)plasmic reticulum calcium ATP-ase in healthy and diseased rat hearts. *St George's, University of London Research Day, St George's, London, UK,* **Poster Communication**.

*14)***Sam C.L.S.**, Read C and Freestone N.S (2010) Negative chronotropic responses mediated via β-3 adrenergic receptors in chick embryo ventricular myocytes. *St George's, University of London Research Day, St George's, London, UK,* **Poster Communication**. (Shortlisted for prize for best research poster).

15)**Sam C.L.S.,** Bolton T.B., Gordienko D., Piper I.T., Freestone N.S., (2010) Is there a relationship between calcium spark initiation sites and cell morphology in rat atrial myocytes? *Physiological Society Main Meeting, Manchester, UK,* **Poster Communication**.

16)**Sam C.L.S.,** Bolton T.B., Gordienko D., Piper I.T., Freestone N.S., (2010) A study of the relationship between calcium spark initiation sites and cell morphology in rat atrial myocytes. *Research Day Kingston University, UK,* **Poster Communication * (Second prize award)**.

List of Publications

1) **Sam C.L.S.,** Bolton T.B., Piper I.T., Freestone N.S., (2012) A novel mechanism for the genesis of arrhythmias? The role of the low affinity β1-adrenergic receptor and CGP12177 in spontaneous calcium release in rat atrial myocytes. *Proceedings (P717) of the 6th European Congress of Pharmacology.* Medimond International Proceedings.

2) **Sam C.L.S.,** Alhakem H., Freestone N.S., (2012) β-Adrenergic subtypes in chick embryonic cardiac myocytes. *Proceedings of the 6th European Congress of Pharmacology.* Medimond International Proceedings.

APPENDICES